ACS APPLIED ELECTRONIC MATERIALS

pubs.acs.org/acsaelm Review

A Review on Optical Applications, Prospects, and Challenges of Rare-Earth Oxides

M. Khalid Hossain,* Shahadat Hossain, Mohammad Hafez Ahmed, Md Ishak Khan, Nazmul Haque, and Gazi A. Raihan

Cite This: *ACS Appl. Electron. Mater.* 2021, 3, 3715−3746 Read Online

ACCESS | Metrics & More | Article Recommendations

ABSTRACT: In small- and large-scale industries, manipulable optical characteristics are desired. In this regard, rare-earth oxides (REOs) have been providing pragmatic attributes in terms of successful implementations and promising prospects throughout the last few decades. Currently, there is no comprehensive literature review on REOs that can aid researchers in focusing on industry-relevant emerging materials. Therefore, this review reports studies that have been able to experimentally utilize the physical, chemical, thermal, electronic, spectroscopic, and photocatalytic properties of REOs in the optical field. The brief and focused review finds that the most pronounced applications of REOs in the optical field are in white light and laser, while the prospective ground likely lies in optoelectronics, fiber optic applications, and miscellaneous repertoires that incorporate an innovative utilization of an electronic configuration of REOs. From the perspective of this review, the versatility of an REO in the optical field has become prominent and quantified by the successful implementations of REOs in white light and nonwhite light applications. Furthermore, the innovative applications of REOs include but are not limited to the development of solid-state optical devices, optoelectronic systems, and photocatalytic agents. Specifically, their futuristic applications are likely to be led by the development of stronger emission devices and the obtaining of flexible doping characteristics by several ions such as Li^{+}, Eu^{3+}, Dy^{3+}, Nd^{3+}, La^{3+}, Yb^{3+}, etc. at different levels, which will render the pathway for further exploration in this regard. However, the improvement in terms of methodological attributes requires a serious consideration of overcoming the limitation of thermal stability, lack of exploration of several types of lights, photodarkening in critical applications, lack of applicability at a wide range of temperatures, and so on. From an industrial perspective, it can be conjectured from the reported literature that the challenges will be overcome at a large scale within a few years due to the expedited technological advancements of the experimental repertoires, rendering the REO applications in the optical field reasonably economic and commercially viable. In short, this is the first review that objectively considers the applications and prospects of REOs, which will essentially invoke several studies to investigate the specific properties and viability of REOs in the optical field.

KEYWORDS: *rare-earth oxides, laser and fiber optic, optoelectronics, nonlinear optics, display and luminescence*

1. INTRODUCTION

There has always been a demand for sustainable development, energy consumption, greener, and safer technology, which has motivated researchers to find the best materials in the field of optics. Rare-earth elements (REEs) individually or doped with other host glass matrices have recently made a prodigious impression in optical applications, especially rare-earth oxides (REOs), which are of an increased interest in modern high-tech optics industries due to their unique characteristics. Therefore, studies focusing on rare-earth (RE) sesquioxide or REO (commonly denoted as R_2O_3, R = rare-earth element) doped inorganic elements have burgeoned throughout the past decade. They have revealed a superiority to other materials such as fluoride- and lithium-based glasses, P_2O_5, etc. in terms of various optical applications[1−12] because of their thermal and chemical stability, longevity, nonlinear refraction, high quantum yield, etc. As a result, REO-doped materials have an enormous prospect in replacing conventional materials. For example, current Hg-based compact fluorescent lamps are not highly efficient for long-term use and pose a threat to the environment when damaged. The use of REO phosphor-based lighting devices can overcome this issue.

Starting from the nomads who used fire for lighting, we have now reached an epoch of light-emitting diodes (LEDs) and liquid crystal displays (LCDs). Normally, both LEDs and

Received: July 31, 2021
Accepted: August 25, 2021
Published: September 8, 2021

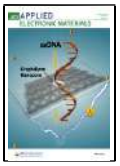

https://doi.org/10.1021/acsaelm.1c00682
ACS Appl. Electron. Mater. 2021, 3, 3715−3746

LCDs are made of phosphors. Because of enhanced chemical stability and photoluminescence properties, REOs are now being exploited as phosphors in these devices.[1,13] Furthermore, the multiphonon relaxation and efficient up−down conversion of REOs might be useful for lessening the nonradiative loss, which will eventually produce quality laser materials. The long-standing demand for substrate stability was satisfied at low temperatures along with a high band gap by using REOs.[14] Nonlinear photonic devices can be manufactured by exploiting REOs, as the third-order optical nonlinearity with large band gaps was achieved in a lab-scale experiment.[15] Moreover, improved lattice strains brought new functional behaviors for REOs, which opens an opportunity for manufacturing innovative optoelectronic devices.[16] Also, successful opto-modifications were done via REOs, which is a recent addition in the domain of fiber optics.[17−19] Even the photocatalytic behavior,[20,21] thermal imaging,[22,23] optical probe,[24] plasma display panel,[25] etc. sectors were vastly improved by the incorporation of REOs in recent years.

Significant research has been conducted by exploring the REO element, its composition, host matrices, growth processes, and other experimental parameters (i.e., growth temperature, pressure, etc.) in a lab scale, whereas industrial applications require a more confirmed synthesis with some other concerns such as production cost and the efficient splitting of REOs.[26−28] Therefore, a piece of combined knowledge and understanding is required for a commercial viability. At present, there is a lack of accumulated studies concentrating on the applications, prospects, and challenges of REOs in optical applications.

This review article broadly discusses the prevailing works related to R_2O_3 (R = Ce, Sm, Eu, Gd, Dy, Y, Er, and Yb) doped inorganic materials, which have shown noteworthy results for optical applications.[1−12] The review begins with a general overview of the optical applications of REOs. Then the applications in various optical sectors are discussed in detail from the available literature, which is followed by discussions of promising prospects in each section. Later, the existing challenges and knowledge gaps in each sector are also narrated separately. Finally, an overall discussion about the reviews along with future directions to tackle the prevailing gaps and major challenges are provided. As a result, this study will eventually invoke several investigations in the optical application area.

2. OVERVIEW OF REO

The lanthanide group together with scandium and yttrium in the periodic table of elements, commonly known as REEs, exhibit interesting physicochemical characteristics. The prime reason behind this is their unique features of f-f intra-configuration.[29] The partially filled inner 4f subshell of REE, rather than the outer shell, includes an electron when incorporated with an atom of a different element. Thus, the ionic radius gets shrunk, which eventually demonstrates expanded physicochemical characteristics.[30]

Technologically important rare-earth sesquioxides (R_2O_3) are well-studied materials. Their crystal phases were divided into five distinct categories depending on their polymorphic form, temperature, and chemical environment, which are (i) A-type (hexagonal), (ii) B-type (monoclinic), (iii) C-type (body-centered cubic), (iv) H-type (high temperature hexagonal), and (v) X-type (high-temperature cubic). The first three types (i.e., A-, B-, and C-type structures) are formed below 2000 °C, while the other two types (i.e., H and X) are formed above this temperature.[31] Because of their unique structural and electronic configurations, they possess handy optical properties. Among the versatile characteristics, a homogeneous light emission due to elongated lifetime excited states, ample energy levels, greater resistance to crystallization, better thermal and chemical stability, isotropic refractive index, intense luminescence, lowered environmental toxicity, less propagation loss, easy manufacturing, etc. are especially notable.[1,13,32−34]

3. CLASSIFICATION OF REO'S OPTICAL APPLICATIONS

It is seen that eight (8) REOs such as Ce_2O_3, Sm_2O_3, Eu_2O_3, Gd_2O_3, Dy_2O_3, Y_2O_3, Er_2O_3, and Yb_2O_3 were significantly applied in various research works for different optical applications. These include UV LED pumped solid-state white light generation,[1] intense and wideband white light emission,[13,35−39] white LED,[40−47] red light emission,[48,49] orange LED,[50] green light emission,[51] solid-state lighting devices,[5,34,52−54] various types of lasers,[6,55−63] UV LED,[7,8] nonlinear optical devices,[9,64,65] near-infrared (NIR) luminescence,[10] NIR light,[66] optoelectronics,[11,16,67,68] optical fiber amplification,[12,19] active and passive optical fiber,[17] optical display,[4,69] multifunctional and enhanced luminescence,[3,70] photocatalytic applications,[20,21] low-temperature thermal imaging,[22,23] optical amplification for medical diagnosis,[71] halide lamp,[72] smart light (circadian cycle),[73] X-ray induced luminescence (XRL),[74] etc. These eight REOs have been preferred in consideration of their significant spectroscopic characteristics and tremendous industrial prospects in the manufacturing of next-generation optical devices. The various optical applications of the aforementioned eight REOs are discussed in an organized manner in the following sections of this article. The applications for which comparatively less literature was found are discussed in a separate section named miscellaneous optical applications. The categorization of optical applications is made as follows.

(i) White light optics
(ii) Nonwhite light optics
(iii) Solid-state optical device
(iv) Laser
(v) UV optics
(vi) Nonlinear optics
(vii) NIR optics
(viii) Optoelectronics
(ix) Optical fiber
(x) Display and luminescence
(xi) Miscellaneous.

4. REOS' OPTICAL APPLICATIONS AND PROSPECTS

4.1. White Light Optics. *4.1.1. White Light Optical Applications.* The generation of white light has gained ample interest among researchers for its vast applications in LED and LCD. These LEDs and LCDs are advantageous over the traditional luminous lamps owing to their extended lifetime, reduced power consumption, and environmentally friendly features.[1] The REOs have shown tremendous success in generating white light where it is mainly used as a dopant material in various hosts.

Yttria (Y_2O_3) phosphor is one of the host materials used in various studies with specific rare-earth elements as activators.[1,13,35−37] The undoped nanosized Y_2O_3 has demonstrated

https://doi.org/10.1021/acsaelm.1c00682
ACS Appl. Electron. Mater. 2021, 3, 3715−3746

Table 1. White Light Optical Applications

specific applications	used REOs	REO composition[a]	refs
Nanophosphor for UV LED pumped solid-state white light	Acetylacetonate (acac) passivated Eu:Y_2O_3 nanocrystal.	2,4-pentadione (acac) passivated Eu (x): Y_2O_3 where x = 0, 2, 9, 11, and 18 wt %.	Dai et al. (2011)[1]
Intense white light emission	Eu^{3+} and Tb^{3+} codoped Y_2O_3 phosphors	Eu^{3+} concentration was varied from 0.6 to 10 mol % whereas Tb^{3+} concentration was varied from 1 to 4 mol %.	Tu et al. (2011)[35]
White light emission	Tm^{3+}, Er^{3+}, Yb^{3+} triply doped Y_2O_3 transparent ceramics	$(Er_xTm_{0.001}Yb_{0.03}Zr_{0.03}Y_{0.939-x})_2O_3$ where x = 0, 0.001, 0.005, 0.01, and 0.02 at.%.	Hou et al. (2011)[36]
Bright and wideband white light emission	Undoped Y_2O_3 nanopowders	N/A	Bilir et al. (2014)[37]
Bright white light emission	Tm^{3+}, Er^{3+}, Yb^{3+}, Li^+-doped Y_2O_3 nanocrystals	Y_2O_3 + 0.3 mol % Tm^{3+} + 0.5 mol % Er^{3+} + 3.5 mol % Yb^{3+} (TEYY) and Y_2O_3 + 0.3 mol % Tm^{3+} + 0.5 mol % Er^{3+} + 3.5 mol % Yb^{3+} + 2 mol % Li^+ (TEYYL).	Bai et al. (2009)[13]
Laser and white light generation	Dy^{3+}-doped lithium lead gadolinium silicate glasses	25 Li_2O + 15 PbO + 5 Gd_2O_3 + (55−x) SiO_2 + xDy_2O_3 where x = 0.0, 0.1, 0.5, 1.0, 1.5, and 2.0 mol %.	Khan et al. (2019)[80]
White light generation using solid-state lighting	Dy^{3+} nanoparticles doped Zinc borotellurite glasses	$\{[(TeO_2)_{0.7}(B_2O_3)_{0.3}](ZnO)_{0.3}\}_{1-x}(Dy_2O_3NP)_x$ (where x = 0.01, 0.02, 0.03, 0.04, and 0.05 M fraction).	Hazlin et al. (2018)[32]
Laser & white light generation	Dy^{3+}-doped LGFDy glasses	x Dy_2O_3 + 40 Li_2O + 5 BaO + 5 GdF_3 + (50−x) SiO_2 where x = 0.0, 0.1, 0.5, 1.0, 1.5, and 2.0 mol %.	Khan et al. (2019)[81]
White light emission	Gd^{3+} and Dy^{3+} codoped borate glasses.	$(B_2O_3)_{0.55-x}$ $(Li_2O)_{0.30}$ $(MgO)_{0.10}$ $(Gd_2O_3)_{0.05}$ $(Dy_2O_3)_x$ where 0.0 < x (mol %) < 1.5	Ullah et al. (2020)[38]
White light emission device	Dy^{3+} activated NKBT piezoelectric powders	$Dy_2O_3Na_{0.25}K_{0.25}Bi_{0.5}TiO_3$	Kuzman et al. (2020)[82]
Fabrication of bright white LED's	Dy^{3+}-doped lithium aluminoborate glasses	27 Li_2O + 3 Al_2O_3 + (70−x) B_2O_3 + xDy_2O_3, where x = 0, 0.1, 0.3, 0.5, and 0.7 mol %.	Pawar et al. (2017)[40]
White light laser and color display devices	Dy^{3+}-activated zinc borotellurite glasses and nanoglass-ceramics	N/A	Kaur et al. (2019)[75]
Ideal white light emission	Eu^{3+} and Dy^{3+} codoped calcium tungstate nanoparticles	2 mol % Eu_2O_3 + 5 mol % Dy_2O_3 + $CaWO_4$	Kaur et al. (2020)[83]
Intense white light generation	Dy^{3+}-doped NBSAZB glasses	25 Na_2O + 10 B_2O_3 + (50−x) SiO_2 + 5Al_2O_3 + 5ZnO + 5BaO + xDy_2O_3 (0 ≤ x ≤ 2.0 mol %)	Jamalaiah et al. (2017)[39]
White LEDs	Ce^{3+} and Tb^{3+} in barium gallium borosilicate glasses	30BaO + 2 Ga_2O_3 + (27.8−x)B_2O_3 + 40SiO_2 + xCe_2O_3 + 0.2Tb_2O_3 (0 ≤ x ≤ 1.0)	Rao et al. (2019)[41]
Cool white LED and glass scintillation applications	Dy^{3+}-doped yttrium calcium silicoborate (YCaSBDy) glasses	25Y_2O_3 + 10CaO + 10SiO_2 + (55−x)B_2O_3 + xDy_2O_3, where x = 0.05, 0.1, 0.5, 1.0, 1.5, 2.0, and 2.5 mol %.	Kesavulu et al. (2017)[42]
White light emission	Dy^{3+}-doped lithium borosilicate glasses	30 Li_2O + (70−$x$$Dy_2O_3$) {1/7$SiO_2$ + 6/7B_2O_3} where x = 0.5, 1, 1.5, and 2 mol %.	Ramteke et al. (2017)[76]
White LEDs	Dy^{3+}-doped calcium bismuth borate glasses	xLiF + (30−x)CaO + 20Bi_2O_3 + 50B_2O_3 + 1 mol % of Dy_2O_3 (x = 0, 2, 5, 7, 10, and 15 mol %.	Narwal et al. (2018)[43]
W-LEDs application and smart lighting	Dy^{3+}-doped calcium boroaluminate glasses	50B_2O_3 + (25−x)CaO + 15Al_2O_3 + 10CaF_2 + xDy_2O_3 (x = 0.0, 0.5, 1, 2, 3, and 5 wt %).	Lodi et al. (2018)[44]
Solid-state white light generation devices	Dy^{3+}-doped trialkali oxyfluoroborate (NKLB) glasses	25LiF + 10Na_2O + 10K_2O + (55−x)B_2O_3 + xDy_2O_3, (x = 0, 0.1, 0.5, 0.7, 1.0, and 1.5 mol %).	Khan et al. (2019)[33]
White light generation	Dy^{3+}-doped lithium zinc borosilicate glasses	(30−x)B_2O_3 + 25SiO_2 + 10Al_2O_3 + 30LiF + 5 ZnO + xDy_2O_3 (x = 0, 0.1, 0.5, 1.0, and 2.0 mol %).	Jaidass et al. (2018)[77]
Bright white LED's and modern white LED bulbs	Dy^{3+}-doped lithium borate glasses	30Li_2O + (70−x)B_2O_3 + xDy_2O_3, where x = 0, 0.1, 0.3, 0.5, and 0.7 mol %.	Pawar et al. (2016)[45]
White LED	Eu^{3+}-activated borate-based phosphors	$LiLa_2O_2BO_3$ + Eu_2O_3	Li et al. (2011)[46]
Red photoluminescent component for white LEDs under n-UV excitation	Eu^{3+}-doped alkaline earth zinc-phosphate glasses	(40−x)ZnO + 35P_2O_5 + 20RO + 5TiO_2 + xEu_2O_3 (where x = 1 mol % and R = Mg, Ca, Sr, and Ba)	Jha et al. (2016)[47]

[a]N/A indicates not applicable.

10 times more efficiency than a commercial 60 W incandescent lamp.[37] By contrast, Eu^{3+}- and Tb^{3+}-doped Y_2O_3 showed excellent chemical durability along with improved photoluminescence and electroluminescence.[35] In other studies, Tm^{3+}-, Er^{3+}-, and Yb^{3+}-doped Y_2O_3 transparent ceramics were used to enhance the green, red, and blue upconversion processes,[36] while a Li^+ ion doping with these three dopants in the same nanocrystal tremendously improved the luminous efficiency.[13] It has been apparent that doping RE ions greatly ameliorates the stability and resistance to crystallization, indicating their influence on structural and optical features of multicomponent glass networks. Several successful studies were conducted in tailoring glass system types and the amount of RE ions to improve the luminescence properties up to the desired range. Among other glass host materials, borate-based glasses showed noteworthy results when doped with Dy^{3+} ions.[32,33,46,75−77,38−45] The incorporation of borate improves the glass property (i.e., the nonlinear refractive index) and provides stability to the glass matrix. The higher phonon energies and fragility problems of borate-based glasses can be resolved by using alkali elements, and several features such as dynamic luminescence center, amplified afterglow due to f-f ion-trapping shell for a prolonged period, robust excitation band around 454 nm, etc., over other RE ions have made the Dy^{3+} ion popular among researchers for a white light generation.[32] Moreover, Dy^{3+} shows $^4F_{9/2} \rightarrow {}^6H_{15/2}$ and $^4F_{9/2} \rightarrow {}^6H_{13/2}$ transitions in the visible region that are influential for a yellow/blue emission and ideal white light generation.[40,44,76] Table 1 demonstrates various studies for efficient white light generations exploiting RE ions. Figure 1 shows various

https://doi.org/10.1021/acsaelm.1c00682
ACS Appl. Electron. Mater. 2021, 3, 3715−3746

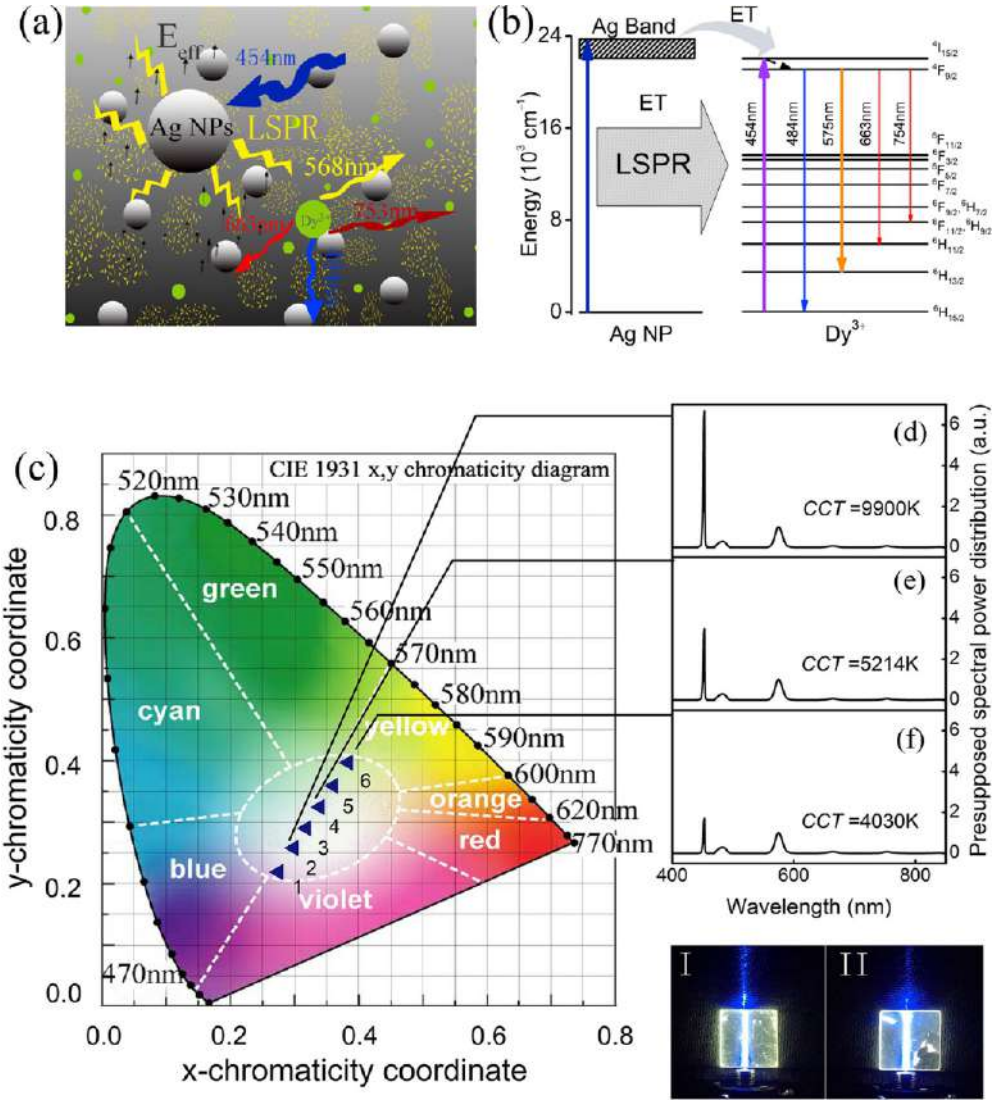

Figure 1. (a) Depiction of localized surface plasmon resonance (LSPR), (b) partial energy level diagram for Dy^{3+}-doped HGT glasses nearby Ag nanoparticles, (c) color coordinates of the same glass (at 453 nm laser excitation), and (d–f) corresponding correlated color temperature (CCT). (I) White fluorescence snaps and (II) resemblance of the HGT-Dy-0.5 and HGT-Dy-0.5/AgH glasses by a long laser-pumping path. Reproduced with permission from ref 78. Copyright 2018 Elsevier.

interesting properties of Dy^{3+}-doped heavy metal germanium tellurite (HGT) glasses containing Ag nanoparticles,[78] and Figures 2 and 3 illustrate promising properties for $Gd_{3.67}EuSi_3O_{13}$ phosphor-fabricated LEDs.[79]

4.1.2. Prospects in White Light Optical Applications. The REOs have promising prospects in an efficient white light generation. The former section, section 4.1.1, has provided a list of studies where RE ions were used, and some of them have great potential in white light generating industries. The Y_2O_3 transparent ceramic showed a broad prospect in white light emission when doped with three RE ions, that is, $Tm^{3+}/Er^{3+}/Yb^{3+}$.[36] A higher lifetime, quantum efficacy, and stimulated emission cross-section for Dy_2O_3-doped zinc borotellurite glasses, nanoglass-ceramics, and NBSAZBDy glasses could be apposite for commercial manufacturing white light lasers.[32,39,75] The 0.6 mol % Ce_2O_3- and Tb^{3+}-doped BaGaBSi glass is much more steady against devitrification and shows extreme intensity, therefore making this composition promising for white LEDs.[41] The Dy_2O_3 blended trialkali oxyfluoroborate (NKLB-Dy), lithium lead gadolinium silicate (LPDy), Li_2O-BaO-GdF_3–SiO_2 (LGFDy), LiF-CaO-Bi_2O_3–B_2O_3, and calcium boroaluminate (CaBAl) glasses have a higher yellow-to-blue ratio indicating the covalent character of the Dy–O bond, making them potential candidates for laser and white light generation applications.[33,43,44,80,81] The 0.5 mol % Dy_2O_3-doped lithium borate glasses have the maximum emission intensity under UV irradiation (i.e., 350 nm) also signifying their practicality in manufacturing contemporary bright white LED bulbs.[45] Furthermore, 2 mol % Eu_2O_3 with 5 mol % Dy_2O_3-doped $CaWO_4$ is also a suitable candidate for white light emission.[83]

4.2. Nonwhite Light Optics. *4.2.1. Nonwhite Light Optical Applications.* The generation of nonwhite light such as red, orange, reddish-orange, green, yellow, etc., has gained considerable traction among researchers due to the prevalent applications in LEDs, optoelectronics, lasers, sensors, and optical communications. Similar to white light generations, the various combinations of REO ions have also shown a superiority over other materials in a nonwhite light generation. This has been possible because of their inimitable attributes

https://doi.org/10.1021/acsaelm.1c00682
ACS Appl. Electron. Mater. 2021, 3, 3715–3746

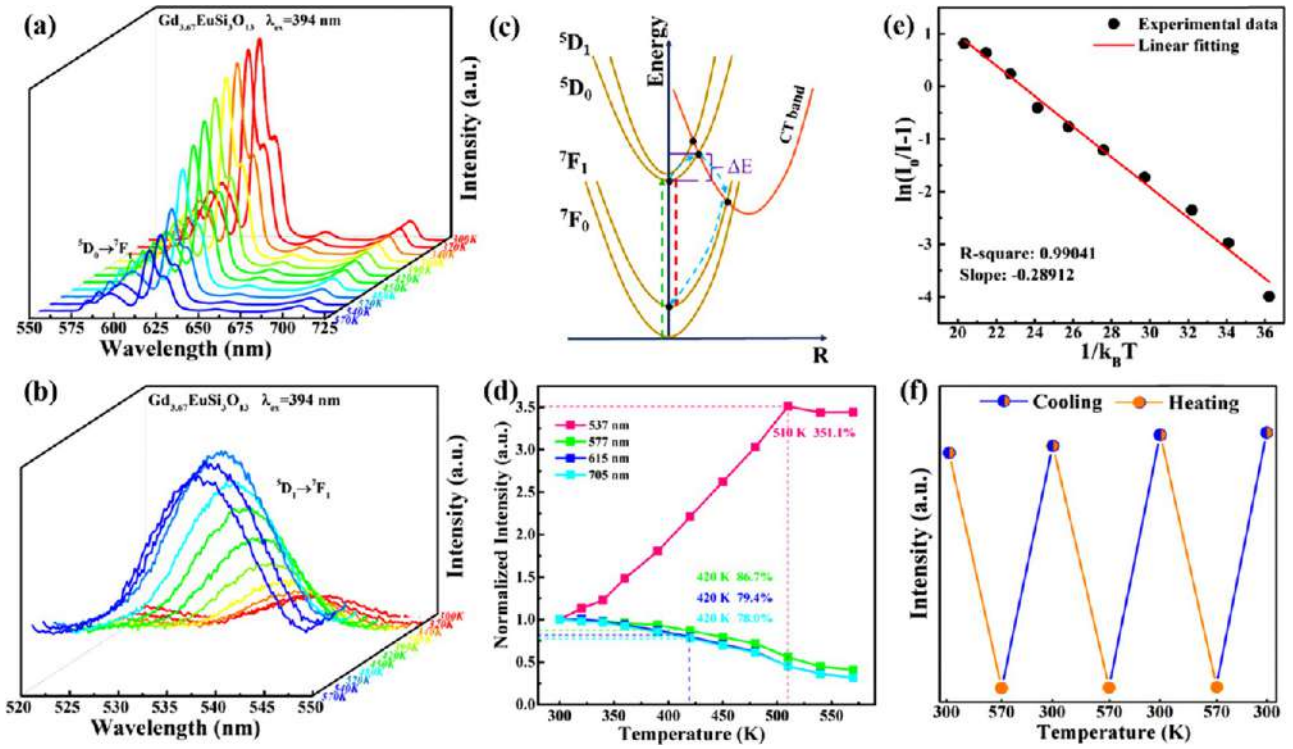

Figure 2. (a, b) Photoluminescence variation of the $Gd_{3.67}EuSi_3O_{13}$ phosphor at different temperatures (excited at 394 nm), (c) depiction of the allowed pathways for thermal quenching, (d) normalized emission intensity for the same phosphor with different temperatures, (e) graph for $\ln(I_0/I - 1)$ vs $1/k_BT$ and (f) temperature−recycle analysis. Reproduced from 79. Copyright 2021 American Chemical Society.

like superior thermal and chemical stability, consistent light emission, uncomplicated manufacturing process, and small production cost. By tailoring some crucial parameters (i.e., the concentration of REO ions, host matrix or glass compositions, processing temperature, etc.), the luminescence properties can be enhanced, and highly efficient materials can be prepared.

Gadolinium oxide (Gd_2O_3) also possesses an excellent chemical and thermal stability alongside a low photon energy, which makes it capable of being used as a host matrix for luminescence properties. Huang et al. (2013) first synthesized Eu^{3+}-doped Gd_2O_3 core−shell microspheres through a prototype-free solvothermal process using poly-(vinylpyrrolidone) (PVP) as a surfactant, which was followed by a calcination process.[48] This material showed a strong red emission when excited at 254 nm.[48] Further, the Eu^{3+}-doped Y_2O_3 nanophosphor is a well-studied material for the red light luminescence, whereas Vini et al. (2020) used Gd^{3+} as a codopant in this material. It has been reported that the 6 wt % Eu^{3+}-doped Y_2O_3 nanophosphors and codoped Gd^{3+} have significantly increased (i.e., ∼4 times) the luminescence.[49] In a different study, Jha et al. (2019) employed three different alkaline network moderators (i.e., BaO, SrO, and CaO) for Eu^{3+}-doped oxy-fluoro telluorophosphate glass composites. However, the maximum quantum efficacy and emission intensity were achieved for a BaO network modifier glass with 5 mol % Eu^{3+} doping. It showed a pure red light emission under near-ultraviolet (n-UV) excitations.[29] The Sm^{3+} ion has also attained popularity among researchers for use as an orange luminescent center. One study showed that Sm^{3+}-doped silicate-based oxide and oxyfluoride glasses are suitable for orange LEDs.[50] Meanwhile, another study revealed that Sm^{3+}-doped barium sodium borate glasses have a high potency for utilization as orange emanating materials.[2]

Eu^{3+} ions have been used for reddish-orange light emissions by several researchers as well. It was reported that 1.48 mol % Eu^{3+}-phosphate glasses have outstanding luminescent properties for reddish-orange light emissions (Figure 4).[69] An addition of 2 mol % Dy^{3+} with 2 mol % Eu^{3+} in sodium−zinc phosphate glasses also has similar properties in generating warm white light to reddish-orange light sources.[34] The Dy^{3+} ion was also used in yellow light generation doping with K−Sr−Al phosphate glasses. The quantum efficiency had increased to ∼76% when 1 mol % of Dy^{3+} was doped with K−Sr−Al phosphate glasses.[84] The green light emission using REO ions has also been reported. The Ho^{3+}-doped bismuth-germanate (GeBiNaGdBaH) glasses demonstrated strong emissions near the green region (i.e., ∼548 nm).[51] The fabrication of 1.0 wt % Tb_2O_3 and 3.0 wt % Yb_2O_3-doped tellurite glass exhibited the maximum green light intensity in the visible region and can be useful for developing green fiber lasers.[85] Figure 5 depicts the energy transfer mechanism between Eu^{2+} ions in various host materials (phosphors).[86] Table 2 shows some of the studies for nonwhite light light generations using REO ions from the past decade.

4.2.2. Prospects in Nonwhite Light Optical Applications. Several studies, as discussed in Section 4.2.1, have shown the prospects of REO ions in nonwhite light generations, especially the red, reddish-orange, yellow, and green light emissions. The uniform and monodisperse Gd_2O_3 core−shell microspheres doped with Eu^{3+} have shown promising prospects in producing nonwhite light with strong red emissions as well as in the growth of a prototype-free synthetic approach for the new hollow metal oxides production.[48] Among the different series of 0.5 mol % Eu_2O_3-doped alkali oxides-modified borosilicate glasses, the Li_2O−Na_2O combination has shown the maximum stimulated emission cross-section and experimental branching

https://doi.org/10.1021/acsaelm.1c00682
ACS Appl. Electron. Mater. 2021, 3, 3715−3746

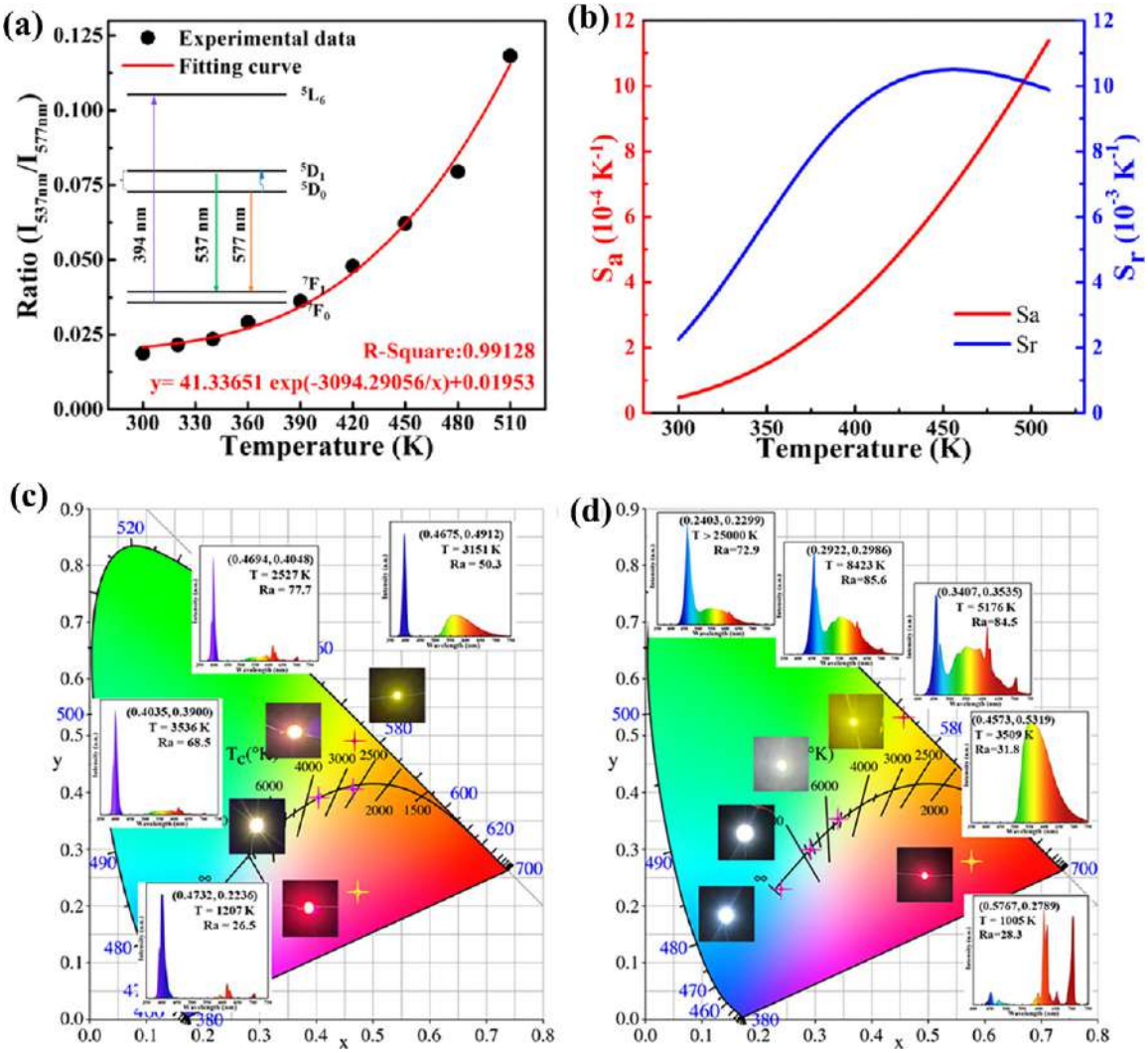

Figure 3. (a) Photoluminescence intensity ratio of $Gd_{3.67}EuSi_3O_{13}$ phosphor with respect to temperature, (b) absolute sensitivity (S_a), and relative sensitivity (S_r) calculation from 300 to 510 K, (c, d) color coordinates, photographs, and electroluminescent spectra of the fabricated LEDs using the same phosphor under 395 nm (c) and 460 nm (d) excitation. Reproduced from ref 79. Copyright 2021 American Chemical Society.

ratios for the $^5D_0 \rightarrow {}^7F_2$ (614 nm) transition, which makes it a possible runner aimed at a red color center for display devices and visible red lasers.[87] The ZnO-TiO_2 has also proved its potentiality for use as a red upconversion phosphor showing very high red emissions when doped with a ratio of Yb_2O_3/Er_2O_3 = 0.06:0.02.[88] The various spectroscopic parameters, that is, the oscillator strength for the $^6H_{5/2} \rightarrow {}^6P_{3/2}$ (400 nm) transition, the stimulated emission cross-section $^4G_{5/2} \rightarrow {}^6H_{7/2}$ (600 nm) transition, and the branching ratio (0.518) obtained from a Judd-Ofelt analysis were the highest for the 0.5 mol % of Sm_2O_3-doped barium sodium borate glass. These properties of the Sm_2O_3-doped glass make it viable for applications as an orange-emitting functional materials design.[2] Meanwhile, the Ho^{3+}-GeBiNaGdBaH glass has shown a strong green emission for the $(^5S_2+{}^5F_4) \rightarrow {}^5I_8$ (452 nm) transition and maximum stimulated emission cross-section (0.18×10^{-20} cm^2) likened to other studied glasses,[51] suggesting its highly promising prospects for use as green lighting functions. The Dy^{3+}-doped K−Sr−Al phosphate glasses might be suitable for yellow laser applications, since an intense yellow emission was found for the $^4F_{9/2} \rightarrow {}^6H_{13/2}$ (572 nm) transition with a higher branching ratio (0.78).[84]

4.3. Solid-State Optical Device. *4.3.1. Solid-State Optical Device Applications.* Solid-state optical materials gained tremendous traction in the past decade, as they offered great solutions to the challenges encountered in the arena of optoelectronics, display technologies, optical amplification, and so on. When these materials were combined with RE ions, they showed significant improvements, especially in the study of a near-infrared solid-state laser, optical sensing, amplification, and thermometry.

As happened previously, various glass host matrices incorporating RE ions were used in numerous studies to enhance the desired properties. For example, Er^{3+} and Nd^{3+} codoping was used in lithium niobate-based tellurite glasses, which showed admirable luminescence responses.[55] Phosphate-based glasses were found to be an exceptional material as a host, and Dy^{3+}, Eu^{3+} doped, separately and in combination, with sodium−zinc phosphate glasses could be appropriate for solid-state lighting sources, because they showed a high quantum efficiency (i.e., 96%) close to unity and yellow, reddish-orange, and neutral/warm white light have been produced successfully by varying doping concentrations (Figure 6 depicts some measured features of this glass

https://doi.org/10.1021/acsaelm.1c00682
ACS Appl. Electron. Mater. 2021, 3, 3715−3746

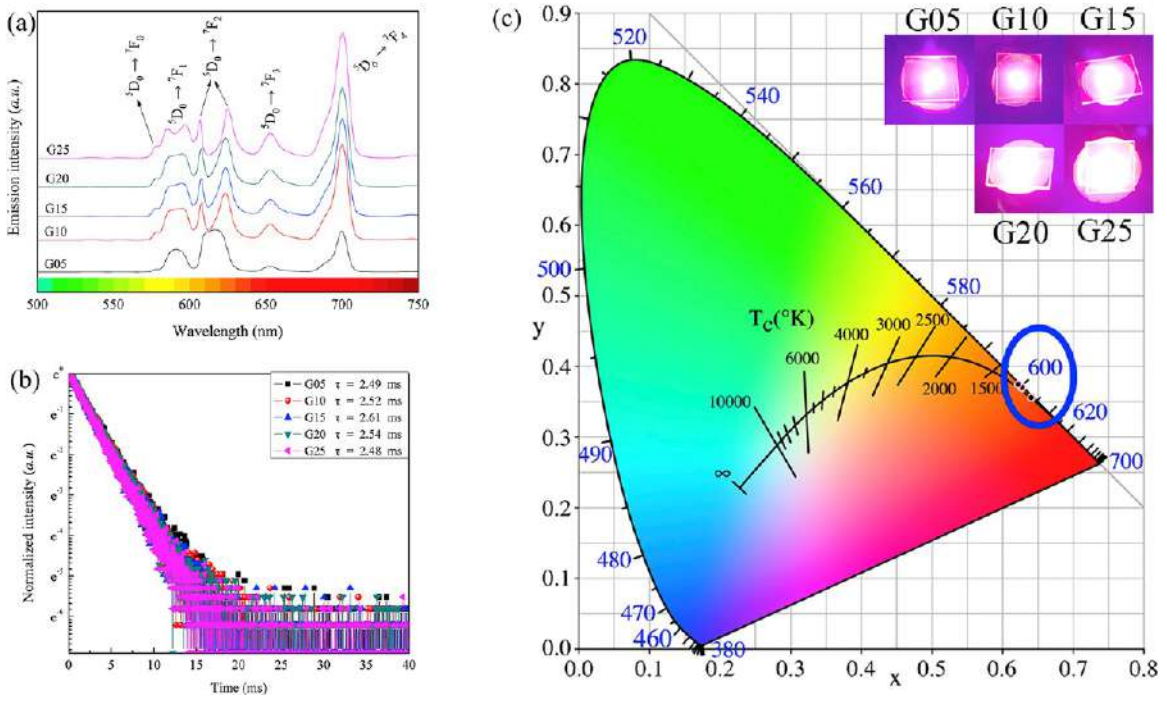

Figure 4. (a) Emission spectrum for Eu_2O_3-doped P_2O_5−SrO−BaO−ZnO (PSBZ) glass, (b) fluorescence decay curves of the same glass matrix, and (c) chromaticity coordinates of glasses using a CIE 1931 chromaticity diagram. Reproduced with permission from ref 69. Copyright 2020 Elsevier.

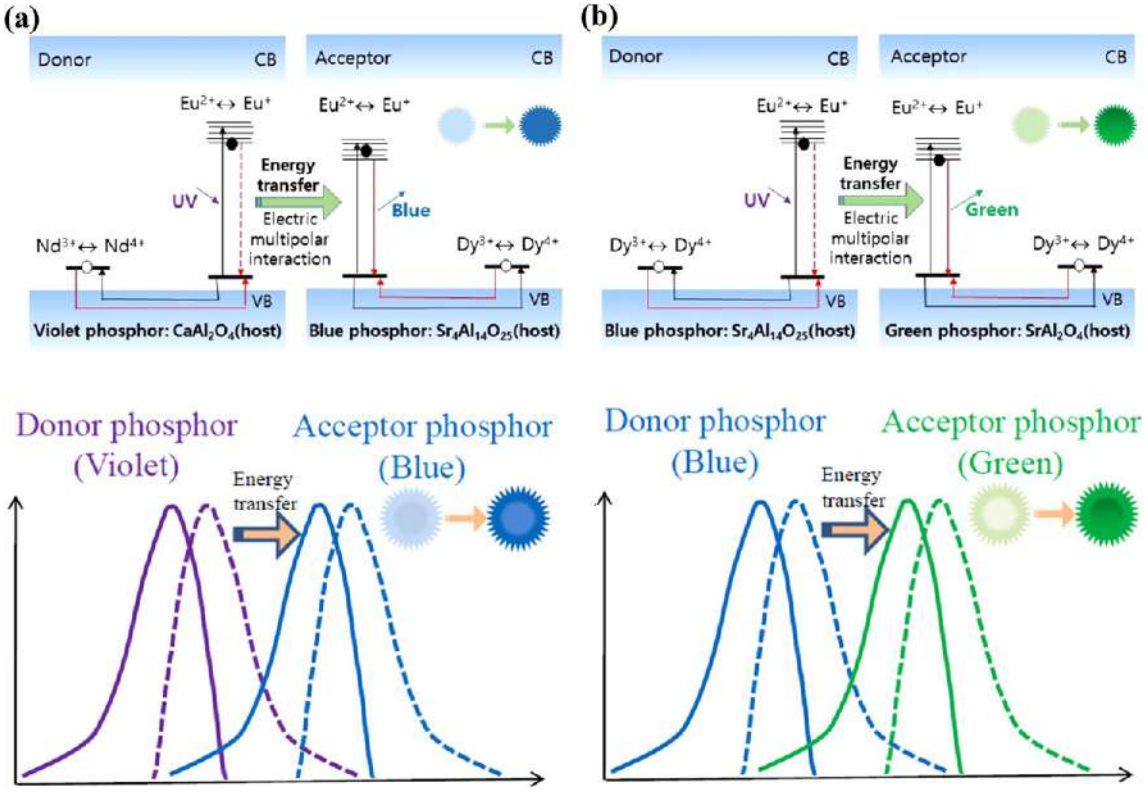

Figure 5. Schematic of the energy transfer model between the donor and acceptor ions in various host materials. (a) Violet-Blue phosphor mixing and (b) blue-green phosphor mixing. Reproduced from ref 86. Copyright 2020 American Chemical Society.

matrix).[34] The Ho^{3+}-doped Y_2O_3 has also been reported to show a green luminescence property upon the blue excitation.[89] The Sm^{3+} ion has also been doped with various host matrices like tellurium oxide-based glasses,[5] zinc oxide nanostructured films,[52] and lithium magnesium borate erbium oxide-based glasses,[90] and most of them are suitable for solid-state lighting. Another RE ion Eu^{3+} has been doped with lead- and bismuth-containing borate glasses,[91] lithium aluminum

https://doi.org/10.1021/acsaelm.1c00682
ACS Appl. Electron. Mater. 2021, 3, 3715−3746

Table 2. Non-White Light Optical Applications

specific applications	used REOs	REO composition	refs
Strong red emission and light emitting phosphors	Homogeneous Gd_2O_3:Eu^{3+} core−shell microspheres	N/A	Huang et al. (2013)[48]
Red light emission	Eu^{3+}- and Gd^{3+}-doped Y_2O_3 nanophosphors	N/A	Vini et al. (2020)[49]
Red photoluminescent component in photonic devices	Eu^{3+}-doped oxy-fluoro tellurophosphate glasses	(40-x) P_2O_5 + 20 TeO_2 + 20 ZnF_2 + 20 RO + x Eu_2O_3 (where R = Ca, Sr, and Ba and x = 1)	Jha et al. (2019)[29]
Red color center in display devices and visible red laser emission	Eu^{3+}-doped alkali oxide modified borosilicate glasses	74.5 B_2O_3 + 10 SiO_2 + 5 MgO + R + 0.5 Eu_2O_3 [where R = 10 (LiO_2/Na_2O/K_2O) for series A and R = 5 (Li_2O + Na_2O/Li_2O + K_2O/K_2O + Na_2O) for series B]	Reddy et al. (2017)[87]
Red upconversion phosphor	Er^{3+}, Yb^{3+}:ZnO-TiO_2 phosphor	Ti/Zn/Yb/Er ratios of 1:1:0:0.06, 1:1:0.02:0.06, 1:1:0.06:0.06, 1:1:0.06:0.02, and 1:1:0.06:0.	Ohyama et al. (2015)[88]
Orange LEDs and laser	Sm^{3+}-doped silicate-based oxide and oxyfluoride glasses	25 Li_2O + 5 Gd_2O_3 + 15 PbO + (55−x) SiO_2: x Sm_2O_3 (LPOSm) and 25 Li_2O + 5GdF_3 + 15 PbO + (55−x) SiO_2: x Sm_2O_3 (LPFSm) where x = 0.00, 0.01, 0.05, 1.00, and 1.50 mol %.	Khan et al. (2020)[50]
Orange emitting material	Sm^{3+}-doped barium sodium borate glasses	10 BaO + 25 Na_2O + (65−x) B_2O_3 + x Sm_2O_3 (where x = 0.00, 0.10, 0.50, 1.00, 1.50, and 2.00 mol %).	Luewarasirikul et al. (2017)[2]
Yellow laser, neutral white, reddish-orange light sources phosphor	Dy^{3+}, Eu^{3+}, and Dy^{3+}/Eu^{3+}-doped sodium−zinc phosphate glasses	98 $NaZn(PO_3)_3$ + 2 Dy_2O_3, 98 $NaZn(PO_3)_3$ + 2 Eu_2O_3 and 96 $NaZn(PO_3)_3$ + 2 Dy_2O_3 + 2 Eu_2O_3	Caldiño et al. (2018)[34]
Reddish orange light emitting material	Eu^{3+}-doped P_2O_5−SrO−BaO−ZnO glasses	N/A	Han et al. (2020)[69]
Green light application	Ho^{3+}-doped bismuth-germanate glasses	(40−x) GeO_2 + 20 Bi_2O_3 + 20 Na_2O + 10 Gd_2O_3 + 10 BaO + x Ho_2O_3 (x = 0.1, 0.5, 1.0, 1.5, and 2.5 mol %)	Prakash et al. (2019)[51]
Yellow laser application	Dy^{3+}-doped K−Sr−Al phosphate glasses	(59-x/2) P_2O_5 + 17 K_2O + (15−x/2) SrO + 9 Al_2O_3 + x Dy_2O_3 (where x = 0.1, 0.5, 1.0, 2.0, and 4.0 mol %)	Linganna et al. (2014)[84]
Green fiber laser emission	Tb^{3+}/Yb^{3+} codoped tellurite glasses	80 TeO_2 + 10 ZnO + 10 Na_2O (mol %) + 1 wt % Tb_2O_3 + x Yb_2O_3 (x = 1, 2, 3, and 4 wt %)	Zhou et al. (2010)[85]

[a]N/A indicates not applicable.

phosphate glasses,[92] and alkaline-earth zinc-phosphate glasses,[47] whereas the Eu^{2+} ion has been doped with $CaAlSiN_3$ red-emitting nitride phosphors.[54] The Tb^{3+} ion has been doped with a ZnO nanophosphor (Figure 7 shows some characteristics of this combination), which is also promising.[93] All these materials showed noteworthy characteristics favorable for a solid-state light emission. Some recent works are listed in Table 3, which gives an idea of using RE ions in solid-state lighting.

4.3.2. Prospects in Solid-State Optical Devices. The previous section briefly discussed some applications of RE ions in solid-state lighting technologies, and a few of them showed huge prospects. For instance, the Sm_2O_3-doped tellurium oxide-based glasses have shown an increased rigidity and transition temperature with the increasing amount of Sm_2O_3. Nine absorption bands were observed following the excitation to various excited states. The Judd-Ofelt parameters and spectroscopic quality factors further validate the higher stability of the material to use as solid-state lasers, optical storage, color displays, and subsea communications.[5] A study suggests that 1 mol % Eu^{3+}-doped lead-containing borate glasses are superior to bismuth-containing borate glasses in terms of lifetime and quantum efficiency, thus making them suitable for red light solid-state lighting applications excited by a blue light.[91]

For a practical manufacturing of solid-state optical materials, cost-effectiveness is an important issue. To mitigate this problem, one study used the carbothermal reduction and nitridation (CTRN) method. This method used cost-effective and air-stable oxide raw materials entirely. Using this method, they prepared $CaAlSiN_3$:Eu^{2+} nitride phosphors, which showed bright red emissions, indicating the prospects of this material.[54] Another study reported that the 0.5 mol % Dy_2O_3-doped yttrium calcium silicoborate glasses had shown the maximum intensity for blue, green, and reddish-orange emission excited at 351 nm. So, this combination of glass material can become a budding candidate for solid-state lighting applications.[53] Further, 30 000 ppm Tm^{3+} and Dy^{3+} codoped tellurite glasses have a bright and shiny white light emission due to the maximum effective bandwidth (i.e., $\Delta\lambda$ = 127 nm), emission cross section (i.e., σ_{em} = 8.86 × 10^{-21} cm^2), and internal gain coefficient (i.e., $\sigma_R(\lambda)$ = 6.3 dB/cm). These results are convincing for futuristic applications of this material as a solid-state laser.[94]

4.4. Laser. *4.4.1. Laser Applications.* A laser is one of the most widely used techniques, and it has applications in numerous branches of materials science. Generally, materials with a low phonon energy and nonlinear refractive index are chosen as hosting materials for lasers. When the RE ions are doped with appropriate host materials, they absorb photons, and successful emission occurs at a precise energy range. The fruitful combination of the host material and RE ions may reduce the nonradiative loss by a multiphonon relaxation. As a result, ample studies were found in a search for the proper combination of these two.[6,95]

Among the various REO ions, Er^{3+} is the most attractive due to its upconversion luminescence without using a sensitizer. When excited by infrared radiation, it can successfully emit distinctive colors such as blue, green, and red.[57] Additionally, the Er_2O_3 is now steadily substituting the conventional regenerative repeaters in telecommunication applications (i.e., fiber optics) due to their characteristic of seizing the loss link by amplification.[6] So, they have been extensively studied with numerous host materials to modify the spectroscopic properties. Some recent works were found where the Er_2O_3 was doped with fluoroquaternary glasses,[96] antimony oxide-based glasses,[56] tellurite based glasses,[95,97] biosilicate borotellurite glasses,[6] yttria-stabilized zirconia (YSZ) single crystals,[57] willemite glass-ceramics,[98] tungstate tellurite glass fibers,[62] etc. In some other works, the Er_2O_3 ion

https://doi.org/10.1021/acsaelm.1c00682
ACS Appl. Electron. Mater. 2021, 3, 3715−3746

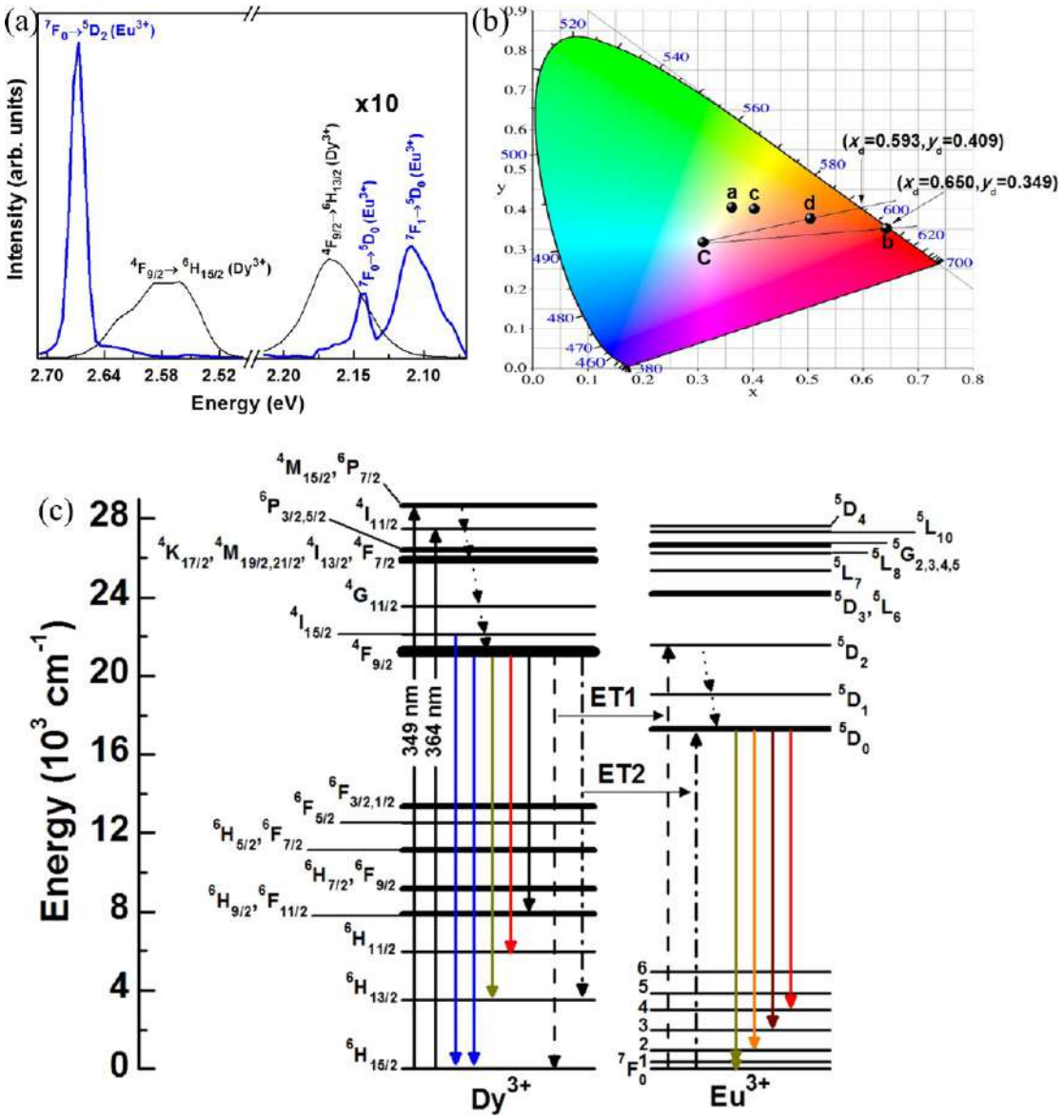

Figure 6. (a) Normalized line-shape functions plot in the spectral overlap areas between Dy^{3+} emission bands (thin black line) and Eu^{3+} absorption bands (thick blue line), (b) chromaticity coordinates in CIE 1931 chromaticity diagram, and (c) energy band diagram of Dy^{3+} and Eu^{3+} showing the probable transitions between a Dy^{3+} and Eu^{3+} energy transfer. Reproduced with permission from ref 34. Copyright 2018 Elsevier.

was codoped with another REO ion Yb_2O_3 in some host glass matrices. For example, $Ho^{3+}/Er^{3+}/Yb^{3+}$ was codoped in bismuth-germanate oxide glasses,[58] $Er^{3+}/Yb^{3+}/Cr^{3+}$ was codoped in phosphate-based glasses,[59] $Nd^{3+}/Er^{3+}/Yb^{3+}/$ was codoped in fluorophosphate glasses,[99] and Er^{3+}/Yb^{3+} was codoped in NbO_3 ceramics.[100]

The other most-studied REO ion for lasing material is Yb_2O_3. The main benefit of the Yb^{3+} ion is that it has a broad energy gap (i.e., ~1.27 eV) between the ground state ($^2F_{7/2}$) and excited state ($^2F_{5/2}$). Furthermore, the codoping of a Yb^{3+} ion with a Nd^{3+} ion can create multiple excitation states that will lead to the enhanced efficiency of the laser medium. So, it can avert cross-relaxation and undesirable effects like excited-state absorption processes. Moreover, it has a long lifetime compared to other RE ions.[101] These features are helpful for mitigating nonradiative de-excitations (quenching to −OH groups). A few studies (codoped with Er^{3+}) were given in the previous paragraph. Now Yb^{3+} has also been singly doped in several host glass materials like yttrium aluminum garnet (YAG) ceramics,[63] tellurite glasses,[102] double-clad fiber,[103] phosphate glasses,[101,104] fluorophosphate glasses,[105] etc. Furthermore, Yb^{3+} has been codoped with Ce^{3+} in aluminosilicate fiber[106] and Ce^{3+}/P in fluoroaluminosilicate fiber.[107]

In other studies, Dy_2O_3 was doped with Li−Y borate glasses,[108] tellurium-borate glass phosphors,[109] Sb−Mg−Sr oxyfluoroborate glasses,[110] etc. Some of these glass matrices showed superior spectroscopic features, which will be discussed in the next section. Table 4 summarizes the recent works using REO ions as laser materials.

4.4.2. Prospects in Laser Applications. A number of host glass matrix and REO ion combinations showed a bright prospect for use as laser materials. For example, the Er^{3+}-doped YSZ single crystal demonstrated an effective upconversion luminescence, slenderer energy distribution, and other advantageous parameters for quality laser production.[57] One study used rice husk to extract biosilicate, and they have

https://doi.org/10.1021/acsaelm.1c00682
ACS Appl. Electron. Mater. 2021, 3, 3715−3746

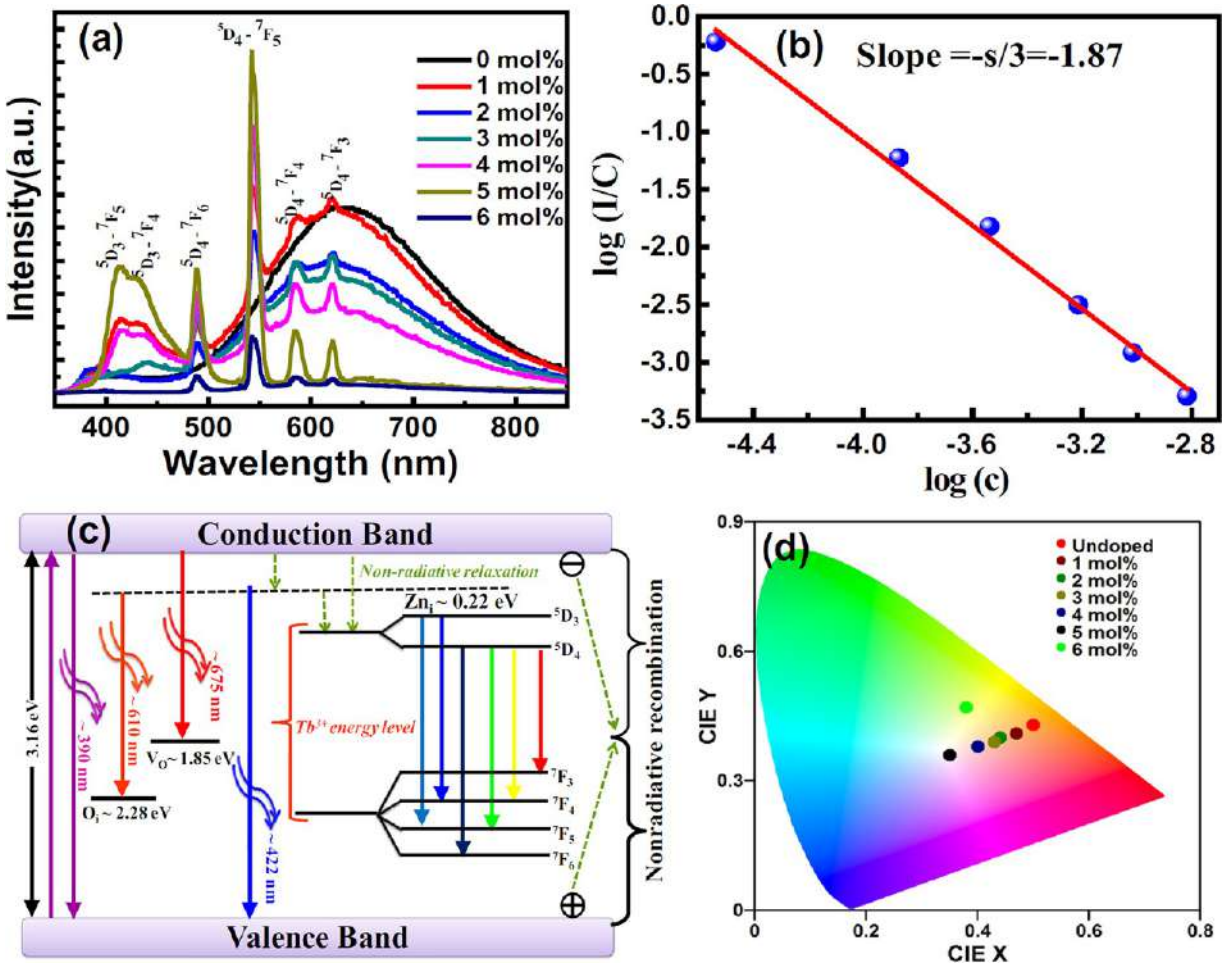

Figure 7. (a) Photoluminescence emission intensity of the ZnO:Tb^{3+} nanophosphor by varying the Tb^{3+} concentration, (b) plot of log(I/C) vs log(C), (c) schematic energy-level diagram for ZnO:Tb^{3+}. (d) The CIE diagram of ZnO:Tb^{3+} nanophosphors by varying the doping concentration of Tb. Reproduced from ref 93. Copyright 2014 Elsevier.

prepared Er^{3+}-doped biosilicate borotellurite (BSBT) glasses. In general, natural silicate is costly. As such 98% of the silicate from rice husk was extracted for a cost reduction. This glass also showed noteworthy spectroscopic properties with strong green and weak red emission (at 380 nm), which are sound for photonics and laser applications.[6] Moreover, the Er^{3+}-doped ternary fluoroglasses (TeO_2−ZnO-NaF-MoO_2) showed remarkable spectroscopic quality factors, refractive index, Urbach energy, and radiative lifetime, which are favorable for using this combination as a laser material.[96] The improved refractive indices and small phonon energies with a high emission cross section (i.e., $^4I_{13/2} \rightarrow {}^4I_{15/2}$ transition of Er^{3+}) recommend the admirable spectroscopic features of Er^{3+}-doped antimony oxide-based glasses, proving their suitability for future applications.[56] When 2 mol % Er^{3+} was doped with the 65TeO_2−15ZnO−10Na_2O−5BaO−3La_2O_3 (TZNBL) glass network, it showed a better thermal steadiness and weak crystallization tendency along with optimum mechanical features.[95] These properties are useful in the fabrication of an amplifier glass. Moreover, a detailed study (both experimental and theoretical examinations for gain-switched laser generation) on the Er^{3+}-doped tungstate-tellurite fiber showed noteworthy results in favor of a practical employment.[62]

Other REO ion Yb^{3+}-doped glass matrices were found promising for future applications. For example, the YAG ceramics doped with Yb^{3+} showed an improved absorption and emission cross section, which are encouraging for an industrial manufacturing of high-power and ultrafast laser materials.[63] The Nd^{3+} and Yb^{3+} codoped phosphate glasses showed an effective energy transfer ($Nd^{3+} \rightarrow Yb^{3+}$), which is in good agreement with the theoretical model. This also shows the prospect of using it as multiple-pump channel lasers.[101] Yb, Ce, and P codoped fluoroaluminosilicate double-clad fiber showed a better photodarkening (PD) suppression, which is admirable for viable elevated power fiber lasers.[107]

The Dy^{3+} ion-doped glass matrices also possess a huge prospect in laser applications as well. One mole percent Dy^{3+}-doped lithium yttrium borate (LiYBDy) glasses showed a greater emission at low temperatures as well as better physical (i.e., refractive index, density, and molar volume) and luminescence (i.e., absorption and emission spectra) properties. The emission intensity varied linearly with temperature and is making this material a suitable candidate for laser medium and other applications.[108] Additionally, multicomponent tellurium borate (MTB) glasses doped with Dy^{3+} were found effective in emitting a bright white light, while the color coordinates and correlated color temperatures (CCTs) had a solid reliance on pumping powers and phosphor size. As a

https://doi.org/10.1021/acsaelm.1c00682
ACS Appl. Electron. Mater. 2021, 3, 3715−3746

Table 3. Solid-State Optical Device Applications

specific application	used REOs	REOs composition	refs
Solid-state laser	Er^{3+}/Nd^{3+} codoped lithium niobate tellurite glasses	$(70-x-y)\ TeO_2 + 15\ Li_2CO_3 + 15\ Nb_2O_5 + x\ Er_2O_3 + y\ Nd_2O_3$ with $x = 0$; 1.0 mol % and $0 \le y \le 1.0$ mol %	Hasim et al. (2016)[55]
Solid-state light technology	Dy^{3+}, Eu^{3+}, and Dy^{3+}/Eu^{3+}-doped sodium−zinc phosphate glasses	$98\ NaZn(PO_3)_3 + 2\ Dy_2O_3$, $98\ NaZn(PO_3)_3 + 2\ Eu_2O_3$ and $96\ NaZn(PO_3)_3 + 2\ Dy_2O_3 + 2\ Eu_2O_3$	Caldiño et al. (2018)[34]
Solid-state lighting	Ho-doped yttrium oxide phosphor	$Y_{2-x}Ho_xO_3$ (x = 0.005, 0.02, 0.04, 0.06, 0.08 and 0.10)	Singh et al. (2020)[89]
Tellurite glass-based optical devices (solid-state laser, optical storage, undersea communication, color display, etc.)	Sm^{3+}-doped tellurium oxide glasses	$75\ TeO_2 + 5\ Li_2O + 10\ ZnO + (10-x)\ Nb_2O_5 + x\ Sm_2O_3$ where (x = 0.0, 0.5, 1.0, 1.5, 2.0, and 2.5 mol %)	Elkhoshkhany et al. (2018)[5]
Solid-state lighting	Sm_2O_3/ZnO nanostructured films	N/A	Matei et al. (2013)[52]
Solid-state white lighting	Dy^{3+}-doped yttrium calcium silicoborate glasses	$25\ Y_2O_3 + 10\ CaO + 10\ SiO_2 + (55-x)\ B_2O_3 + x\ Dy_2O_3$, where x = 0.0, 0.1, 0.2, 0.3, 0.4, and 0.5 mol %	Chanthima et al. (2016)[53]
Solid-state laser	Tm^{3+}/Dy^{3+} codoped tellurite glasses	$90\ TeO_2 + 10\ Nb_2O_5 + 10\ ZnO$ in mol % + x (Tm_2O_3/Dy_2O_3), where x = 10,000, 20 000 and 30 000 ppm	Algarni et al. (2018)[94]
Red light solid-state lighting	Eu^{3+}-doped lead and bismuth containing borate glasses	$10\ La_2O_3 + 50$ HMO + $(40-x)\ B_2O_3 + x\ Eu_2O_3$ (with x = 0, 0.5, 1, and 2 mol % and HMO = PbO, Bi_2O_3)	Ramesh et al. (2020)[91]
Solid-state lighting	Eu^{2+}-doped $CaAlSiN_3$ nitride phosphors	$Ca_{0.9}AlSiN_3$: $_{0.1}Eu^{2+}$ nitride phosphors with variable C/O molar ratios (1.15, 1.19, 1.23 and 1.27)	Yang et al. (2016)[54]
Solid-state laser (reddish orange regions)	Eu^{3+}-doped lithium aluminum phosphate glasses	$15\ Li_2O + 20\ Al_2O_3 + (65-x)\ P_2O_5 + x\ Eu_2O_3$ (where x = 0.0, 0.1 0.5, 1.0, and 2.0 mol %)	Chanthima et al. (2018)[92]
Red photoluminescent for solid-state light	Eu^{3+}-doped alkaline earth zinc-phosphate glasses	$(40-x)\ ZnO + 35\ P_2O_5 + 20\ RO + 5\ TiO_2 + x\ Eu_2O_3$ (where x = 1 mol % and R = Mg, Ca, Sr, and Ba)	Jha et al. (2016)[47]
Solid-state laser, telecommunication, and radiation shielding	Sm_2O_3 codoped lithium magnesium borate erbium oxide glasses	$30\ Li_2O + (59.5-x)\ B_2O_3 + 10\ MgO + 0.5\ Er_2O_3 + x\ Sm_2O_3$ where x = 0, 0.3, 0.5, 0.7, and 1.0 mol %	Mhareb (2020)[90]

[a]N/A indicates not applicable.

result, a laser-driven white light medium with an elevated power density can be manufactured using this material.[109] Moreover, 0.5 mol % Dy^{3+}-doped antimony−magnesium-strontium-oxyfluoroborate (BMFSrSbD) glasses demonstrated promising results for white light laser applications.[110]

Among other REO-doped glasses, 0.75 mol % Sm^{3+}-doped $20ZnO-10Li_2O-10Na_2O-60P_2O_5$ glasses demonstrated elevated emission cross-section and branching ratio parameters, which showed better prospects for fiber optic amplifier and visible laser applications.[112] The Nd^{3+}-doped yttrium oxide showed a large branching ratio and radiative decay rate, which are also promising for laser applications.[114] Figure 8 demonstrates the visualized electron localization function along with the crystal structure for yttrium oxide and Nd^{3+}-doped yttrium oxide.[114]

4.5. UV Optics. *4.5.1. UV Optical Applications.* The REOs have been applied in lower-scale UV-related applications (Table 5). For instance, Gd_2O_3 was successfully employed in multilayer coatings for varying UV wavelengths (i.e., 0.2−0.35 μm).[115] The electron beam property of Gd^{3+} films showed a substrate durability at low temperatures with a high band-energy gap (i.e., 6.36 eV). The optical absorption-emission properties of Dy^{3+} ions doped with oxyfluorotellurite glass were explored at the visible-infrared wavelength region.[14] The integration of Dy^{3+} ions considerably improved the thermal tolerance of the glass composite. The optical feature of Dy_2O_3 doped with borosilicate glasses was also tested via the transmission of UV lights.[116] The addition of Dy_2O_3 reduced both the UV transmittance and band-energy gaps while enhancing the refractive index. In addition, the Eu^{3+}-doped Lu_2WMoO_9 phosphors demonstrated enhanced excitation and photoluminescence spectra with UV chips (i.e., 365 nm) (Figure 9).[7,8]

4.5.2. Prospects in UV Optical Applications. The durability and high energy gaps of Gd^{3+} film depositions were evident at low substrate temperatures.[115] The optothermal stabilities make these composites attractive in constructing multicoatings on materials, where maintaining the ambient room temperature is warranted.

The phosphor (lutetium molybdenum oxides)-UV light (365 nm) blend provided a red spectrum to the LED under the influence of forwarding bias current.[7,8] This attribute can potentially be applied in phosphors-converted LEDs near the UV region.

4.6. Nonlinear Optics. *4.6.1. Applications in Nonlinear Optics.* The photomodulated nonlinear optical features of various REO-doped materials were reported in a few studies. The Gd/Dy_2O_3 codoped with $(K_{0.5}Na_{0.5})NbO_3$ (KNN) demonstrated nonlinear attributes in pulsed laser depositions.[15] The enhanced tetragonal nanocrystalline structures of the doped compound and the larger ratio of atoms/particles had caused the third-order nonlinear optical response of the synthesized thin films. The Dy_2O_3 had also been applied in borosulfophosphate glasses, where the Dy^{3+}-doped glass composites demonstrated the nonlinear optophysical properties.[64] The optical and physical parameters of the characterized materials nonlinearly varied with the Dy_2O_3 concentrations. The metallization characteristics of Sm^{3+}-biosilica borotellurite glass also demonstrated the nonlinear properties.[9] Similarly, two novel RE^{3+} (i.e., Gd^{3+}/Y^{3+})-doped beryllium borates exhibited nonlinear optical properties excited at less than 200 nm, as demonstrated in Figure 10.[117]

The properties of nonlinear refractivity and high thermal stability (i.e., a strong bond of Eu−O) were evident in the application of Eu^{3+} in ZnO boro-tellurite glass composites.[65] The addition of Eu_2O_3 in molar concentrations decreased the nonlinear susceptibility because of the enhanced electron excitations. In a similar study, SiO_2 and Dy_2O_3 were used as refractory materials to prepare gold−bismuth borosilicate glass nanocomposites.[118] The addition of Dy^{3+} enhanced the nonlinearity of glass-gold compounds. Some of these nonlinear applications were summarized in Table 6.

https://doi.org/10.1021/acsaelm.1c00682
ACS Appl. Electron. Mater. 2021, 3, 3715−3746

Table 4. Laser Applications

specific application	used REOs	REOs composition	references
Laser material	Er_2O_3-doped fluoroquaternary glasses	70 TeO_2 + 10 ZnO + 10 NaF + (10−x) MoO_2 + x Er_2O_3 where x = 0.5, 1.0, 1.5, 2.5, 3.5, 4.0, and 5.0 mol %	AbouDeif et al. (2018)[96]
Infrared laser	Er_2O_3-doped antimony oxide based glasses	88 Sb_2O_3 + 10 Na_2O + 2 Bi_2O_3 and 60 Sb_2O_3 + 20 WO_3 + 19 Na_2O + 1 Bi_2O_3 (both doped with 0.25 mol % Er_2O_3)	Ouannes et al. (2017)[56]
Laser application and amplification	Er^{3+}-doped tellurite based glasses	65 TeO_2 + 15 ZnO + 10 Na_2O + 5 BaO + 3 La_2O_3 + Er_2O_3 (2 mol %)	Benmadani et al. (2013)[95]
Photonics and laser	Er_2O_3-doped biosilicate borotellurite glasses	$\{[(TeO_2)_{0.8}\ (B_2O_3)_{0.2}]_{0.8}\ (SiO_2)_{0.2}\}_{1-y}\ (Er_2O_3)_y$, y = 0.01, 0.02, 0.03, 0.04, and 0.05 mol %	Hamza et al. (2019)[6]
Laser	Er_2O_3-doped yttria-stabilized zirconia single crystals	N/A	Wang et al. (2020)[57]
Midinfrared fiber amplifier and laser	$Ho^{3+}/Er^{3+}/Yb^{3+}$ codoped bismuth-germanate oxide glasses	(59.75−x−y) (Bi_2O_3 + GeO_2) + 40 (Na_2O + Ga_2O_3) + x Ho_2O_3 + y Er_2O_3 + 0.25 Yb_2O_3 where x = 0, 0.1 mol % and y = 0.0, 0.25, 0.4, 0.55, 0.7 mol %	Ragin et al. (2018)[58]
Eye safe laser system (rods for lamp pumped lasers)	$Er^{3+}/Yb^{3+}/Cr^{3+}$ codoped phosphate glasses	Different wt.% and mol % of P_2O_5 + Al_2O_3 + BaO + PbO + K_2O + Yb_2O_3 + Er_2O_3 + Cr_2O_3	Stepien et al. (2001)[59]
Laser induced optical emission	Eu^{3+} Sites in polycrystalline powders of monoclinic and body-centered cubic Eu_2O_3	N/A	Sheng et al. (1988)[111]
Red, green lasers and display device application	Eu^{3+}/Tb^{3+}-doped alkali oxide modified boro phosphate glasses	69.5 B_2O_3 + 10 P_2O_5 + 10 CaF_2 + 5 ZnO + R + 0.5 (Eu_2O_3/Tb_4O_7) [where R = 5 ($Li_2O/Na_2O/K_2O$)]	Moulika et al. (2018)[60]
Green laser application and optoelectronic devices	Er^{3+}-doped willemite glass-ceramics	$[(ZnO)_{0.5}(SLS)_{0.5}]_{1-x}\ (Er_2O_3)_x$ where x = 1 wt.%	Effendy et al. (2016)[98]
Photonic materials in the display, white LED, laser device, scintillation detector, temperature sensor	Dy^{3+}-doped lithium yttrium borate glasses	60 Li_2O + 10 Y_2O_3 + (30−x) B_2O_3 + x Dy_2O_3, where x = 0.05, 0.1, 0.5, 1.0, and 1.5 mol %	Kaewnuam et al. (2017)[108]
Laser-driven white illumination	Dy^{3+}doped tellurium-borate glass phosphors	[10 Na_2O + 4 K_2O + 10 ZnO + 6 MgO + 13 TeO_2 + 57 B_2O_3] (mol %) + x Dy_2O_3 where x = 0.1, 0.5, 1.0, 2.0, and 3.0 wt.%	Li et al. (2019)[109]
Visible & NIR fiber laser application	Er^{3+}, Dy^{3+}-doped and Er^{3+}/Dy^{3+} codoped multicomponent borotellurite glasses	(50−x−y) B_2O_3 + 10 TeO_2 + 10 PbO + 10 ZnO + 10 Li_2O + 10 Na_2O + (x) Er_2O_3 + (y) 0.5 Dy_2O_3 ((x = 0.5, 1.0; y = 0); (x = 0; y = 0.5, 1.0); and (x = 0.5; y = 0.5, 1.0; x = 1.0; y = 0.5, 1.0)) (mol %)	Lakshminarayana et al. (2019)[61]
Display device and laser	Dy^{3+}-doped antimony−magnesium-strontium-oxyfluoroborate glasses	(70−x) B_2O_3 + 10 MgF_2 + 15 SrO + 5 Sb_2O_3 + x Dy_2O_3, where x = 0.1, 0.5, 1.0, 1.5, 2.0, and 2.5 mol %	Farooq et al. (2018)[110]
Visible laser application	Sm^{3+}-doped zinc−lithium-sodium-phosphate glasses	20 ZnO + 10 Li_2O + 10 Na_2O + 60 P_2O_5 + Sm_2O_3 (0 to 1 mol %)	Ramteke et al. (2017)[112]
Faraday devices for Tm^{3+} and Ho^{3+} lasers	Dy_2O_3 based ceramics	$(Dy_xY_{0.95-x}La_{0.05})_2O_3$, where x = 0.7, 0.85, and 0.9	Snetkov et al. (2018)[113]
Fiber drawing, laser, nonlinear optical application	Er^{3+}-doped quinary tellurite glass system	5 TeO_2 + 5 Li_2O + 10 ZnO + (10−x) Nb_2O_5 + x Er_2O_3 where (x = 0.0, 0.5, 1.0, 1.5, 2.0, and 2.8 mol %)	Elkhoshkhany et al. (2018)[97]
Gain-switched laser generation	Er^{3+}-doped tungstate tellurite glass fibers	72 TeO_2 + 24 WO_3 + 4 La_2O_3 and 71.2 TeO_2 + 23.7 WO_3 + (4 − x) La_2O_3 + 1.1 Bi_2O_3 + xEr_2O_3 where x = 0.4, 4 mol %	Anashkina et al. (2017)[62]
Low dispersion stable laser host	Nd_2O_3, Er_2O_3, and Yb_2O_3-doped fluorophosphate glasses	0.4 MgF_2 + 0.4 BaF_2 + 0.1 $Ba(PO_3)_2$ + 0.1 $Al(PO_3)_3$ + $Nd_2O_3/Er_2O_3/Yb_2O_3$	Choi et al. (2005)[99]
High power and ultrafast laser application	Yb^{3+}-doped yttrium aluminum garnet (YAG) ceramics	Y_2O_3 + Al_2O_3 + Yb_2O_3 + 5 at.% Yb_2O_3	Luo et al. (2012)[63]
Ultrashort pulse laser	Yb^{3+}-doped tellurite glass	80 TeO_2 + 10 Al_2O_3 + 10 Cs_2O + x Yb_2O_3 (x = 0−1.6 mol %)	Li-quan et al. (2013)[102]
High power laser	Yb_2O_3/Ce_2O_3 codoped Aluminosilicate fiber	Yb_2O_3 (0.16 mol %) + Ce_2O_3 (0.08 mol %) + Al_2O_3 (0.7 mol %) + SiF_4 (0.35 mol %)	Li et al. (2018)[106]
High power laser fiber	Yb_2O_3-doped double-clad fiber	SiO_2 + Yb_2O_3 + Al_2O_3 + P_2O_5	Wang et al. (2018)[103]
Fiber laser	Yb_2O_3-doped phosphate glass	P_2O_5 + Al_2O_3 + BaO + ZnO + MgO + Na_2O + Yb_2O_3 (6 mol %)	Stepień et al. (2014)[104]

https://doi.org/10.1021/acsaelm.1c00682
ACS Appl. Electron. Mater. 2021, 3, 3715−3746

Table 4. continued

specific application	used REOs	REOs composition	references
High power fiber laser	Yb/Ce/P codoped fluoroaluminosilicate fiber	0.21 mol % Yb_2O_3 + 0.05 mol % Ce_2O_3 + 0.83 mol % P_2O_5 + 0.37 mol % SiF_4 + 1.61 mol % Al_2O_3	Liu et al. (2020)[107]
Multiple pump channel laser	Yb_2O_3-doped phosphate glasses	(59−x/2−y/2) P_2O_5 + 17 K_2O + (15−x/2−y/2) BaO + 9 Al_2O_3 + x Nd_2O_3 + y Yb_2O_3 (x = 1 and y ranges from 0 to 4 mol %)	Rivera-López et al. (2011)[101]
High-power and ultrashort pulse laser	Yb^{3+}-doped fluorophosphate glasses	(54−x/2) P_2O_5 + 14 K_2O + 10 KF + (13−x/2) BaO + 9 Al_2O_3 + x Yb_2O_3, where x = 0.1, 1.0, 2.0, and 4.0 mol %	Krishnaiah et al. (2013)[105]
Multifunctional device (using up-conversion luminescence)	Er^{3+}/Yb^{3+} codoped (K,Na)NbO_3 ceramics	$(K_{0.49}Na_{0.51})NbO_3$ + 0.5% Er_2O_3/x Yb_2O_3 (x = 0%, 0.25%, 0.5%, 0.75% and 1%.	Wang et al. (2016)[100]

[a]N/A indicates not applicable.

4.6.2. Prospects in Nonlinear Optics. The higher order of optical nonlinearity is a key property in optoelectronics. The third-order optical nonlinearity of a KNN crystal composite with a large band energy and biggish optical transmittance and dielectric constant, therefore, makes it well-suited for nonlinear photonics.[15] The Dy_2O_3 concentrations significantly ameliorated the density of the glass structure.[64] The high band energy gap (2.120−3.376 eV) and nonlinear refractive indices also indicate Dy_2O_3 as a suitable substitute for P_2O_5 in nonlinear optoelectronic applications. The Dy_2O_3 also prevented the surface coagulation of the gold−bismuth borosilicate glass composites while preserving structural integrity at high temperatures.[118] It can therefore show a prospect as an excellent stabilizer in nonlinear optoelectronic devices as well.

An augmented number of nonbinding oxygens with the addition of Eu oxides suppressed the band-energy gap of Eu_2O_3-glass composites.[65] The high thermal stability and nonlinear refractivity also demonstrate the promising prospect of Eu_2O_3 in fiber optics and laser applications. The demonstrated properties of REO composites are, therefore, expected to have a promising potential to increase the nonlinear characterizations in optical device applications.

4.7. NIR Optics. *4.7.1. NIR Optical Applications.* The REOs have shown effective photoluminescence properties at the NIR range in a few studies (Table 7). For example, the sensitizer feature of Yb_2O_3 was exploited in Bi-doped borophosphate glasses at the NIR (i.e., 976 nm) excitation.[10] The strong absorption capacity of Yb^{3+} greatly enhanced the photoillumination of the glass composites.

The optothermal properties of phosphate glasses were sensitive at the NIR (i.e., 1510−1550 nm) emissions with the addition of Er_2O_3.[66] The prominent gain coefficient and solubility of Er^{3+}-glass composites led to the enhanced photoluminescence in the NIR region. Further, the Tb^{3+}-doped Dy_2O_3 nanostructures were employed in multimodal contrast agents in magnetic and optical imagery.[119]

4.7.2. Prospects in NIR Optical Applications. The observed properties of several REOs discussed in the previous sections have a high potential for laser applications. For instance, the properties of a stronger (i.e., ∼37 times) photoluminescence intensity at the NIR and longer lifetime (i.e., 8 times) due to the addition of Yb_2O_3 in Bi-doped borophosphate glasses can be capitalized in tunable laser applications.[10]

The single-phase bimodal contrasting effect of Tb^{3+}-Dy_2O_3 nanocrystals[119] can be potentially applied in high-field (i.e., 7.0 T) magnetic and fluorescent nanoprobes. The Er^{3+}-phosphate glasses achieved a high luminescence at higher wavelengths (i.e., 1510−1550 nm).[66] These Er^{3+}-doped glasses, therefore, can be used in laser applications and in the generation of green lights as well.

4.8. Optoelectronics. *4.8.1. Optoelectronics Applications.* The REOs were effective in a few optoelectronic studies (Table 8). The Eu^{3+} was used in a boro-tellurite glass synthesis for a photoluminescence demonstration. The noncrystalline surface morphology led to the emission of five distinct bands at the 394 nm wavelength, as depicted in Figure 11.[11] In a different study, the Eu^{3+} ion was used as a sputtering material on soda-lime glass substrates alongside two codopants (i.e., Lu^{3+} and Ga^{3+}).[120] The uniform nanostructures and lucid surface caused the high phototransmission (i.e., 83%) within the visible range and large band energy gap (i.e., 3.96 eV). Moreover, the Yb^{3+}-La_2MoWO_9 at room temperature demonstrated an intense luminescence by forming a novel cubic

https://doi.org/10.1021/acsaelm.1c00682
ACS Appl. Electron. Mater. 2021, 3, 3715−3746

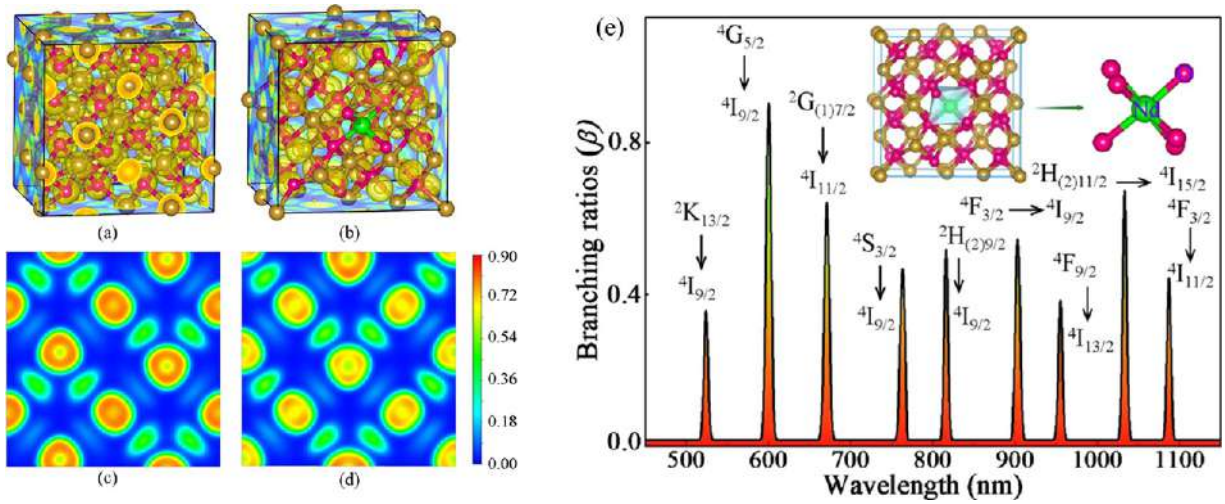

Figure 8. Visualized electron localization function (ELF) of (a) Y_2O_3 and (b) Nd:Y_2O_3 crystals and the ELF of the (010) plane for (c) Y_2O_3, (d) Nd:Y_2O_3, and (e) calculated branching ratios of the promising ED transitions for Nd^{3+} in Y_2O_3. Reproduced from ref 114. Copyright 2020 American Chemical Society.

Table 5. UV Optical Applications

specific applications	used REOs	REOs composition	refs
Ultraviolet Laser	Electron beam deposited Gd_2O_3 films	N/A	Sahoo et al. (2003)[115]
UV transmission and the optical energy gap, increase the refractive index	Dy^{3+}-lead alkali borosilicate glasses	60 PbO + (40−x) SiO_2 + x (0.1 Li_2O + 0.86 B_2O_3 + 0.04 Dy_2O_3) (where $0 \leq x \leq 30\%$)	Shaaban et al. (2019)[116]
Near UV LED	Eu^{3+}-lutetium molybdenum oxides	N/A	Cao et al. (2019)[7]
UV LED	Eu^{3+}-lutetium tungsten molybdenum oxides	$Lu_2W_xMo_yO_9$ ($x + y = 2$)	Cao et al. (2020)[8]
UV-excited visible phosphors	Dy^{3+}-oxyfluorotellurite glasses	(65−x) TeO_2 + 20ZnF_2 + 12Pb_2O_5 + 3Nb_2O_5 + xDy_2O_3 (x = 0.5, 2, 5 mol %)	Klimesz et al. (2015)[14]

[a]N/A indicates not applicable.

structure. The self-quenching and the creation of vacancies into the structures led to this enhanced luminescence as demonstrated in Figure 12.[121]

The Er^{3+} ion was applied as a dopant in photoactive glass-ceramics.[16] The higher chemical attraction between Er^{3+} and a glass structure and an improved thermal stability led to multiphase crystallizations. In addition, the incorporation of Er_2O_3 significantly increased the specific surface area (SSA) of Er^{3+}-TiO_2 films.[67] This is attributable to the increased electrolytic concentrations that induced the enhancement of electrostatic repulsion and limited aggregation.

4.8.2. Prospects in Optoelectronics Applications. The nanosized (i.e., ∼14 nm) crystalline morphology and high SSA (i.e., 152−174 m^2/s) of the highly stable Er^{3+}-TiO_2 films[67] showed the potential for optoelectronic applications, that is, gas sensing. The addition of Er^{3+} improved the crystal structure (i.e., hexagonal) of Er^{3+}-ZnO.[68] The increased size and lattice strains of the synthesized nanorods highlight the new functional trait of Er^{3+}. The enhanced photoluminescence emissions (i.e., 3 and 8 times, respectively) from $^4S_{3/2}$ and $^4F^{9/2}$ states create an opportunity for constructing novel optoelectronic materials using Er^{3+} as an effective dopant as well. The multiphase crystallizations of Er^{3+}-oxyfluoride glass composites demonstrated the larger chemical affinity of Er^{3+} to the silicate-glass network compared to La^{3+}.[16]

The noncrystalline structure of Eu^{3+}-boro-tellurite glasses and enhanced photoluminescence spectra of red emission with an increasing Eu^{3+} [11] revealed the potential use of Eu^{3+} in making photoluminescence optical devices. The high optical transmission and light absorption capacity of Eu^{3+} soda lime glass compounds[120] will be beneficial for devices at a high operating temperature and enhanced speed optoelectronic devices (i.e., radar and LED).

4.9. Optical Fiber. *4.9.1. Optical Fiber Applications.* REOs were also used in different glass networks for their opto-modification properties (Table 9). Yb_2O_3 was applied in fiber-laser operations where silica glasses (SiO_2−Al_2O_3−La_2O_3) (SAL) worked as core materials.[17] The Yb^{3+}-SAL glass composite also exerted a higher nonlinearity and refractive index (i.e., 1.5−1.7) compared to SiO_2. The Yb_2O_3 was utilized as a modifier in investigating the thermal and mechanical properties of alkali-free aluminoborosilicate glass composites.[18] The addition of Yb^{3+} significantly attenuated the dielectric constant (from 4.96 to 4.52) and thermal expansion coefficient. The effective penetration of Yb^{3+}/Ho^{3+} ions into the $Bi_4Ti_3O_{12}$ lattice further demonstrated enhanced optical properties with an extraordinary repeatability at higher temperatures (Figure 13 and Figure 14).[122] Further, Er^{3+} was used for a nonlinear opto-fiber enhancement in rice husk silicate-borotellurite nanocomposites.[19] The higher molecular weight of Er^{3+} caused the increased density (i.e., 4.1900−4.6003 g cm^{-3}) of the glass composite.

4.9.2. Prospects in Optical Fiber Applications. An improved doping level compared to that of La^{3+} and the reduced photodarkening effect of Yb^{3+}-SAL glasses make it a potential alternative to commercially produced pure silicate

https://doi.org/10.1021/acsaelm.1c00682
ACS Appl. Electron. Mater. 2021, 3, 3715−3746

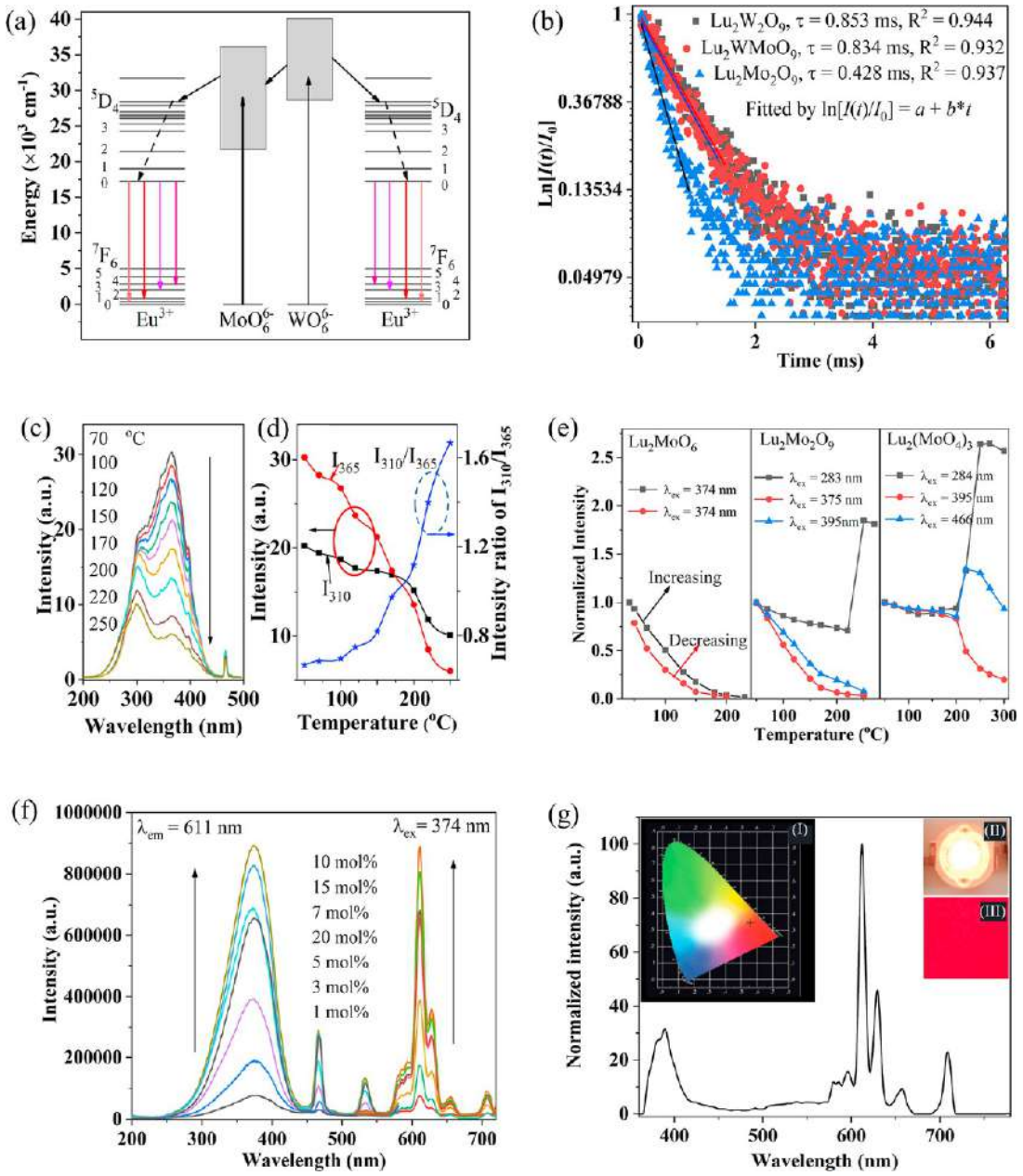

Figure 9. (a) Energy level and probable energy process diagram of MoO_6^{6-}, WO_6^{6-}, and Eu^{3+}, (b) photoluminescence decay plots of Eu^{3+}-doped $Lu_2W_2O_9$, Lu_2WMoO_9, and $Lu_2Mo_2O_9$, (c) temperature-reliant photoluminescence excitation spectra (i.e., 613 nm) of Eu^{3+}-doped $Lu_2W_{1.4}Mo_{0.6}O_9$, and (d) photoluminescence excitation intensities and the intensities vs temperature ratio of Lu_2WMoO_9. Reproduced with permission from ref 8. Copyright 2019 Elsevier. (e) Temperature-dependent emission intensity of Eu^{3+} as a function of wavelength, (f) wavelength-dependent emission intensity of Eu^{3+}-doped $Lu_2(MoO_4)_3$ as a function of temperature, and (g) normalized photoluminescence of LED lamps for 50 mA. (insets) (I) LED lamp, (II) chromaticity diagram, and (III) phosphor excited at 365 nm. Reproduced with permission from ref 7. Copyright 2019 Elsevier.

glasses (Suprasil F300).[17] The increased transition temperature of glass (i.e., reduced viscosity) and softening points due to the addition of Yb^{3+} [18] also suggest potential applications in an elevated temperature glass fiber melting and drawing process.

The infrared light of higher wavelength (i.e., 1550 nm) emission invokes the notion that the Er^{3+}-glass materials[12] can be a pronounced optical waveguide for numerous optical-fiber applications. The high refractive index (i.e., 2.6050−2.6794) and metallization metric (i.e., 0.3268−0.3414) of Er^{3+}-borotellurite nanocomposites[19] suggest that the Er^{3+} has high potentials in optical-fiber amplifications.

4.10. Display and Luminescence. *4.10.1. Applications as Display and Luminescence.* REOs recently achieved considerable attention in various photoluminescence display studies (Table 10). The enhanced photoluminescence and quenching impact of Er^{3+} were utilized in borate glasses.[70] The luminescence amplification was observed at 980 nm because of the quenching effect of Er^{3+} concentrations. Moreover, the Er^{3+} was used as a multifunctional dopant in both $(Li,K,Na)NbO_3$ (Li-KNN)[3] and $(K,Na)NbO_3$[123] ceramics. The addition of 0.5% Er_2O_3 significantly improved the ferro- and piezoelectric properties (i.e., due to the doping impact of the donor) of the ceramic synthesis and resulted in an intense photolumines-

https://doi.org/10.1021/acsaelm.1c00682
ACS Appl. Electron. Mater. 2021, 3, 3715−3746

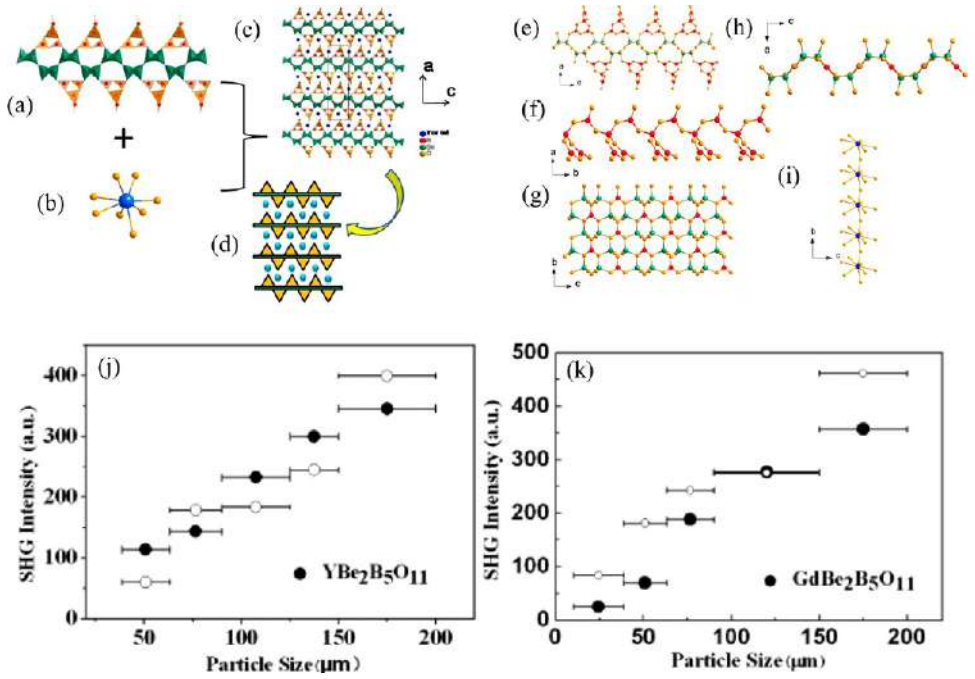

Figure 10. (a) Platelike (i.e., polyhedral) superlayer structures of RE^{3+}-$Be_2B_5O_{11}$ (RE^{3+} = Y or Gd), (b–d) neighboring layer connections through RE^{3+} (i.e., Y or Gd) in coordination with O atom, (e–i) superlayer connections and projections of groups in $YBe_2B_5O_{11}$, (j) second-harmonic generation signal measurements of (j) $YBe_2B_5O_{11}$, and (k) $GdBe_2B_5O_{11}$ as a function of particle size. Reproduced from ref 117. Copyright 2014 American Chemical Society.

Table 6. Applications in Nonlinear Optics

specific applications	used REOs	REOs composition	refs
Nonlinear photonic application	Gd/Dy_2O_3-$(K_{0.5}Na_{0.5})NbO_3$	N/A	Peddigari et al. (2016)[15]
Nonlinear optics	Sm^{3+}-biosilica borotellurite glass	$\{[(TeO_2)_{0.7}\ (B_2O_3)_{0.3}]_{0.8}\ [SiO_2]_{0.2}\}_{1-x}\ \{Sm_2O_3\ NPs\}_x$ where x = 0.01 to 0.05	Aysikin et al. (2020)[9]
Nonlinear optics applications	Dy^{3+}-borosulfophosphate glasses	$15Li_2O + 30B_2O_3 + 15SO_3 + (40-x)P_2O_5 + xDy_2O_3$ ($0 \le x \le$ 1:0 mol %	Bulus et al. (2017)[64]
Nonlinear optical device	Eu^{3+}-doped with ZnO-boro-tellurite glass	$24B_2O_3 + (25-x)ZnO + 51TeO_2$, xEu_2O_3, mol % (where x = 0.0, 0.5, 1, and 3%)	Ali et al. (2017)[65]
Nonlinearity for optics	SiO_2 and Dy_2O_3 doped with gold–bismuth borosilicate glass	$(50-x)Bi_2O_3 + 30H_2BO_3 + 20SiO_2 + xDy_2O_3$ (x = 0.0 and 1.0 mol %)	Singla et al. (2019)[118]

[a]N/A indicates not applicable.

Table 7. NIR Optical Applications

specific applications	used REOs	REOs composition[a]	refs
NIR Luminescence	Bi/Yb^{3+} codoped with boro-phosphate glasses	N/A	Sheng et al. (2014)[10]
NIR Light	Er^{3+} doped with phosphate glasses	$50P_2O_5 + 30ZnO + 20CdO$ + 30000pp Er_2O_3, and $50P_2O_5 + 30ZnO +$ 20SrO + 30,000 ppm Er_2O_3	Afef et al. (2017)[66]
Nanocrystals for MRI and fluorescence	Tb^{3+}-doped Dy_2O_3 nanocrystals	N/A	Das et al. (2011)[119]

[a]N/A indicates not applicable.

cence. Additionally, the codoping of Er^{3+} with Yb_2O_3 greatly improved the upconversion intensity of the $(K,Na)Li_{0.04}NbO_3$ host material (as demonstrated in Figure 15 and Figure 16) when compared with only Er^{3+}-doped samples.[124]

In a different study, the Mg-borate glass properties were found to be sensitive to Dy^{3+} concentrations.[125] The 0.7% Dy^{3+} was hypersensitive at 1260 nm. Besides, the Eu^{3+} was also efficiently employed in quaternary glasses for its photoluminescence and laser features.[4] The multiphonon relaxation phenomenon increased the photoluminescence intensity of the red emission at 614 nm.

4.10.2. Prospects in Display and Luminescence Applications. The unique features of REOs suggest potential applications of these materials in optical displays. For instance, the optical properties of Eu^{3+}-quaternary glasses, that is, intense red emission and longer half-life (i.e., ~2.8 ms),[4] are suitable for glass-laser applications near the visible red spectrum (i.e., 614 nm). The increased photoluminescence peak of Er^{3+}-borate glasses at 980 nm[70] indicates a high prospect in long-range photoamplification applications (i.e., broadband telecommunication). Further, the improved ferro- and piezoelectric properties of Er^{3+}-Li/KNN ceramics[3,123]

https://doi.org/10.1021/acsaelm.1c00682
ACS Appl. Electron. Mater. 2021, 3, 3715–3746

Table 8. Optoelectronics Applications

specific applications	used REO	materials composite	refs
Optoelectronics	Er^{3+} doped with TiO_2	N/A	Mohammadi et al. (2006)[67]
Optoelectronics	Eu^{3+}-Pb-borotellurite glasses	$(70-y)(B_2O_3) + 15TeO_2 + 5PbO + 10Na_2O + yEu_2O_3$ (y = 0, 0.1, 0.2, 0.3, 0.4, and 0.5 mol %)	Devaraja et al. (2020)[11]
Optoelectronics	Er^{3+}-ZnO nanorods	N/A	Achehboune et al. (2019)[68]
Optoelectronics	Er^{3+}-oxyfluoride glass−ceramics	$55SiO_2 + 17Al_2O_3 + 5Na_2F_2 + 8Na_2O + 10GdF_3 + 5BaO$	Sroda et al. (2015)[16]
Optoelectronic devices	Eu^{3+}-soda lime glass substrates codoped with Lu^{3+} and Ga^{3+}	N/A	Mandal et al. (2020)[120]

[a]N/A indicates not applicable.

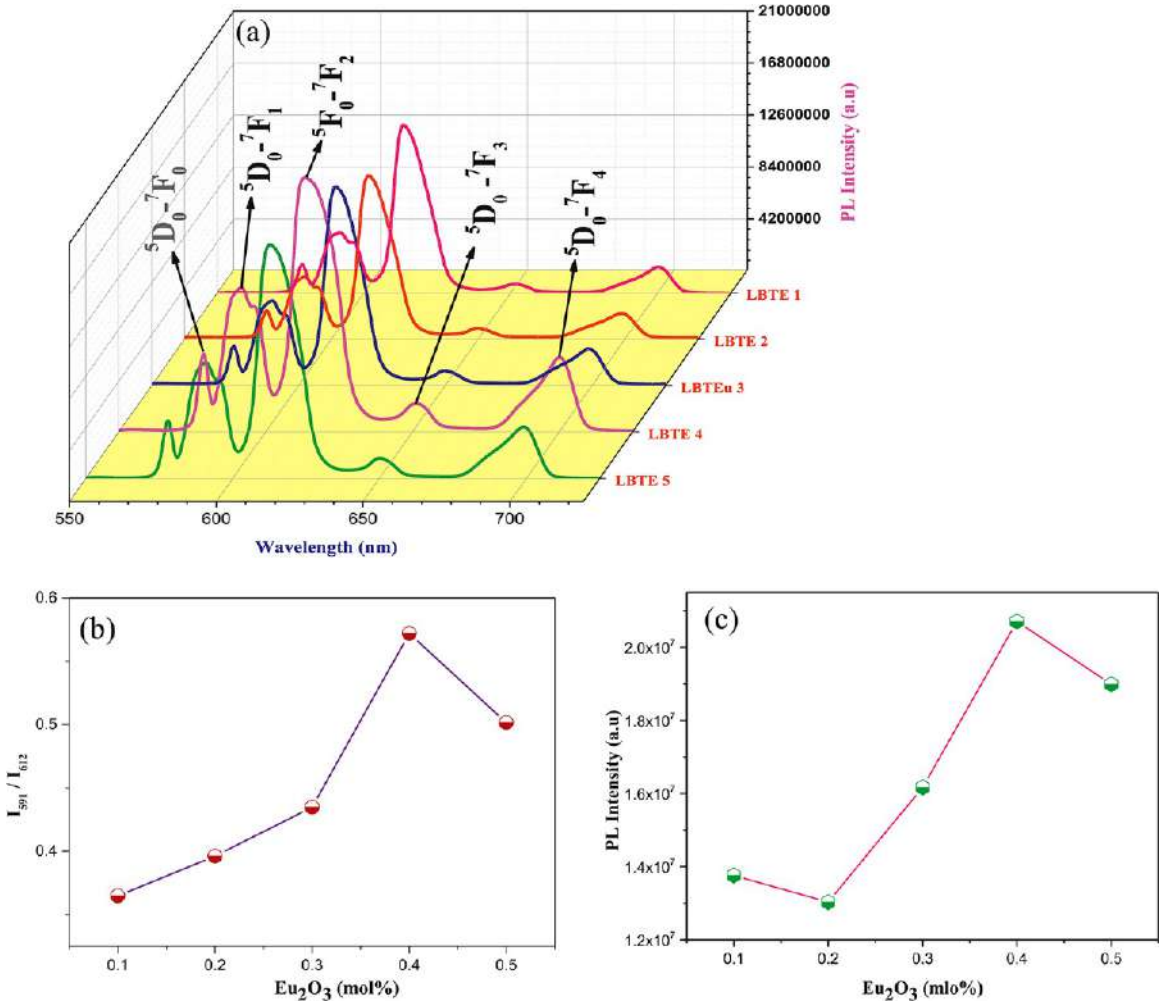

Figure 11. (a) Emission spectra of Eu^{3+}-Pb-borotellurite (LBTE) glasses, (b) the asymmetric ratio of LBTE with Eu^{3+}, and (c) the photoluminescence intensity of LBTE with Eu^{3+}. Reproduced with permission from ref 11. Copyright 2020 Elsevier.

caused by the addition of Er_2O_3 indicates great potential in multifunctional device applications as well.

The elongated luminescence (i.e., 2.61 ms) and reddish emission from Eu^{3+}-phosphate glasses show potential implications in display devices and plant lighting.[69] The intense photoluminescence of Dy^{3+}-Mg-borate glasses in the visible spectra[125] can also be useful in diverse technological, that is, solid-state laser, applications.

4.11. Miscellaneous. *4.11.1. Miscellaneous Optical Applications.* The REOs are acquiring a rising traction in optics industries because of their excellent photocatalytic traits. The Nd-TiO_2 composites[20] and synthesized Gd_2O_3[21] had exhibited remarkable photoluminescence properties in degrading organic substrate. The application of REOs was also evident in thermal imaging,[22,23] where the ZnO-Eu_2O_3 composite enhanced the photoluminescence property because of the heterogeneous surface. The synthetic Eu_2O_3 nanoparticles were proven effective as an illuminating label for an atrazine detection.[126] The hydrothermally fabricated Eu/Tb (Bisphenol A)$_3$phen nanocomposites had demonstrated a remarkable thermal stability up to 334 °C.[24] The stable Eu/Tb_2O_3 also exhibited color spectra under the influence of an ultraviolet irradiance (350 nm). The heat tolerance and co-photoluminescence color adjustability of the REOs, therefore,

https://doi.org/10.1021/acsaelm.1c00682
ACS Appl. Electron. Mater. 2021, 3, 3715−3746

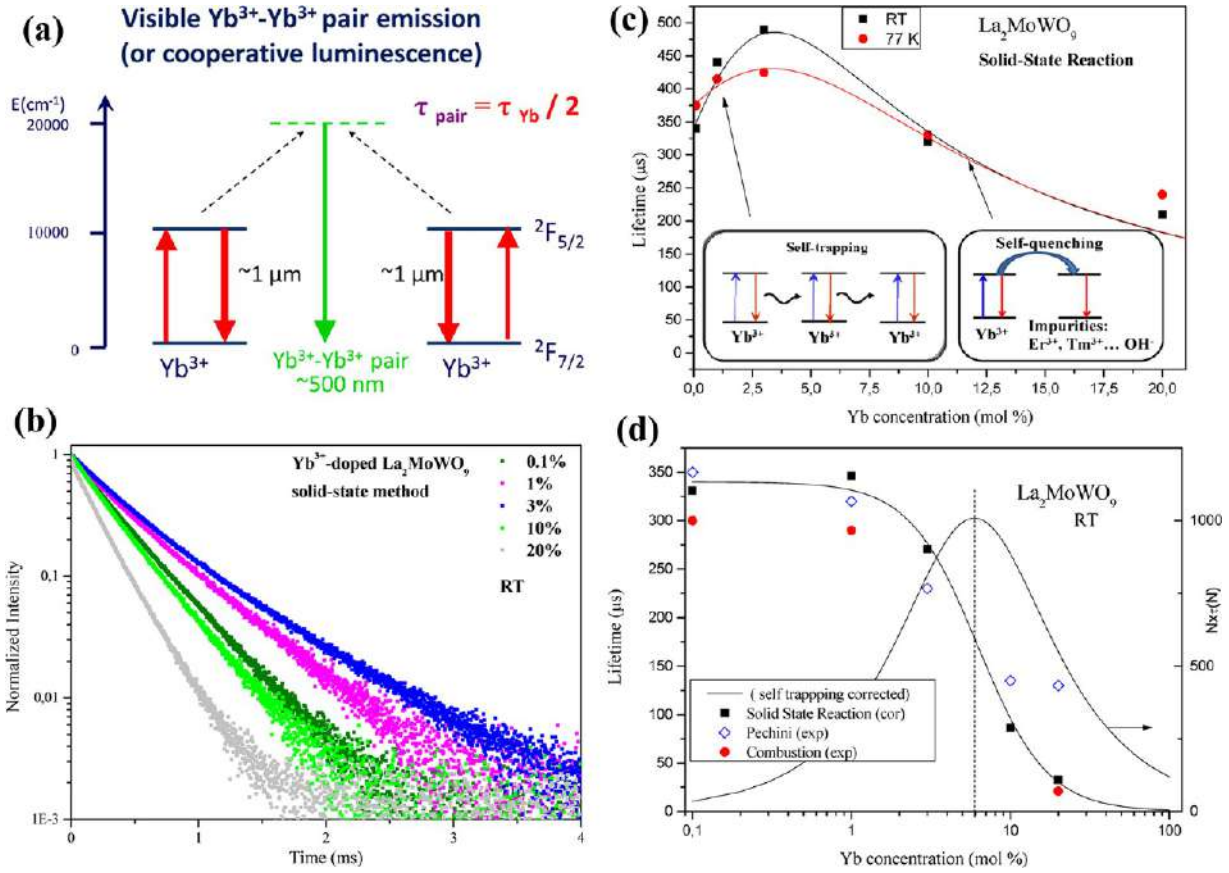

Figure 12. (a) Conjunctive luminescence spectrum of the Yb^{3+}-Yb^{3+} pair, (b) plot of luminescence intensity vs time of Yb^{3+}-La_2MoWO_9 at room temperature, (c) concentration-dependent decay of Yb^{3+}-La_2MoWO_9 considering both self-trapping and self-quenching, and (d) concentration-dependent decay considering only self-quenching. Reproduced from ref 121. Copyright 2017 American Chemical Society.

Table 9. Optical Fiber Applications

specific applications	Used REO	materials composite	refs
Optical Fiber Amplification	Er^{3+}-barium lithium fluoroborate glasses	$(70-x)\ H_3BO_3 + 10Li_2CO_3 + 10BaCO_3 + 5CaF_2 + 5ZnO + xEr_2O_3$ ($x = 0.05-2$ in wt %)	Mariselvam et al. (2019)[12]
Passive and active optical fibers	Yb^{3+}-SiO_2–Al_2O_3–La_2O_3	N/A	Litzkendorf et al. (2012)[17]
glass fiber melting and drawing process.	La^{3+}/ Pr^{3+}/ Gd^{3+}/Yb^{3+}-aluminoborosilicate glasses	$xLa_2O_3 + xPr_2O_3 + xGd_2O_3 + xYb_2O_3$ (x = 1.5 mol %)	Zhang et al. (2020)[18]
Fiber optic amplifier	Er^{3+}-borotellurite glasses	$\{[(TeO_2)_{0.7}\ (B_2O_3)_{0.3}]_{0.8}\ (SiO_2)_{0.2}\}_{1-x}\ (Er_2O_3\ NPs)_x$; x = 0.01–0.05	Umar et al. (2019)[19]

[a]N/A indicates not applicable.

underscore the potential applications in optoelectronic probes. Among REOs, the Er_2O_3 is diverse and showed high chemical and mechanical stabilities with inorganic host materials, that is, silica.[71] The hybrid mesoporous composites and the outer surface modification, respectively, increased the luminescence longevity (2.42–4.93 μs) and relative intensity (35–97%) of Er_2O_3 in an image analysis. Such applications of REOs are referred to in Table 11.

Gd_2O_3 with other codoped REOs (i.e., La^{3+}, Dy^{3+}, Y^{3+}, Yb^{3+}, etc.) was used as a protective layer to obtain a high photoluminescence efficiency for plasma display panels (PDPs) of an alternating current (AC).[25] A similar antireflective attribute of Gd_2O_3 was also observed where a Cr and Cu addition improved the absorption of the thin films.[127] The hydrolysis-aided synthesized Eu^{3+}-Y_2O_3 nanoparticles (i.e., 7–14 nm) were applied in a phosphors application with 1% Eu^{3+}.[128] The increased particle size bettered the crystal structures that also enhanced the photoluminescence intensity with the annealing temperature.

Additionally, an enhanced thermoluminescence signal was observed in phosphate glasses due to the addition of Dy^{3+}/Gd_2O_3.[129] The incorporation of Dy^{3+}/Gd^{3+} significantly influenced the electron trap structures in the glass composite. The Dy^{3+} was doped with alkali fluoroborate glass composites for the generation of low-cost while light.[130] The Dy_2O_3 worked as a potent modifier that converted BO_3 to BO_4 without producing a nonbridging oxygen. Furthermore, the polycrystalline Dy_2O_3 was applied in a metal halide lamp as a potential arc tube material (Figure 17).[72]

Eu_2O_3 has also been used in different phosphors. For example, the Eu^{3+} ion was doped in the production of a γ-aluminum oxynitride (γ-AION) phosphor.[131] The solid-state reaction led to the formation of an AION-0.25% mol Eu^{3+} phosphor that demonstrated two dominant spectra of 410 and

https://doi.org/10.1021/acsaelm.1c00682
ACS Appl. Electron. Mater. 2021, 3, 3715–3746

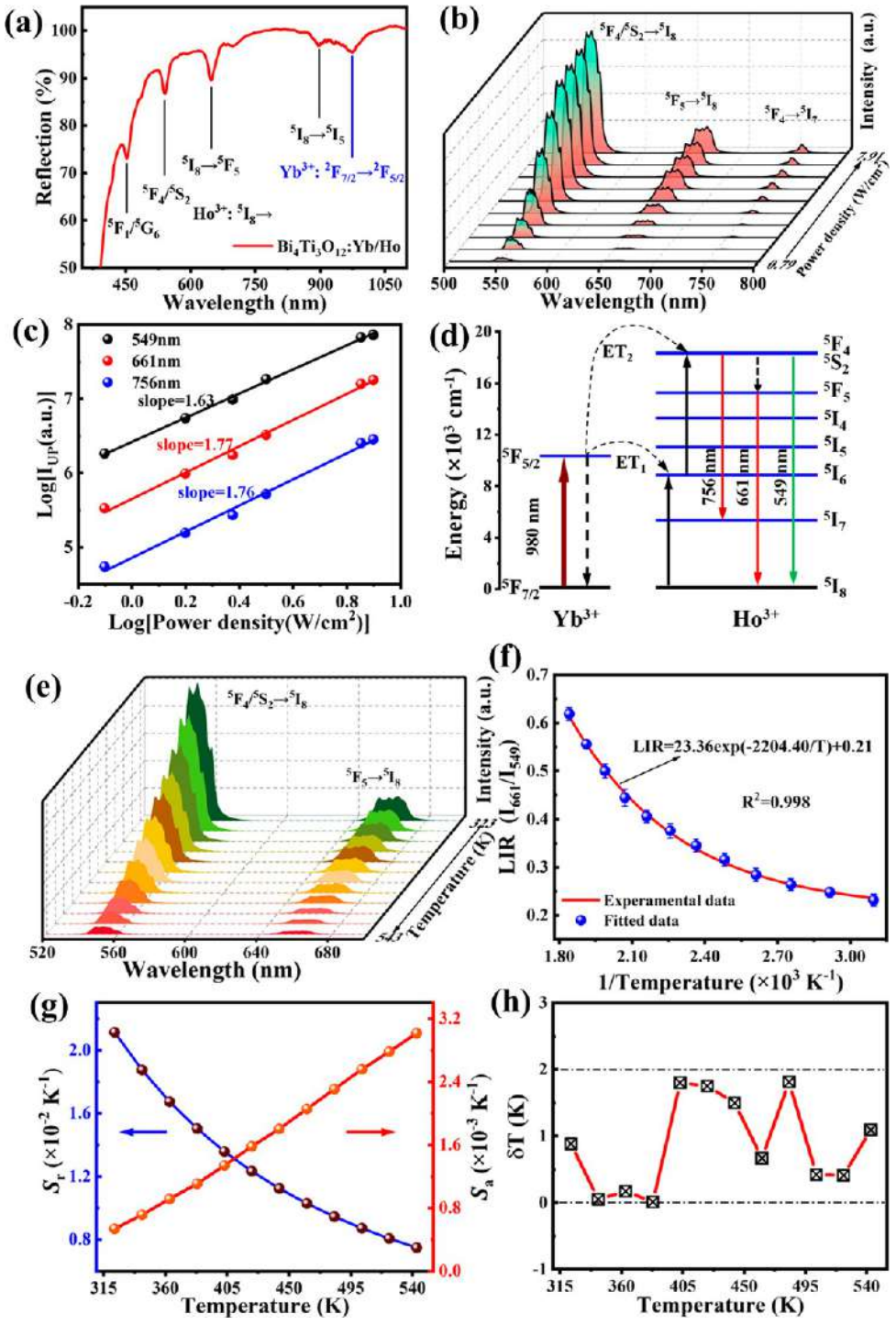

Figure 13. (a) The reflectance of a Yb/Ho-doped $Bi_4Ti_3O_{12}$ sample at different wavelengths, (b) power-dependent upconversion intensity of that sample, (c) wavelength-dependent logarithmic intensity, (d) energy-level scheme and excitation tract, (e) temperature-dependent upconversion intensity at 980 nm excitation, (f) temperature-dependent upconversion intensity between 549 and 661 nm, (g) temperature-dependent relative and absolute intensity, and (h) the temperature precision of fabricated materials. Reproduced from ref 122. Copyright 2020 American Chemical Society.

475 nm. The Eu^{3+}-barium glasses exhibited a high quantum yield of scintillations.[74] The concentration quenching effect due to the addition of Eu_2O_3 significantly increased the photoluminescence intensity of the glass composites. The Eu^{3+} with other low-cost oxide raw materials (i.e., $SrCO_3$ and SiO_2) were applied in the synthesis of nitride phosphors.[132] The red luminescence of the phosphor was achieved at a controlled C/O ratio (i.e., 1.5).

Besides an image analysis, the incorporation of Er_2O_3 nanoparticles in borotellurite glasses showed potential for optical amplification.[19] Borate glass is an important host material for optical applications. The Er^{3+}-sodium borate glass composites displayed multiluminescence emission peaks within the visible range (i.e., 401−700 nm).[133] The optical and spectroscopic traits of Er^{3+} codoped with Yb_2O_3 were utilized in photothermo-refractive (PTR) glasses.[134] The kinetics of

https://doi.org/10.1021/acsaelm.1c00682
ACS Appl. Electron. Mater. 2021, 3, 3715−3746

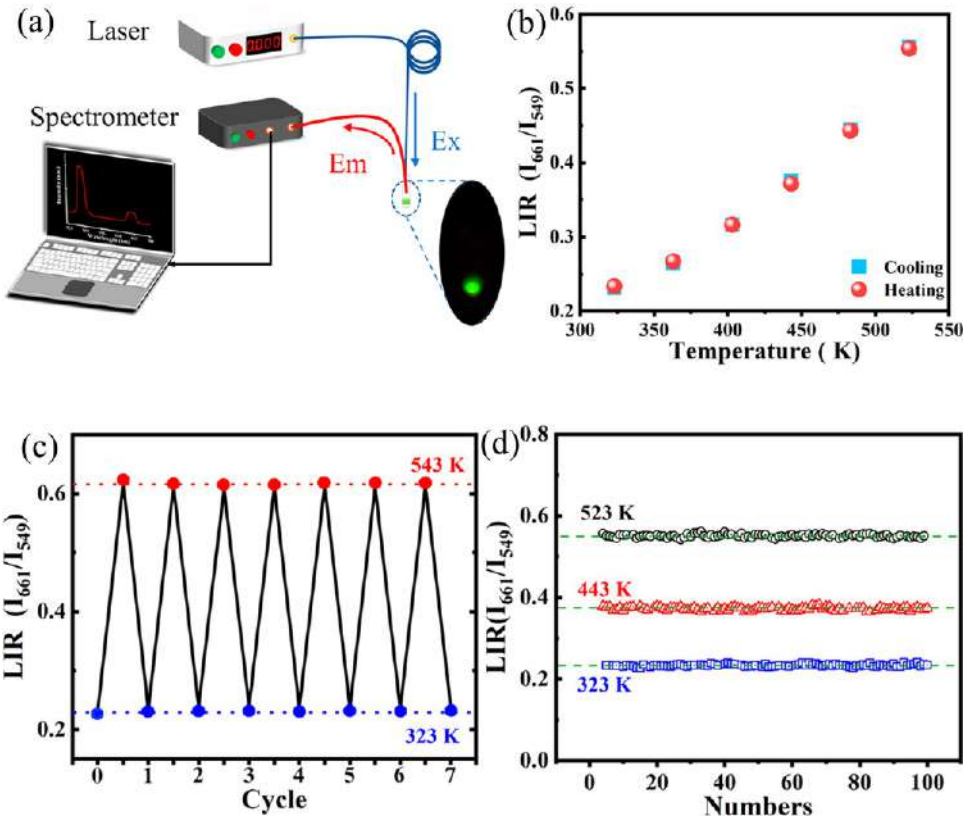

Figure 14. (a) The optical scheme based on a Yb/Ho-doped $Bi_4Ti_3O_{12}$ sensor, (b) temperature-dependent upconversion intensity of the $Bi_4Ti_3O_{12}$ sensor between a cooling and heating system, (c) the repetition of the cooling and heating cycle, and (d) the fluctuation in sensor readings at fixed temperatures. Reproduced from ref 122. Copyright 2020 American Chemical Society.

Table 10. Applications in Displays and Luminescence

specific applications	used REO	materials composite[a]	refs
Optical display	Eu^{3+}-quaternary glasses	20SrO + 5CaO + 40Li_2O + (35−x) B_2O_3 + xEu_2O_3 (x = 0.3, 0.5, and 1 mol %)	Venugopal et al . (2020)[4]
Display glass	Eu^{3+}-phosphate glasses	N/A	Han et al. (2020)[69]
Multifunctional device (luminescence)	Er^{3+}-(Li,K,Na)NbO_3 ceramics	$[Li_{0.04}(K_{0.49}Na_{0.51})_{0.96}]NbO_3$ + x Er_2O_3 (x = 0, 0.25, 0.5, 0.75, 1 mol %)	Zhao et al. (2016)[3]
Intense luminescence	Dy^{3+}-magnesium borate glasses	N/A	Ichoja et al. (2018)[125]
Enhanced luminescence	Er^{3+}-borate glasses	20ZnO + 20PbO + (20−x)Bi_2O_3 + xEr_2O_3 + 40B_2O_3 (x = 0,0.1,0.5,1,2, 3 mol %)	Madhu et al. (2020)[70]
Multifunctional device (luminescence)	Er^{3+}-(K,Na)NbO_3 ceramics	N/A	Zhao et al. (2016)[123]

[a]N/A indicates not applicable.

the crystalline composites showed the highest quantum efficiency at 1.53 μm for 0.1% Er^{3+} and 1% mole Yb^{3+}, respectively. Moreover, the nanolaminate films (i.e., Er^{3+}-doped Yb oxides) were constructed on silicon-based LEDs.[135] The presence of $Yb_2Si_2O_7$ resulted in an enhanced photoluminescence, whereas the limited conduction of electrons suppressed the electroluminescence. In addition to the Er^{3+} concentration, the color coordinates (i.e., fluorescence intensity) of Yb^{3+}/Er^{3+}-doped gadolinium gallium garnet (GGG) color tunable crystals were affected by the optical temperature (Figure 18) and the crystalline size (Figure 19).[136]

The fluoroaluminosilicate optical fiber codoped with $Yb^{3+}/Ce^{3+}/P_2O_5$ demonstrated a magnificent photodarkening inhibition.[107] The coordination of Al/P increased the solubility of codopants in the core materials, which resulted in an enhanced photodarkening resistance. In addition, the semiconductor attributes of Ce^{3+}-modified TiO_2 nanotubes (TNTs) were reported.[137] The Ce^{3+}-modified TNTs (i.e., energy gap 2.92 eV) demonstrated an increased photocurrent reaction under the visible spectrum. Furthermore, the chemical stability of Ce_2O_3 was employed on the chemosynthesis of low-cost nanocrystalline ceria (i.e., CeO_2) films.[138] The incorporation of Ce^{3+} improved the crystallization of the films at an optimum annealing temperature of 500 °C.

4.11.2. Prospects in Miscellaneous Optical Devices. The photocatalytic activities of different REOs in the optics industry were discussed in the application section and can be capitalized across various vital sectors. The Nd-TiO_2 doping was a one-step hydrothermal process and did not require any postsynthesis.[20] The homogeneous hydrolysis of $TiSO_4$ and the high SSA of mesopores (i.e., 256 m^2/g) can be utilized in a

https://doi.org/10.1021/acsaelm.1c00682
ACS Appl. Electron. Mater. 2021, 3, 3715−3746

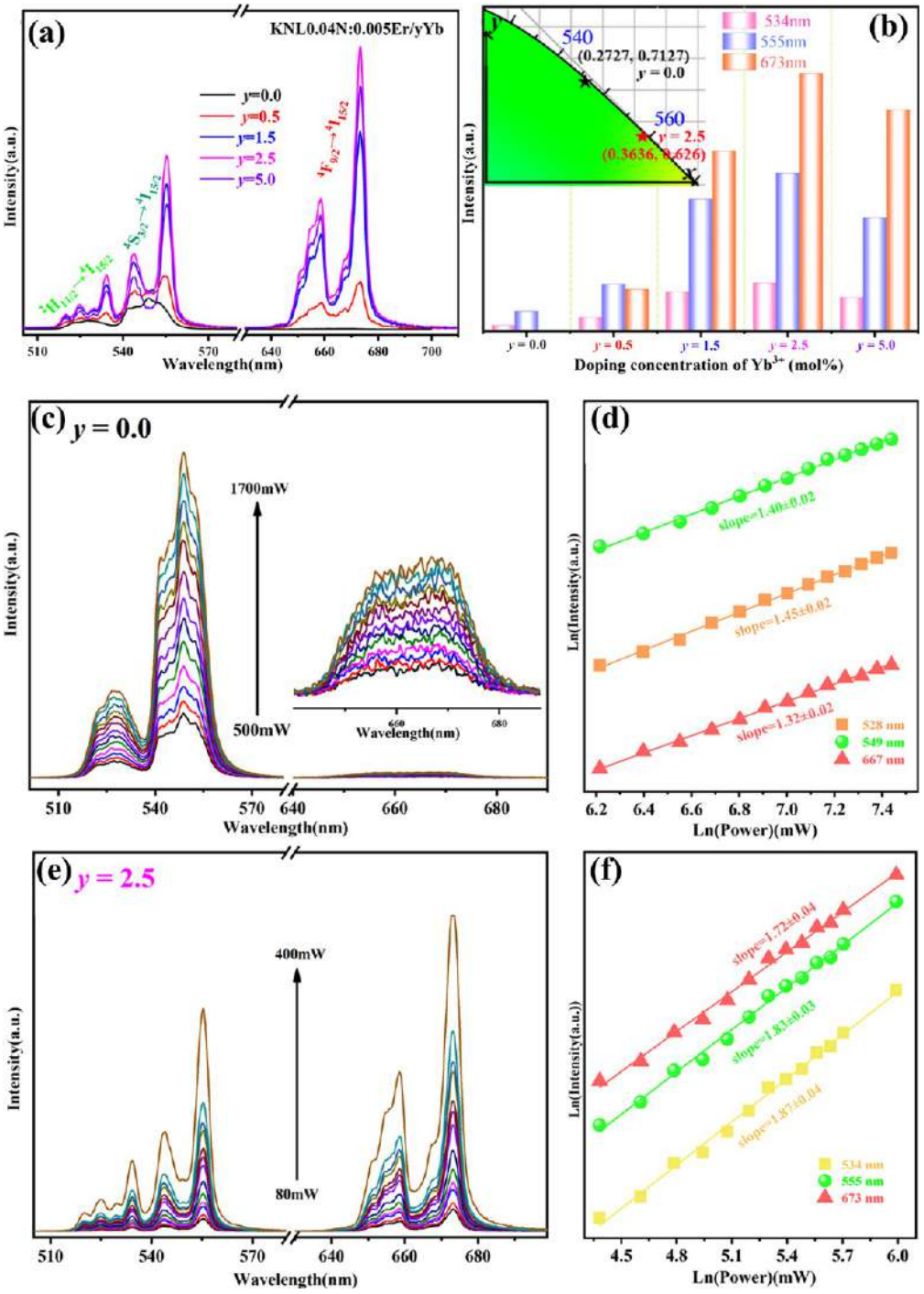

Figure 15. (a) Upconversion spectrum of Yby/0.5Er:KNLxN (x = 0.04; y = 0−5), (b) red-green emission intensity at different doping concentrations, (c, e) upconversion intensity at different wavelengths, and (d, f) logarithmic intensity vs logarithmic power at different wavelengths. Reproduced from ref 124. Copyright 2020 American Chemical Society.

large-scale industrial photocatalyst production. The easy manufacturing, unvarying internal morphology with high purity, and strong photocatalytic properties of Gd_2O_3 microspheres[21] indicate the promising aspect of a low-cost and environmentally friendly alternative of Degussa P25. The reciprocal relation between the photocatalytic intensity of ZnO-Eu_2O_3 and temperature[22] implies a potential of temperature-dependent photoelectronics applications. The atrazine detection using a derivatized Eu_2O_3 as an illuminating label[126] has potential in the microbial conjugation of water bodies to limit contaminations. The introduction of Er^{3+} impurities led to an increased density and improved spectroscopic properties of the Er^{3+}-TiO_2 barium glass[149] and can be useful for optical applications. The density and refractive index were greater for the Er_2O_3 nanoparticles-zinc borotellurite glass compared to its original counterpart,[148] suggesting a potential for nanophotonic applications. Moreover, the potent photocatalytic activity (both in duration and magnitude) of Er_2O_3-silica[71] also highlights the potential in thermal imaging for a clinical diagnosis.

https://doi.org/10.1021/acsaelm.1c00682
ACS Appl. Electron. Mater. 2021, 3, 3715−3746

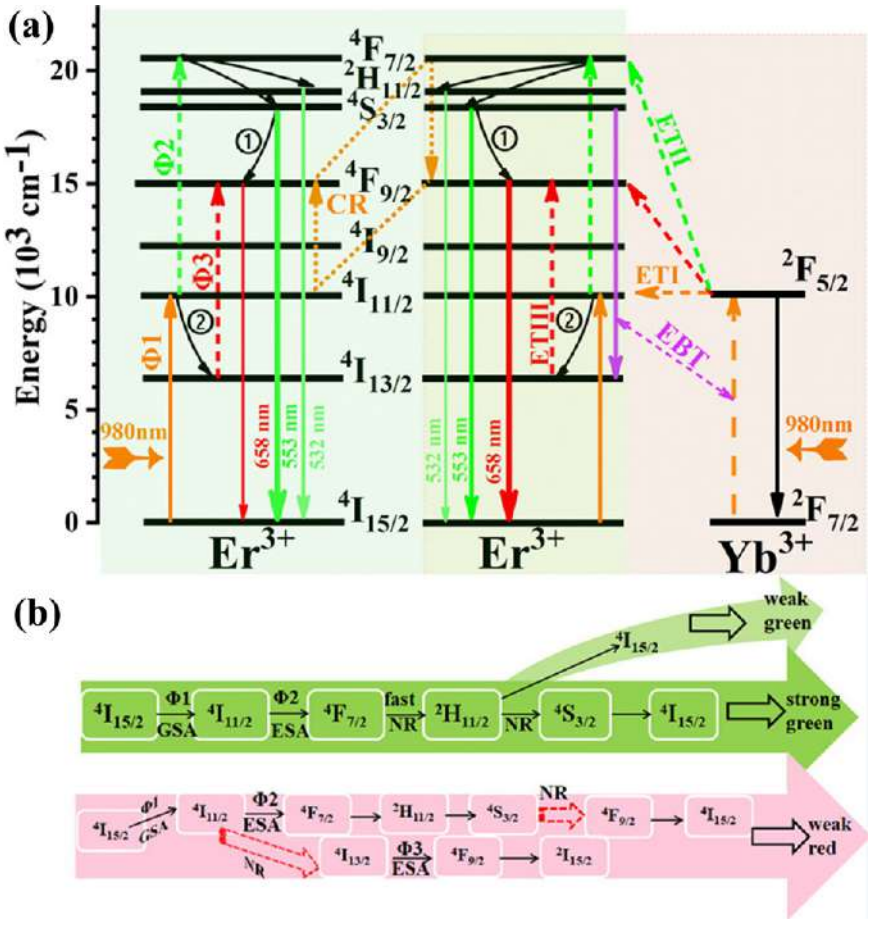

Figure 16. (a) Upconversion luminescence mechanism of Yb*y*/0.5Er:KNL*x*N (x = 0.04; y = 0−5) and (b) upconversion flowcharts of green and red lights. Reproduced from ref 124. Copyright 2020 American Chemical Society.

Sm_2O_3 is also of great interest because of its unique physical and optical properties. For instance, the noncrystalline structure of Sm^{3+}-tellurite glass ceramics, increased photon interaction, and reduced half-layer values indicate the prospect of fabricating shielding materials against γ-radiation.[143] Samarium codoped with ZnO-tellurite glass materials showed an enhanced absorption.[140] The physical properties (i.e., density and molar volume) and photoluminescence spectra (i.e., excited at 452 nm) of four bands suggest a potential for building different optical devices. Apart from that, the Sm^{3+}-alkali-bismuth germanate glass composite demonstrated a vivid orange-red spectrum excited at 405 nm.[142] The chromaticity diagram suggests a potential for color-tunable optical display applications as well. The incorporation of an L-lysin surfactant into Sm^{3+}/Eu^{3+}-poly(methyl methacrylate) (i.e., three-dimensional (3D) ordered macroporous (3DOM)) improved the SSA and UV-optical absorption compared to their counterparts.[141] These physical properties and the 3DOM structures will be useful for optical and nonuniform catalysis applications. In addition, the enhanced photoluminescence (i.e., nonexponential) and shortened lifespan of Sm^{3+}-fluorosilicate glasses clearly entail the photonic applications of tilted glasses.[144]

The unique feature, that is, modified/tunable photoluminescence, allows Dy^{3+} to be used in different phosphors and optical device applications. The Dy^{3+}/Eu^{3+} calcium boroaluminate glass composites, for instance, showed a modified emission (i.e., white to red) due to the incorporation of Eu^{3+} concentrations.[73] The unaltered lifetime and combined emission will be useful to achieve smart lighting like the circadian light cycle. The simultaneous emission of Dy^{3+} and Eu^{3+} (at 390 nm) was evident from Dy^{3+}/Eu^{3+} tellurite glass materials.[145] The emission color was hinged on the Dy/Eu ratio; hence, it is suitable for fabricating color-tunable phosphors. An effective yellowish-white photoluminescence of Dy^{3+} was evident in Ge-tellurite glass.[78] The incorporation of Ag nanoparticles into the glass composite significantly enhanced (i.e., by 29%) the emission intensity and can be considered a good candidate for high-quality lightings.

In an earlier study, the nanostructured CeO_{2-x} films showed unique physical and mechanical properties.[150] These properties significantly affect the dielectric function at the UV and IR emission spectra and, therefore, will be useful for developing optical devices with good mechanical performances.

The Yb^{3+}-silicate glass demonstrated an improved absorption and shortened lifetime.[152] These attributes can potentially lead to a limited concentration quenching and improved laser performance and, therefore, are good candidates for high-performance photonic crystal laser applications. The nonappearance of co-operative photoluminescence and optical attributes (i.e., improved absorption and reduced lifetime) of Yb^{3+}-phosphate laser glass showed prospects for a photonic device application.[153] In addition, the thermally stable and low-cost Eu^{2+}-doped β-Sialon phosphors can be a promising prospect in producing UV-based green LEDs.[146]

https://doi.org/10.1021/acsaelm.1c00682
ACS Appl. Electron. Mater. 2021, 3, 3715−3746

Table 11. Miscellaneous Optical Applications

specific applications	used REO	materials composite	refs
Production of low-priced photocatalytic nanoparticles	Nd^{3+}-TiO_2	N/A	Stengl et al. (2009)[20]
Photooxidation of methyl orange	Gd_2O_3 hollow microspheres	N/A	Jiang et al. (2016)[21]
Enhanced visible-light photocatalyst	ZnO−Dy_2O_3	N/A	Josephine et al. (2014)[139]
Fluorescence low-temperature thermal imaging	ZnO-Eu_2O_3	N/A	Rauwel et al. (2016)[22]
Low-temperature thermal imaging using photoluminescence	ZnO-Eu_2O_3	N/A	Rauwel et al. (2014)[23]
Optical and electronic devices, fluorescent probe and labels	Eu/Tb(Bisphenol A)$_3$phen	N/A	Xie et al. (2018)[24]
Optical amplification and medical diagnosis	Composites of Er_2O_3 and silica	N/A	Yu et al. (2013)[71]
Luminous efficiency (plasma display)	Gd_2O_3 codoped REOs (i.e., La^{3+}, Dy^{3+}, Y^{3+}, Yb^{3+})	N/A	Koiwa et al. (1996)[25]
Optical device (absorption-emission)	Sm^{3+}-Zn tellurite glasses	$(80-x)$ TeO_2 + 20ZnO + xSm_2O_3 ($0.0 \le x \le 1.5$ mol %)	Tanko et al. (2015)[140]
Optics	Sm^{3+}/ Eu^{3+}-poly(methyl methacrylate)	N/A	Zhang et al. (2011)[141]
Tunable color display	Sm^{3+}-alkali-bismuth germanate glasses	$(40-x)$ GeO_2 + 20 Bi_2O_3 + 20Na_2O + 10BaO + 10Gd_2O_3 + xSm_2O_3 (x = 0.05−2.5 mol %)	Prakash et al. (2019)[142]
Tellurite glass application	Sm^{3+}-tellurite glass ceramics	65TeO_2 + 25Na_2O + $(10-x)$ $NdCl_3$ + xSm_2O_3 ($0.0 \le x \le 2.5$ mol %)	Al-Hadeethi et al. (2020)[143]
Phosphor applications	Eu^{3+}-Y_2O_3	N/A	Srinivasan et al. (2010)[128]
Photonic absorption of fluorosilicate glasses	Sm^{3+}- fluorosilicate glasses	N/A	Linganna et al. (2015)[144]
Antireflective thin films with enhanced absorption	Dy_2O_3 with Cr/Cu	N/A	Ramay et al. (2018)[127]
Good thermoluminescence for beta radiation	Dy^{3+}/Gd^{3+}-phosphate glasses	N/A	Gasiorowski et al. (2020)[129]
Alkali Fluoroborate Glasses for WLEDs	Dy^{3+}-fluoroborate glasses	10K_2O + 10BaO + 10ZnF_2 + $(70-x)$ B_2O_3 + xDy_2O_3, (x = 0.1−2.0 mol %)	Gopi et al. (2019)[130]
HID Lamp	Lucid polycrystalline Dy_2O_3 ceramics	N/A	Wei et al. (2008)[72]
Smart light (circadian cycle)	Dy^{3+}/Eu^{3+}- calcium boroaluminate glasses	N/A	Lodi et al. (2018)[73]
Color tunable phosphors	Dy^{3+}/Eu^{3+}- tellurite glasses	73TeO_2 + 4BaO + 3 Bi_2O_3 + 1Ag:xEu_2O_3 + $(2-x)$ Dy_2O_3 (x = 0.5−2.0 mol %)	Lewandowski et al. (2018)[145]
High-quality lighting device	Dy^{3+}- tellurite glasses	N/A	Hua et al. (2018)[78]
Nitride Phosphor	Eu^{3+}-doped with $SrCO_3$ and SiO_2	N/A	Yang et al. (2016)[132]
AION ceramics and phosphors	Eu^{3+}-γ-aluminum oxynitride phosphor	N/A	Zhang et al. (2018)[131]
Color tunable luminescence	Eu/Tb(Bisphenol A)$_3$phen	N/A	Xie et al. (2018)[24]
X-ray induced luminescence (XRL)	Eu^{3+}-barium glasses	yEu_2O_3 + 50BaF_2 + xAl_2O_3 + $(50-x)$ B_2O_3 (x = 0−25, y = 1−10, in mol %)	Shinizaki et al. (2018)[74]
UV-based green LED	Eu^{2+}-doped β-Sialon phosphors	$Eu_xSi_5Al_{1-x}O_z$ + xN_{8-z-x} (x = 0.05, 0.06, 0.07; $0 < z \le 4.2$)	Xing et al. (2017)[148]
Enhanced optical properties	Eu^{3+}-phosphate glass	N/A	Jimenez (2015)[147]
Borotellurite Glass	Er^{3+}-borotellurite glasses	$\{[(TeO_2)_{0.7}$ $(B_2O_3)_{0.3}]_{0.8}$ $(SiO_2)_{0.2}\}_{1-x}$ $(Er_2O_3$ NPs$)_x$; x = 0.01−0.05	Umar et al. (2019)[19]
Multispectrum emissions	Er^{3+}-sodium borate glass	$(80-x)$ B_2O_3 + 10Na_2O + 10ZnO+ x Er_2O_3 (x= 0.5−1.5 mol %)	Mardhia et al. (2013)[133]
Nanophotonic	Er_2O_3/Er_2O_3 nanoparticles-zinc borotellurite glass	$\{[(TeO_2)_{0.70}$ $(B_2O_3)_{0.30}]_{0.70}$ $(ZnO)_{0.30}\}_{1-y}$ $(Er_2O_3/Er_2O_3$ nanoparticles$)_y$; (y = 0.005, 0.05 mol %)	Azlan et al. (2017)[148]
Enhanced luminescence	Er^{3+}-borate glasses	20ZnO + 20PbO + $(20-x)Bi_2O_3$ + xEr_2O_3 + 40B_2O_3 (x = 0 ,0.1,0.5,1,2,3 mol %)	Madhu et al. (2020)[70]
Optical application	Er^{3+}-TiO_2 barium glass	0.6TeO_2+ $(0.35-y)$ BaO + 0.05ZnO + yEr_2O_3 (y = 0.01−0.05 mol %)	Gaafar (2017)[149]
Photodarkening application	Yb^{3+}/Ce^{3+}-fluoroaluminosilicate	N/A	Liu et al. (2020)[107]
Metal-oxide-semiconductor LEDs	Er^{3+}-doped Yb oxides	N/A	Ouyang et al. (2018)[135]
Optical application	Yb^{3+}/Er^{3+}-PTR glasses	N/A	Nasser et al. (2020)[134]
Photoelectrode	Ce^{3+}-modified TiO_2 nanotubes	N/A	Tan et al. (2014)[137]
Photodarkening application	Yb^{3+}/Ce^{3+}-fluoroaluminosilicate	N/A	Liu et al. (2020)[107]

https://doi.org/10.1021/acsaelm.1c00682
ACS Appl. Electron. Mater. 2021, 3, 3715−3746

Table 11. continued

specific applications	used REO	materials composite	refs
Photoluminescence of nanocrystal thin films	Photodarkening application	N/A	Desouky et al. (2020)[138]
Optical device	Nanostructured cerium oxide	CeO_{2-x} ($x < 0.2$)	Charitidis et al. (2005)[150]
Enhanced photocatalytic application	Nanohybrid CeO_2/Ce_2O_3	N/A	Ma et al. (2016)[151]
Photonic crystal fiber	Yb^{3+}-doped silicate glass	$SiO_2 + Li_2O + Na_2O + K_2O + MgO + Al_2O_3 + Yb_2O_3$ (70−x−y−z 8−2−2 mol %), and $x + y + z = 18$	Jingxia et al. (2010)[152]
Photonic device	Yb^{3+}-phosphate laser glass	N/A	Venkatramu et al. (2011)[153]

[a]N/A indicates not applicable.

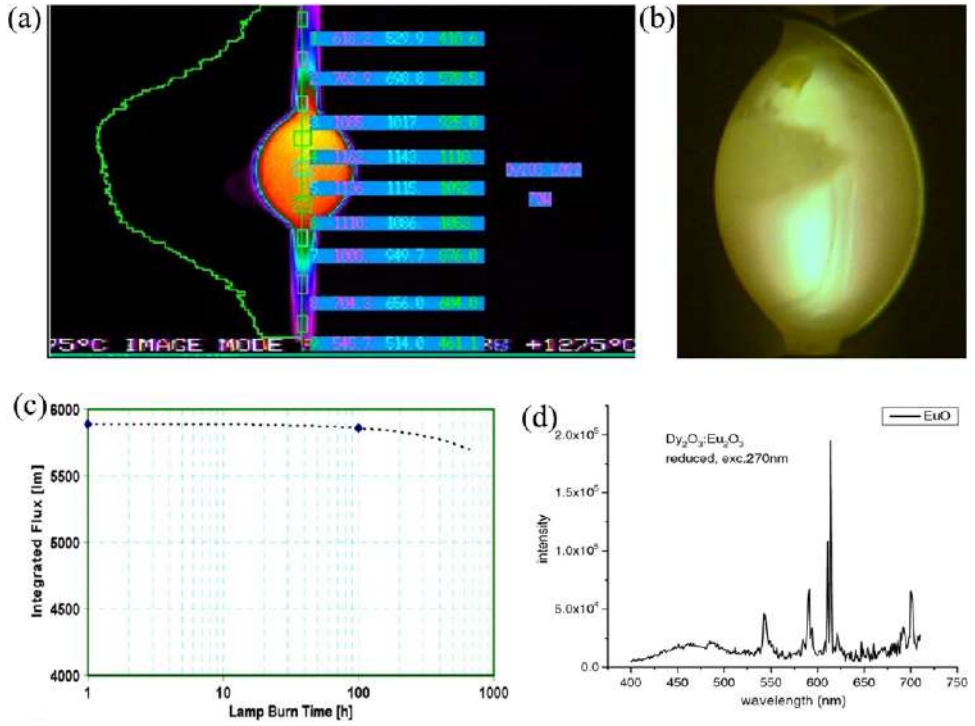

Figure 17. (a) False color image displaying an outer surface temperature at 70 W: ∼10 μm images of 100 h burner (The green line is a comparative vertical temperature profile, and the small squares are sample areas for more precise temperature measurements.), (b) the optical image demonstrating the difficulty in constructing good core luminance measurements, (c) flux vs burn time, and (d) the emission spectrum for polycrystalline Dy^{3+}. Reproduced with permission from ref 72. Copyright 2008 IOP Publishing Ltd.

5. CHALLENGES IN OPTICAL APPLICATIONS OF REOS

Challenges in White Light Applications. Vigorous studies have been done using RE ions to develop white light-emitting devices but still need to overcome some challenges. For example, the acetylacetonate (acac)-passivated Eu^{3+}-doped Y_2O_3 white light phosphors have shown ideal characteristics for use as a single-component phosphor. But a higher downconversion from the acac charge transfer (CT) band to defect levels along with Eu^{3+} guest ion energy levels indicated that the modifying and fabricating of a metal acac passivation layer might steer to further competent white light conversion.[1] Li^+ doping into Y_2O_3 nanocrystals has increased luminous efficiency greatly, whereas a proper tailoring of the Li^+ ion concentration could lead to standard equivalent energy white light illuminates (X = 0.33, Y = 0.33).[13] Dy^{3+}-Doped YCaSBDy glasses have shown yellowish-white light emission, while the doping concentration modification might pave the way to perfect white light emission.[42]

Challenges in Non-White Light Applications. The oxide glasses show a luminescence property when it is incorporated by some trivalent RE ion activators. The reason behind this is the transition between the energy levels of these RE ions, which eventually give rise to many energy levels in absorption and emission bands. But the luminescence can be enhanced more if a sensitizer can be added. This sensitizer acts as a donor, whereas the activator acts as an acceptor.[49] Finding a proper combination of acceptor and sensitizer along with a host glass matrix can lead to perfect non-white light generation. In the case of a non-white light emission, most studies concentrated on red light emission; however, very few studies have been found for a yellow, orange, blue, or green light emission. So, extensive studies are required for the generation of these lights.

Challenges in Solid-State Optical Devices. A combination of low phonon energy host material with a high thermal stability is a major challenge in this domain. The prepared glass system should have a high thermal stability along with a small optical loss and higher photoluminescence (PL). Now a higher

https://doi.org/10.1021/acsaelm.1c00682
ACS Appl. Electron. Mater. 2021, 3, 3715−3746

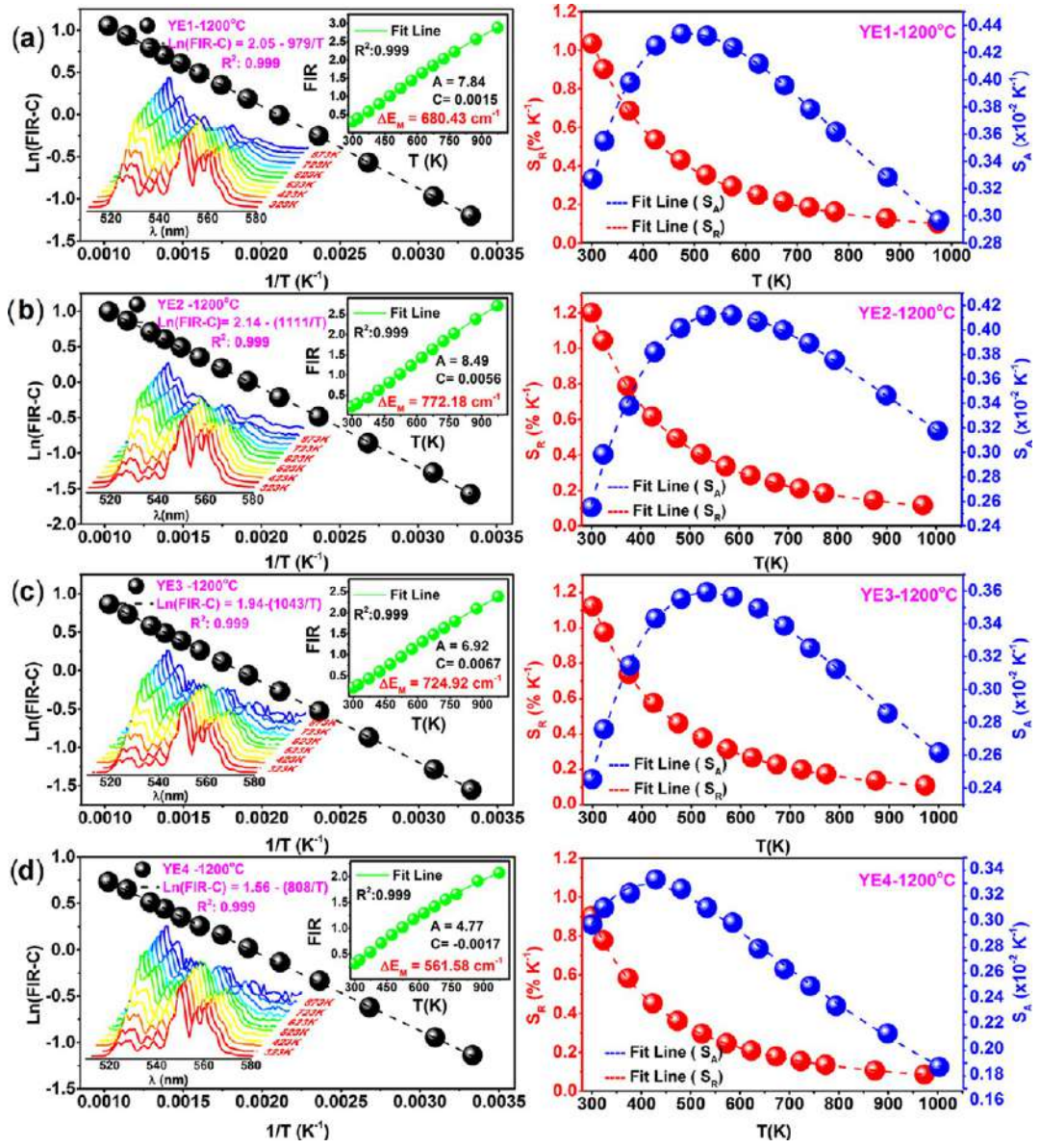

Figure 18. Fluorescence intensity and sensing as a function of temperature for (a–d) four different sizes of Yb^{3+}/Er^{3+}-doped GGG nanocrystals. Reproduced from ref 136. Copyright 2021 American Chemical Society.

PL can be achieved by using RE ions when they are in a host material with low phonon energies. Some reported studies have tried to overcome this problem in lab scales,[90,91,94] but more studies are necessary for a practical implementation. Furthermore, most of the studies of the preparation of solid-state lighting materials require complex and costly processes. So, cost reduction is one of the main challenges. To do so, researchers need to develop such a method or process by which large-scale commercial manufacturing can be done in a lucrative way.

Challenges in Laser Applications. A high-power fiber laser with a long-term stability is an ultimate demand for industrial, medical, and defense system applications. Moreover, low maintenance and operation costs are also wanted. But the photodarkening phenomenon is one of the prominent limitations in long-term operations. Additionally, the minimization of an optical loss is also a formidable challenge.[106,107] Some studies used fluoride-based elements as a host material due to their small phonon energies and developed upconversion efficacies, but they lack chemical and thermal stability along with difficulty in preparation.[57,62] On the one hand, borate glasses have become popular, as they offer a superior RE ion solubility, comparatively lower melting temperature, low cost, lofty thermal and chemical stability, and good transparency. On the other hand, higher phonon energy and a hygroscopic nature limit their execution. Higher phonon energy increases multiphonon relaxation rates, that is, nonradiative decay rates, and thus decreases the fluorescence and quantum efficacy.[61] Furthermore, because of the hygroscopic nature, they absorb humidity and turn into volatile materials.[110]

Challenges in UV Optical Applications. Applications of REOs in the UV wavelength range experienced some challenges as well. The Gd^{3+} films showed a high refractive index at high temperatures.[115] Moreover, the beam deposition rate varied between 0.5 and 2.0 nm/s at different substrate temperatures. An optimum temperature and oxygen pressure need to be maintained to get the full benefit of the electron

https://doi.org/10.1021/acsaelm.1c00682
ACS Appl. Electron. Mater. 2021, 3, 3715–3746

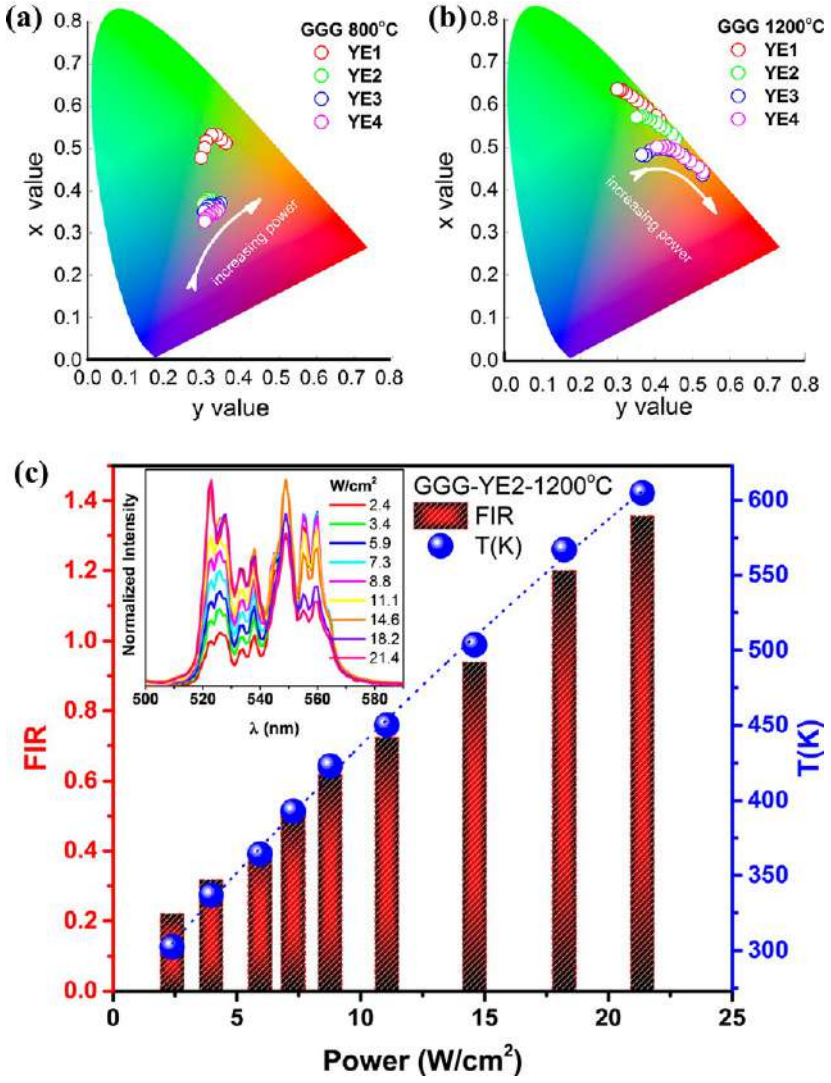

Figure 19. Chromaticity diagrams of Yb^{3+}/Er^{3+}-doped GGG nanocrystals with the increasing pump for (a) small and (b) large nanocrystals and (c) the intensity ratio (*y*-left) and host temperature (*y*-right) as a function of power. Reproduced from ref 136. Copyright 2021 American Chemical Society.

beam evaporation process and to avoid unstable film composites.

Although the Dy^{3+}-borosilicate glasses showed an enhanced refractive index,[116] the effectiveness of Dy_2O_3 at the UV region depends on the absorption capacity of the host glasses.

Challenges in Nonlinear Optics Applications. Despite the high-order optical nonlinearity of Gd/Dy_2O_3−KNN crystals,[15] the REO doping can lead to the reduction in the defects caused by the volatilized alkali materials. Although the addition of Dy_2O_3 instead of P_2O_5 significantly enhanced the glass density,[64] the atoms of low molecular weight (i.e., the presence of lithium) in the glass network cannot be detected. The Eu_2O_3-glass composites demonstrated a high mechanical stability and nonlinear refractivity.[65] However, the higher concentration of Eu_2O_3 can alter the photoluminescence intensity and peak because of the conversion of BO_3 to BO_4. Further research is warranted to overcome these technical issues.

Challenges in NIR Optical Applications. Applications of REOs in the NIR range also have challenges that require further attention. The optical luminescence mechanism of Yb_2O_3 in Bi-doped borophosphate glasses is poorly understood.[10] Further, the prolonged melting time caused the weaker fluorescence of 808 nm and stronger fluorescence of 976 nm, respectively. This dichotomy is difficult to address and represents a challenge.

Challenges in Optoelectronics Applications. There are some unelucidated mechanisms of REOs despite having shown potential in optoelectronic studies. The increased molar ratio of Er^{3+}/TiO_2 led to the formation of oxygen-deficient titania (TiO_{2-x}).[67] This TiO_{2-x} formation is subject to further research. The mechanical-stability-enhanced photoluminescence of Eu^{3+}-boro-tellurite glasses was primarily owing to the presence of nonbridging oxygens.[11] Although it showed the influence of Eu_2O_3, it did not provide evidence for the presence of Eu^{3+}. These unexplained mechanisms need further motivation.

Challenges in Optical Fiber Applications. Albeit the all-SAL fibers can be drawn at a high temperature (i.e., ∼1100 °C), it is mechanically less stable compared to SiO_2.[17] Further, the construction of a hybrid SAL-SiO_2 represents a major technical barrier because of their difference in thermochemical properties (i.e., a large gap in viscosity).

https://doi.org/10.1021/acsaelm.1c00682
ACS Appl. Electron. Mater. 2021, 3, 3715−3746

The Yb^{3+} only worked as a modifier in the alkali-free aluminoborosilicate glass composites.[18] It cannot participate in the bond formation of glass composites. Thus, a strong electric field might weaken the oxygen-bridging bond in the glass network at an elevated temperature. The molar volume of Er^{3+}-borotellurite nanocomposites was increased because of the presence of high-molecular Er^{3+}.[19] However, the pyroborate (BO_3) production can cause material compactness in the glass network that can result in fewer nonbridging oxygens.

Challenges in Display and Luminescence Applications. Some challenges of REO applications are also apparent in display and photoluminescence studies. Although the ferroelectric attribute of Er^{3+}-Li/KNN ceramics was enhanced with the addition of Er_2O_3,[3,123] the surplus amount could demolish the microstructure of the ceramic composites. The photoluminescence peak of Eu^{3+}-quaternary glasses can also alter at different wavelengths due to the presence of divalent metal contents (i.e., Ca^{2+}, Sr^{2+}, Eu^{2+}, etc.).[4] This phenomenon can be ascribed to the development of ligand-divalent metal complexes and their intricate charge-transfer mechanisms.

Challenges in Miscellaneous Optical Applications. There are also some formidable challenges even though various REOs nanocomposites offer prominent potential applications. For example, if the optimum dosage of Nd^{3+} ions (~3−4 wt %) is excessively large, the photodegradation of an organic substance by TiO_2 can be considerably reduced because of the ease of an electron−hole pair recombination.[20] Although the photooxidation of ZnO−Dy_2O_3 was active across a wide range of pH, the maximum efficiency was observed at neutral pH. The competition with the organic moiety for adsorption on the catalyst surface due to the surplus amount of H^+/OH^- can result in a lower activity of ZnO−Dy_2O_3.[139] The destabilized surface also played a critical role in the enhanced photocatalytic activity of ZnO-Eu_2O_3 composites.[23] However, the antenna effect (i.e., charge accumulation) from the indirect excitation of Eu^{3+} with ZnO can suppress the photoluminescence trait. Despite having the bioassessment potential of Eu_2O_3 nanocomposites in controlling water pollution,[126] the impure Eu_2O_3 is readily dissolved in acidic conditions, demeriting their desirable photocatalytic characteristics. The complex formation between Er^{3+} and oxygen can repress the lattice vibrations between 4f electrons and silica compounds.[71] This phenomenon could reduce the energy transmission and restrain the temperature quenching outcome; thus, in turn, it will experience a lower photocatalytic activity.

Although Gd^{3+} as a protective film obtained the high photoluminescence of AC-PDPs,[25] the attainment of a low firing voltage is difficult. Furthermore, even though the intense photoluminescence of Eu^{3+}-phosphate glass appears attractive,[147] the level of Cu^{2+} impurities in the composite should be reduced for practical implications. Addressing these issues is quite challenging, and further in-depth research is warranted.

6. CONCLUSIONS AND FUTURE DIRECTIONS

This article has offered a focused and comprehensive review of the recent applications and commercial prospects of REOs in the optical industry. The incorporation of RE ions into the glass matrices has significantly improved the optical attributes of the glasses, and a consideration of the improvement of the field via successful implementations of REOs will invoke several future studies. The major applications found in the review are as follows.

(i) REOs have unique properties that can greatly enhance stability (i.e., thermal and chemical tolerance) and facilitate the prevention of the crystallization of the glasses. Consequently, various REOs independently or in concert with other doping materials are now being increasingly used as phosphors in LEDs and LCDs.

(ii) High-quality lasers are fabricated due to their effective up−down conversion processes.

(iii) Third-order optical nonlinearity has paved the way for applying them in nonlinear photonic devices.

(iv) Next-generation optoelectronics and fiber-optical device fabrication are improved by implementing REOs.

(v) The extensive range of applications and immense prospects imply that REOs usage will increase significantly on an industrial scale in the near future.

In addition to widespread applications and the enormous potential of REOs in optics, some critical challenges persist that need careful attention for the commercial manufacture of low-cost and eco-friendly optical devices. Some future directions to tackle the existing challenges are provided below.

(i) The photodarkening effect can be modified in different ways, such as by manipulating the design for fiber composition and structure, loading mechanism for gas, thermal bleaching, photobleaching, etc. However, the most effective one is a modification of the core fiber configuration. Now, the accumulation of codopants such as Al, Ce, or P in the core composition may largely shorten the PD effect, but an excess of them will create −OHC color centers, which will eventually increase the PD again.

(ii) Borate-based glasses have attained much interest for their advantageous features, but the hygroscopic nature confines their functionalities. The addition of the moderators such as a base or high-pH metallic ions could be a probable solution to this issue.

(iii) The fluoride-based glasses are normally used for an upconversion luminescence while they have a weak thermal and chemical stability. Replacing them with oxide-based glasses could improve the situation.

(iv) Although the incorporation of Dy_2O_3 is a potential alternative to P_2O_5 for the enhancement of glass density, the presence of lithium can considerably hamper the detection limit. Thus, lithium should be avoided, or lithium passivity materials can be used.

(v) The emergence of ligand-divalent metal compounds and their convoluted charge transfer mechanisms is one of the key challenges in display and luminescence applications. In-depth lab-scale research is required that would help us understand the ligand-aversion mechanism to mitigate this technical blockade.

(vi) The presence of alloyed Eu_2O_3 in acidic conditions can further significantly reduce the detection accuracy of Eu_2O_3 nanocomposites as an illuminating label in controlling water pollution due to its high dissolution. This can easily be avoided by maintaining pH levels in alkaline media.

To conclude, it is worthwhile to mention that more exhaustive research is needed to exploit the diversified utility of REOs in optical industries in a cost-effective and environmentally acceptable manner.

https://doi.org/10.1021/acsaelm.1c00682
ACS Appl. Electron. Mater. 2021, 3, 3715−3746

AUTHOR INFORMATION

Corresponding Author

M. Khalid Hossain − *Interdisciplinary Graduate School of Engineering Science, Kyushu University, Fukuoka 816-8580, Japan; Bangladesh Atomic Energy Commission, Dhaka 1207, Bangladesh;* orcid.org/0000-0003-4595-6367; Email: khalid.baec@gmail.com, khalid@kyudai.jp

Authors

Shahadat Hossain − *Interdisciplinary Graduate School of Engineering Science, Kyushu University, Fukuoka 816-8580, Japan; Bangladesh Atomic Energy Commission, Dhaka 1207, Bangladesh;* orcid.org/0000-0001-7680-9891

Mohammad Hafez Ahmed − *West Virginia University, Morgantown 26506-6103 West Virginia, United States;* orcid.org/0000-0001-8788-095X

Md Ishak Khan − *University of Pennsylvania, Philadelphia 19104 Pennsylvania, United States;* orcid.org/0000-0001-7680-9613

Nazmul Haque − *School of Materials Engineering, Purdue University, West Lafayette 47907 Indiana, United States*

Gazi A. Raihan − *University of New Orleans, New Orleans 70148 Louisiana, United States*

Complete contact information is available at: https://pubs.acs.org/10.1021/acsaelm.1c00682

Notes

The authors declare no competing financial interest.

LIST OF ABBREVIATIONS

acac, acetylacetonate
AION, aluminum oxynitride
BaGaBSi, barium gallium borosilicate
BMFSrSbD, Dy^{3+}-doped antimony-magnesium-strontium-oxyfluoroborate
BSBT, biosilicate borotellurite
CaBAl, calcium boroaluminate
CCT, correlated color temperatures
CTRN, carbothermal reduction and nitridation
GeBiNaGdBaH, Ho^{3+}-doped bismuth-germanate
HGT, heavy metal germanium tellurite
KNN, $(K_{0.5}Na_{0.5})NbO_3$
LCD, liquid crystal display
LED, light emitting diode
LGFDy, Li_2O-BaO-GdF_3−SiO_2
Li-KNN, $(Li,K,Na)NbO_3$
LiYBDy, Dy^{3+}-doped lithium yttrium borate
LPDy, Dy^{3+}-doped lithium lead gadolinium silicate
LSPR, localized surface plasmon resonance
MTB, multicomponent tellurium borate
NIR, near-infrared
n-UV, near-ultraviolet
NKBT, $Na_{0.25}K_{0.25}Bi_{0.5}TiO_3$
NBSAZB, Na_2O−B_2O_3−SiO_2−Al_2O_3−ZnO-BaO
NKLB, LiF-Na_2O−K_2O−B_2O_3
PD, photodarkening
PL, photoluminescence
PTR, photothermo-refractive
PVP, polyvinylpyrrolidone
REE, rare earth element
REO, rare earth oxide
R_2O_3, rare earth sesquioxides
SAL, SiO_2−Al_2O_3−La_2O_3
SSA, specific surface area
TNT, TiO_2 nanotube
TZNBL, $65TeO_2$−$15ZnO$−$10Na_2O$−$5BaO$−$3La_2O_3$
UV, ultraviolet
XRL, X-ray induced luminescence
YAG, yttrium aluminum garnet
YCaSBDy, Dy^{3+}-doped yttrium calcium silicoborate
YSZ, yttria-stabilized zirconia

REFERENCES

(1) Dai, Q.; Foley, M. E.; Breshike, C. J.; Lita, A.; Strouse, G. F. Ligand-Passivated Eu:Y_2O_3 Nanocrystals as a Phosphor for White Light Emitting Diodes. *J. Am. Chem. Soc.* **2011**, *133* (39), 15475−15486.

(2) Luewarasirikul, N.; Kaewkhao, J. Spectroscopic Properties and Judd-Ofelt Analysis of Sm^{3+} Ions in Barium Sodium Borate Glasses. *Mater. Today Proc.* **2017**, *4* (5), 6224−6233.

(3) Zhao, Y.; Ge, Y.; Zhang, X.; Zhao, Y.; Zhou, H.; Li, J.; Jin, H. Comprehensive Investigation of Er_2O_3 Doped $(Li,K,Na)NbO_3$ Ceramics Rendering Potential Application in Novel Multifunctional Devices. *J. Alloys Compd.* **2016**, *683*, 171−177.

(4) Venugopal, A. R.; Kaewkhao, J.; Abhiram, J.; Rajashekara, K. M.; Rajaramakrishna, R.; Pramod, N. G.; Rao, C. Eu^{3+} Ions Doped SrO-CaO-Li_2O-B_2O_3 Glasses Foroptical Display Material Application. *J. Phys.: Conf. Ser.* **2020**, *1485*, 012053.

(5) Elkhoshkhany, N.; Marzouk, S. Y.; Khattab, M. A.; Dessouki, S. A. Influence of Sm_2O_3 Addition on Judd-Ofelt Parameters, Thermal and Optical Properties of the TeO_2-Li_2O-ZnO-Nb_2O_5 Glass System. *Mater. Charact.* **2018**, *144*, 274−286.

(6) Hamza, A. M.; Halimah, M. K.; Muhammad, F. D.; Chan, K. T. Physical Properties, Ligand Field and Judd-Ofelt Intensity Parameters of Bio-Silicate Borotellurite Glass System Doped with Erbium Oxide. *J. Lumin.* **2019**, *207*, 497−506.

(7) Cao, C.; Xie, A.; Zhou, T.; Zhong, H.; Lu, X.; Xie, A.; Noh, H. M.; Jeong, J. H. Eu^{3+} Doped Lutetium Molybdenum Oxides: Synthesis, Optical Properties, Thermal Behavior, and LED Packaging. *J. Lumin.* **2020**, *217*, 116759.

(8) Cao, C.; Yang, X.; Chen, X.; Xie, A. Enhanced Emission of Eu^{3+} in Lutetium Tungsten Molybdenum Oxide Phosphors: Synthesis, Optical Properties, Thermal Behavior, and LED Packaging. *J. Lumin.* **2020**, *223*, 117269.

(9) Asyikin, A. S.; Halimah, M. K.; Latif, A. A.; Faznny, M. F.; Nazrin, S. N. Physical, Structural and Optical Properties of Bio-Silica Borotellurite Glass System Doped with Samarium Oxide Nanoparticles. *J. Non-Cryst. Solids* **2020**, *529*, 119777.

(10) Sheng, Q.; Wang, X.; Chen, D. Enhanced Broadband Near-Infrared Luminescence and Its Origin in Yb/Bi Co-Doped Borophosphate Glasses and Fibers. *J. Quant. Spectrosc. Radiat. Transfer* **2014**, *141*, 9−13.

(11) Devaraja, C.; Jagadeesha Gowda, G. V.; Keshavamurthy, K.; Eraiah, B.; Devarajulu, G.; Jagannath, G. Physical, Structural and Photo Luminescence Properties of Lead Boro-Tellurite Glasses Doped with Eu^{3+} Ions. *Vacuum* **2020**, *177*, 109426.

(12) Mariselvam, K.; Arun Kumar, R.; Rajeswara Rao, V. Concentration-Dependence and Luminescence Studies of Erbium Doped Barium Lithium Fluoroborate Glasses. *Opt. Laser Technol.* **2019**, *118*, 37−43.

(13) Bai, Y.; Wang, Y.; Peng, G.; Zhang, W.; Wang, Y.; Yang, K.; Zhang, X.; Song, Y. Enhanced White Light Emission in Er/Tm/Yb/Li Codoped Y_2O_3 Nanocrystals. *Opt. Commun.* **2009**, *282* (9), 1922−1924.

(14) Klimesz, B.; Ryba-Romanowski, W.; Lisiecki, R. Oxyfluorotellurite Glasses Doped by Dysprosium Ions. Thermal and Optical Properties. *Opt. Mater. (Amsterdam, Neth.)* **2015**, *42*, 538−543.

(15) Peddigari, M.; Pattipaka, S.; Bharti, G. P.; Khare, A.; Dobbidi, P. Nonlinear Optical Properties of Pulsed Laser Deposited Gd_2O_3 and

Dy_2O_3 Doped $K_{0.5}Na_{0.5}NbO_3$ Thin Films. *Opt. Mater. (Amsterdam, Neth.)* **2016**, *58*, 9−13.
(16) Środa, M.; Szlósarczyk, K.; Różański, M.; Sitarz, M.; Jeleń, P. Spectroscopic Properties of Transparent Er-Doped Oxyfluoride Glass−Ceramics with GdF_3. *Spectrochim. Acta, Part A* **2015**, *134*, 631−637.
(17) Schuster, K.; Litzkendorf, D.; Grimm, S.; Kobelke, J.; Schwuchow, A.; Ludwig, A.; Leich, M.; Jetschke, S.; Dellith, J.; Auguste, J.-L.; Leparmentier, S.; Humbert, G.; Werner, G. Study of Lanthanum Aluminum Silicate Glasses for Passive and Active Optical Fibers. *Proceedings of SPIE OPTO, San Francisco, CA, 2013;* Digonnet, M. J. F., Jiang, S., Dries, J. C., Eds.; SPIE, 2013; Vol. *8621*, p 86210Q. DOI: 10.1117/12.2004011.
(18) Zhang, L.; Qu, Y.; Wan, X.; Zhao, J.; Zhao, J.; Yue, Y.; Kang, J. Influence of Rare Earth Oxides on Structure, Dielectric Properties and Viscosity of Alkali-Free Aluminoborosilicate Glasses. *J. Non-Cryst. Solids* **2020**, *532*, 119886.
(19) Umar, S. A.; Halimah, M. K.; Chan, K. T.; Amirah, A. A.; Azlan, M. N.; Grema, L. U.; Hamza, A. M.; Ibrahim, G. G. Optical and Structural Properties of Rice Husk Silicate Incorporated Borotellurite Glasses Doped with Erbium Oxide Nanoparticles. *J. Mater. Sci.: Mater. Electron.* **2019**, *30* (20), 18606−18616.
(20) Štengl, V.; Bakardjieva, S.; Murafa, N. Preparation and Photocatalytic Activity of Rare Earth Doped TiO_2 Nanoparticles. *Mater. Chem. Phys.* **2009**, *114* (1), 217−226.
(21) Jiang, X.; Yu, L.; Yao, C.; Zhang, F.; Zhang, J.; Li, C. Synthesis and Characterization of Gd_2O_3 Hollow Microspheres Using a Template-Directed Method. *Materials* **2016**, *9* (5), 323.
(22) Rauwel, E.; Galeckas, A.; Rauwel, P.; Hansen, P.-A.; Wragg, D.; Nilsen, O.; Fjellvåg, H. Metal Oxide Nanoparticles Embedded in Rare-Earth Matrix for Low Temperature Thermal Imaging Applications. *Mater. Res. Express* **2016**, *3* (5), 055010.
(23) Rauwel, E.; Galeckas, A.; Rauwel, P.; Hansen, P.-A.; Wragg, D.; Nilsen, O.; Fjellvag, H. ALD Applied to Conformal Rare-Earth Coating of ZnO Nanoparticles for Low Temperature Thermal Imaging Applications. *ECS Trans.* **2014**, *64* (9), 23−31.
(24) Xie, G.; Zhang, Z.; Zhang, J. Synthesis and Characterization of the Novel Color-Tunable Eu/Tb$(BPA)_3$ Phen Composites. *MATEC Web Conf.* **2018**, *207*, 03021.
(25) Koiwa, I.; Kanehara, T.; Mita, J. Application of Screen-Printed Rare Earth Oxide Protective Film to Alternating-Current Plasma Display Panels. *Electron. Commun. Japan (Part II Electron.* **1996**, *79* (8), 31−41.
(26) Hossain, M. K.; Khan, M. I.; El-Denglawey, A. A Review on Biomedical Applications, Prospects, and Challenges of Rare Earth Oxides. *Appl. Mater. Today* **2021**, *24*, 101104.
(27) Hossain, M. K.; Kawaguchi, K.; Hashizume, K. Conductivity of Gadolinium(III) Oxide (Gd_2O_3) in Hydrogen-Containing Atmospheres. *Proc. Int. Exch. Innov. Conf. Eng. Sci.* **2020**, *6*, 1−6.
(28) Hossain, M. K.; Hashizume, K.; Jo, S.; Kawaguchi, K.; Hatano, Y. Hydrogen Isotope Dissolution and Release Behavior of Rare Earth Oxides. *Fusion Sci. Technol.* **2020**, *76* (4), 553−566.
(29) Jha, K.; Jayasimhadri, M.; Haranath, D.; Jang, K. Influence of Modifier Oxides on Spectroscopic Properties of Eu^{3+} Doped Oxy-Fluoro Tellurophosphate Glasses for Visible Photonic Applications. *J. Alloys Compd.* **2019**, *789*, 622−629.
(30) Hossain, M. K.; Kawaguchi, K.; Hashizume, K. Isotopic Effect of Proton Conductivity in Gadolinium Sesquioxide. *Fusion Eng. Des.* **2021**, *171*, 112555.
(31) Eyring, L. The Binary Rare Earth Oxides. In *Handbook on the Physics and Chemistry of Rare Earths;* North-Holland Publishing Company: Amsterdam, Netherlands, 1979; Vol. 3, pp 337−399. DOI: 10.1016/S0168-1273(79)03010-5.
(32) Ami Hazlin, M. N.; Halimah, M. K.; Muhammad, F. D. Absorption and Emission Analysis of Zinc Borotellurite Glass Doped with Dysprosium Oxide Nanoparticles for Generation of White Light. *J. Lumin.* **2018**, *196*, 498−503.
(33) Khan, I.; Shoaib, M.; Rooh, G.; Kaewkhao, J.; Khattak, S. A.; Ahmad, T.; Zaman, F.; Ataullah; Tufail, M. Investigation of Luminescence Properties of Dy^{3+} Doped LiF−Na_2O− K_2O−B_2O_3 Glasses for White Light Generation. *J. Alloys Compd.* **2019**, *805*, 896−903.
(34) Caldiño, U.; Lira, A.; Meza-Rocha, A. N.; Camarillo, I.; Lozada-Morales, R. Development of Sodium-Zinc Phosphate Glasses Doped with Dy^{3+}, Eu^{3+} and Dy^{3+}/Eu^{3+} for Yellow Laser Medium, Reddish-Orange and White Phosphor Applications. *J. Lumin.* **2018**, *194*, 231−239.
(35) Tu, D.; Liang, Y.; Liu, R.; Li, D. Eu/Tb Ions Co-Doped White Light Luminescence Y_2O_3 Phosphors. *J. Lumin.* **2011**, *131* (12), 2569−2573.
(36) Hou, X.; Zhou, S.; Jia, T.; Lin, H.; Teng, H. White Light Emission in $Tm^{3+}/Er^{3+}/Yb^{3+}$ Tri-Doped Y_2O_3 Transparent Ceramic. *J. Alloys Compd.* **2011**, *509* (6), 2793−2796.
(37) Bilir, G.; Bartolo, B. Di. Production of Bright, Wideband White Light from Y_2O_3 Nano-Powders Induced by Laser Diode Emission. *Opt. Mater. (Amsterdam, Neth.)* **2014**, *36* (8), 1357−1360.
(38) Ullah, I.; Shah, S. K.; Rooh, G.; Srisittipokakun, N.; Khan, A.; Kaewkhao, J.; Kim, H. J.; Kothan, S. Spectroscopic Study and Energy Transfer Behavior of Gd^{3+} to Dy^{3+} for Li_2O−MgO-Gd_2O_3−B_2O_3−Dy_2O_3 Glasses for White Emission Material. *J. Lumin.* **2020**, *226*, 117380.
(39) Jamalaiah, B. C.; Pakardin, G.; Lokeswara Reddy, G. V.; Vijaya Kumar, M. V. White Light Generation in Dy_2O_3-Doped NBSAZB Glasses. *Opt. Mater. (Amsterdam, Neth.)* **2017**, *73*, 545−549.
(40) Pawar, P. P.; Munishwar, S. R.; Gautam, S.; Gedam, R. S. Physical, Thermal, Structural and Optical Properties of Dy^{3+} Doped Lithium Alumino-Borate Glasses for Bright W-LED. *J. Lumin.* **2017**, *183*, 79−88.
(41) Sambasiva Rao, T.; Krishna Reddy, D. V.; Taherunnisa, S. K.; Siva Sesha Reddy, A.; Venkateswara Rao, P.; Veeraiah, N.; Rami Reddy, M. Studies on Structural Characterization and near White Light Emission through Energy Transfer between Ce^{3+} and Tb^{3+} in Barium Gallium Borosilicate Glasses. *J. Mol. Struct.* **2019**, *1190*, 184−195.
(42) Kesavulu, C. R.; Kim, H. J.; Lee, S. W.; Kaewkhao, J.; Chanthima, N.; Tariwong, Y. Physical, Vibrational, Optical and Luminescence Investigations of Dy^{3+}-Doped Yttrium Calcium Silicoborate Glasses for Cool White LED Applications. *J. Alloys Compd.* **2017**, *726*, 1062−1071.
(43) Narwal, P.; Dahiya, M. S.; Yadav, A.; Hooda, A.; Agarwal, A.; Khasa, S. Improved White Light Emission in Dy^{3+} Doped LiF−CaO−Bi_2O_3−B_2O_3 Glasses. *J. Non-Cryst. Solids* **2018**, *498*, 470−479.
(44) Lodi, T. A.; Dantas, N. F.; Gonçalves, T. S.; de Camargo, A. S. S.; Pedrochi, F.; Steimacher, A. Dy^{3+} Doped Calcium Boroaluminate Glasses and Blue Led for Smart White Light Generation. *J. Lumin.* **2019**, *207*, 378−385.
(45) Pawar, P. P.; Munishwar, S. R.; Gedam, R. S. Intense White Light Luminescent Dy^{3+} Doped Lithium Borate Glasses for W-LED: A Correlation between Physical, Thermal, Structural and Optical Properties. *Solid State Sci.* **2017**, *64*, 41−50.
(46) Liu, L.; Yuan, X.-m.; Xie, A.; Yang, M.; Chen, F. Synthesis and Luminescent Properties of Eu^{3+}-Activated Novel Borate-Based Red-Emitting Phosphors for White LED. *Faguang Xuebao* **2011**, *32* (7), 686−692.
(47) Jha, K.; Jayasimhadri, M. Structural and Emission Properties of Eu^{3+}-Doped Alkaline Earth Zinc-Phosphate Glasses for White LED Applications. *J. Am. Ceram. Soc.* **2017**, *100* (4), 1402−1411.
(48) Huang, J.; Song, Y.; Wang, G.; Sheng, Y.; Zheng, K.; Li, H.; Zhang, H.; Huo, Q.; Xu, X.; Zou, H. Surfactant-Assisted Synthesis and Luminescent Properties of Gd_2O_3:Eu^{3+} Core−Shell Microspheres. *J. Alloys Compd.* **2013**, *574*, 310−315.
(49) Vini, K.; Kumar, H. P.; Nissamudeen, K. M. Red Light Emission of Y_2O_3:Eu^{3+} Nanophosphors and Luminescent Enhancement by the Addition of Gadolinium Oxide as Co-Dopant. *J. Mater. Sci.: Mater. Electron.* **2020**, *31* (7), 5653−5666.
(50) Khan, I.; Rooh, G.; Rajaramakrishna, R.; Srisittipokakun, N.; Kim, H. J.; Kothan, S.; Kaewkhao, J.; Kirdsiri, K. Comparative Study of Optical and Luminescence Properties of Sm^{3+}-Ions Doped Li_2O−

Gd_2O_3−PbO−SiO_2 and Li_2O-GdF_3-PbO−SiO_2 Glasses for Orange Emission Solid State Device Application. *J. Lumin.* **2020**, *222*, 117136.
(51) Prakash, M. R.; Neelima, G.; Kummara, V. K.; Ravi, N.; Viswanath, C. D.; Rao, T. S.; Jilani, S. M. Holmium Doped Bismuth-Germanate Glasses for Green Lighting Applications: A Spectroscopic Study. *Opt. Mater. (Amsterdam, Neth.)* **2019**, *94*, 436−443.
(52) Matei, E.; Enculescu, M.; Enculescu, I. Single Bath Electrodeposition of Samarium Oxide/Zinc Oxide Nanostructured Films with Intense, Broad Luminescence. *Electrochim. Acta* **2013**, *95*, 170−178.
(53) Chanthima, N.; Ruangtaweep, Y.; Kaewkhao, J. Optical Properties and White Emission from Dy^{3+} Doped in Y_2O_3-CaO-SiO_2-B_2O_3 Glasses. *Key Eng. Mater.* **2016**, *702*, 62−65.
(54) Yang, Y.; Zhao, Y.; Chen, J.; Mao, Z.; Li, G.; Xu, J.; Wang, D.; Fahlman, B. D. Synthesis of $CaAlSiN_3$:Eu^{2+} Nitride Phosphors from Entire Oxides Raw Materials and Their Photoluminescent Properties. *J. Mater. Sci.: Mater. Electron.* **2017**, *28* (1), 715−720.
(55) Hasim, N.; Rohani, M. S.; Sahar, M. R.; Ghoshal, S. K. Luminescence of Er^{3+}/Nd^{3+} Co-Doped Lithium Niobate Tellurite Glass. *Mater. Sci. Forum* **2016**, *846*, 131−136.
(56) Ouannes, K.; Lebbou, K.; Walsh, B. M.; Poulain, M.; Alombert-Goget, G.; Guyot, Y. Antimony Oxide Based Glasses, Novel Laser Materials. *Opt. Mater. (Amsterdam, Neth.)* **2017**, *65*, 8−14.
(57) Wang, X.; Tan, X.; Xu, S.; Liu, F.; Goodman, B. A.; Deng, W. Preparation and Up-Conversion Luminescence of Er-Doped Yttria Stabilized Zirconia Single Crystals. *J. Lumin.* **2020**, *219*, 116896.
(58) Ragin, T.; Baranowska, A.; Sołtys, M.; Górny, A.; Kochanowicz, M.; Zmojda, J.; Miluski, P.; Jadach, R.; Dorosz, D. Intense and Wide Mid-Infrared Luminescence in Bismuth-Germanate Glass Co-Doped with Ho^{3+}/Er^{3+}/Yb^{3+} Ions. *Infrared Phys. Technol.* **2018**, *92*, 139−143.
(59) Stepien, R.; Jedrzejewski, K. P.; Kwasny, M.; Mierczyk, Z. Er^{3+}- and Yb^{3+}-Doped Phosphate Glasses for Eye-Safe Laser Systems. In *Proceedings of the International Symposium on Photonics and Applications, Singapore*, Design, Fabrication, and Characterization of Photonic Devices II; Osinski, M., Chua, S.-J., Ishibashi, A., Eds.; SPIE, 2001; p 51. DOI: 10.1117/12.446571.
(60) Moulika, G.; Sailaja, S.; Reddy, B. N. K.; Reddy, V. S.; Dhoble, S. J.; Reddy, B. S. Optical Properties of Eu^{3+} & Tb^{3+} Ions Doped Alkali Oxide (Li_2O/Na_2O/K_2O) Modified Boro Phosphate Glasses for Red, Green Lasers and Display Device Applications. *Phys. B* **2018**, *535*, 2−7.
(61) Lakshminarayana, G.; Bashar, K. A.; Baki, S. O.; Lira, A.; Caldiño, U.; Meza-Rocha, A. N.; Falcony, C.; Camarillo, E.; Kityk, I. V.; Mahdi, M. A. Er^{3+}/Dy^{3+} Codoped B_2O_3-TeO_2-PbO-ZnO-Li_2O-Na_2O Glasses: Optical Absorption and Fluorescence Features Study for Visible and near-Infrared Fiber Laser Applications. *J. Non-Cryst. Solids* **2019**, *503*−*504*, 366−381.
(62) Anashkina, E. A.; Dorofeev, V. V.; Koltashev, V. V.; Kim, A. V. Development of Er^{3+}-Doped High-Purity Tellurite Glass Fibers for Gain-Switched Laser Operation at 2.7 μm. *Opt. Mater. Express* **2017**, *7* (12), 4337.
(63) Luo, D. W.; Zhang, J.; Xu, C. W.; Yang, H.; Qin, X. P.; Ma, J.; Tang, D. Y. Fabrication and Spectroscopic Properties of Transparent Yb:YAG Laser Ceramics. *Solid State Phenom.* **2012**, *185*, 44−47.
(64) Bulus, I.; Dalhatu, S. A.; Hussin, R.; Wan Shamsuri, W. N.; Yamusa, Y. A. The Role of Dysprosium Ions on the Physical and Optical Properties of Lithium-Borosulfophosphate Glasses. *Int. J. Mod. Phys. B* **2017**, *31* (13), 1750101.
(65) Ali, A. A.; Shaaban, H. M.; Abdallah, A. Spectroscopic Studies of ZnO Borate−Tellurite Glass Doped with Eu_2O_3. *J. Mater. Res. Technol.* **2018**, *7* (3), 240−247.
(66) Afef, B.; Alqahtani, M. M.; Hegazy, H. H.; Yousef, E.; Damak, K.; Maâlej, R. Green and near Infrared Emission of Er^{3+} Doped PZS and PZC Glasses. *J. Lumin.* **2018**, *194*, 706−712.
(67) Mohammadi, M. R.; Ghorbani, M.; Fray, D. J. Preparation and Characterisation of Nanostructural TiO_2−Er_2O_3 Binary Oxides with High Surface Area Derived from Particulate Sol−Gel Route. *Mater. Sci. Technol.* **2006**, *22* (8), 965−974.
(68) Achehboune, M.; Khenfouch, M.; Boukhoubza, I.; Mothudi, B.; Zorkani, I.; Jorio, A. Study on the Effect of Er Dopant on the Structural Properties of ZnO Nanorods Synthesized via Hydrothermal Method. *J. Phys.: Conf. Ser.* **2019**, *1292*, 012020.
(69) Han, L.; Zhang, Q.; Song, J.; Xiao, Z.; Qiang, Y.; Ye, X.; You, W.; Lu, A. A Novel Eu^{3+}-Doped Phosphate Glass for Reddish Orange Emission: Preparation, Structure and Fluorescence Properties. *J. Lumin.* **2020**, *221*, 117041.
(70) Madhu, A.; Srinatha, N.; Munisudhakar, B. Concentration Dependent Enhanced Luminescence and Its Quenching Effect in Erbium Incorporated Heavy Metal Oxide—Borate Glasses. *Mater. Res. Express* **2019**, *6* (12), 125212.
(71) Yu, H.; Zhang, H.; Yang, W.; Feng, J.; Fan, W.; Song, S. Luminescent Character of Mesoporous Silica with Er_2O_3 Composite Materials. *Microporous Mesoporous Mater.* **2013**, *170*, 113−122.
(72) Wei, G. C.; Lapatovich, W. P.; Browne, J.; Snellgrove, R. Dysprosium Oxide Ceramic Arc Tube for HID Lamps. *J. Phys. D: Appl. Phys.* **2008**, *41* (14), 144014.
(73) Lodi, T. A.; Sandrini, M.; Medina, A. N.; Barboza, M. J.; Pedrochi, F.; Steimacher, A. Dy:Eu Doped CaBAl Glasses for White Light Applications. *Opt. Mater. (Amsterdam, Neth.)* **2018**, *76*, 231−236.
(74) Shinozaki, K.; Fujimoto, Y.; Okada, G.; Kawaguchi, N.; Yanagida, T.; Akai, T.; Koshimizu, M.; Asai, K. Scintillation and VUV-Excited Photoluminescence of Europium-Doped BaF_2−Al_2O_3−B_2O_3 Glasses. *J. Mater. Sci.: Mater. Electron.* **2018**, *29* (14), 11824−11829.
(75) Kaur, S.; Pandey, O. P.; Jayasankar, C. K.; Chopra, N. Spectroscopic, Thermal and Structural Investigations of Dy^{3+} Activated Zinc Borotellurite Glasses and Nano-Glass-Ceramics for White Light Generation. *J. Non-Cryst. Solids* **2019**, *521*, 119472.
(76) Ramteke, D. D.; Gedam, R. S.; Swart, H. C. Physical and Optical Properties of Lithium Borosilicate Glasses Doped with Dy^{3+} Ions. *Phys. B* **2018**, *535*, 194−197.
(77) Jaidass, N.; Krishna Moorthi, C.; Mohan Babu, A.; Reddi Babu, M. Luminescence Properties of Dy^{3+} Doped Lithium Zinc Borosilicate Glasses for Photonic Applications. *Heliyon* **2018**, *4* (3), e00555.
(78) Hua, C.; Shen, L.; Pun, E. Y. B.; Li, D.; Lin, H. Dy^{3+} Doped Tellurite Glasses Containing Silver Nanoparticles for Lighting Devices. *Opt. Mater. (Amsterdam, Neth.)* **2018**, *78*, 72−81.
(79) Ye, W.; Zhao, C.; Shen, X.; Ma, C.; Deng, Z.; Li, Y.; Wang, Y.; Zuo, C.; Wen, Z.; Li, Y.; Yuan, X.; Wang, C.; Cao, Y. High Quantum Yield $Gd_{4.67}Si_3O_{13}$:Eu^{3+} Red-Emitting Phosphor for Tunable White Light-Emitting Devices Driven by UV or Blue LED. *ACS Appl. Electron. Mater.* **2021**, *3* (3), 1403−1412.
(80) Khan, I.; Rooh, G.; Rajaramakrishna, R.; Srisittipokakun, N.; Kim, H. J.; Kaewkhao, J.; Ruangtaweep, Y. Photoluminescence Properties of Dy^{3+} Ion-Doped Li_2O-PbO-Gd_2O_3-SiO_2 Glasses for White Light Application. *Braz. J. Phys.* **2019**, *49* (5), 605−614.
(81) Khan, I.; Rooh, G.; Rajaramakrishna, R.; Srisittipokakun, N.; Kim, H. J.; Kaewkhao, J. Energy Transfer and Spectroscopic Investigation of Dy_2O_3 Doped Li_2O−BaO−GdF_3−SiO_2 for White Light LED. *Glass Phys. Chem.* **2019**, *45* (5), 332−343.
(82) Kuzman, S.; Medić, M.; Đorđević, V.; Zeković, I.; Ristić, Z.; Far, L. Đ.; Dramićanin, M. D. Luminescence Thermometry Using Dy^{3+}-Activated $Na_{0.25}K_{0.25}Bi_{0.5}TiO_3$ Powders. *J. Electron. Mater.* **2020**, *49* (6), 4002−4009.
(83) Kaur, P.; Khanna, A.; Singh, M. N.; Sinha, A. K. Structural and Optical Characterization of Eu and Dy Doped $CaWO_4$ Nanoparticles for White Light Emission. *J. Alloys Compd.* **2020**, *834*, 154804.
(84) Linganna, K.; Haritha, P.; Venkata Krishnaiah, K.; Venkatramu, V.; Jayasankar, C. K. Optical and Luminescence Properties of Dy^{3+} Ions in K−Sr−Al Phosphate Glasses for Yellow Laser Applications. *Appl. Phys. B: Lasers Opt.* **2014**, *117* (1), 75−84.
(85) Zhou, Z.; Lin, A.; Guo, H.; Liu, X.; Hou, C.; Lu, M.; Wei, W.; Peng, B.; Zhao, W.; Toulouse, J. Tb^{3+}/Yb^{3+} Heavily-Doped Tellurite Glasses with Efficient Green Light Emission. *J. Non-Cryst. Solids* **2010**, *356* (50−51), 2896−2899.

(86) Kim, D.; Kim, H.-E.; Kim, C.-H. Enhancement of Long-Persistent Phosphorescence by Solid-State Reaction and Mixing of Spectrally Different Phosphors. *ACS Omega* **2020**, *5* (19), 10909−10918.
(87) Reddy, B. N. K.; Raju, B. D.; Thyagarajan, K.; Ramanaiah, R.; Jho, Y.-D.; Reddy, B. S. Optical Characterization of Eu^{3+} Ion Doped Alkali Oxide Modified Borosilicate Glasses for Red Laser and Display Device Applications. *Ceram. Int.* **2017**, *43* (12), 8886−8892.
(88) Ohyama, K.; Nonaka, T.; Kanamori, T.; Yamamoto, S.-I. Strong Light of Red Up-Conversion in a ZnO-TiO_2 Composite Containing Er^{3+} and Yb^{3+}. In *2015 22nd International Workshop on Active-Matrix Flatpanel Displays and Devices (AM-FPD)*; IEEE, 2015; pp 89−90. DOI: 10.1109/AM-FPD.2015.7173204.
(89) Singh, V.; Dabre, K. V.; Dhoble, S. J.; Lakshminarayana, G. Green Emitting Holmium (Ho) Doped Yttrium Oxide (Y_2O_3) Phosphor for Solid State Lighting. *Optik (Munich, Ger.)* **2020**, *206*, 164339.
(90) Mhareb, M. H. A. Physical, Optical and Shielding Features of $Li_2O-B_2O_3-MgO-Er_2O_3$ Glasses Co-Doped of Sm_2O_3. *Appl. Phys. A: Mater. Sci. Process.* **2020**, *126* (1), 71.
(91) Ramesh, P.; Hegde, V.; Pramod, A. G.; Eraiah, B.; Agarkov, D. A.; Eliseeva, G. M.; Pandey, M. K.; Annapurna, K.; Jagannath, G.; Kokila, M. K. Compositional Dependence of Red Photoluminescence of Eu^{3+} Ions in Lead and Bismuth Containing Borate Glasses. *Solid State Sci.* **2020**, *107*, 106360.
(92) Chanthima, N.; Tariwong, Y.; Kim, H. J.; Kaewkhao, J.; Sangwaranatee, N. Effect of Eu^{3+} Ions on the Physical, Optical and Luminescence Properties of Aluminium Phosphate Glasses. *Key Eng. Mater.* **2018**, *766*, 122−126.
(93) Kumar, V.; Som, S.; Kumar, V.; Kumar, V.; Ntwaeaborwa, O. M.; Coetsee, E.; Swart, H. C. Tunable and White Emission from ZnO:Tb^{3+} Nanophosphors for Solid State Lighting Applications. *Chem. Eng. J.* **2014**, *255*, 541−552.
(94) Algarni, H.; Reben, M.; Almoeed, S.; Maâlej, R.; Yousef, E. S. Luminescence Emission of Tm-Dy Ions Codoped Tellurite Glasses under Visible Light Excitation. *Optik (Munich, Ger.)* **2018**, *160*, 340−347.
(95) Benmadani, Y.; Kermaoui, A.; Chalal, M.; Khemici, W.; Kellou, A.; Pellé, F. Erbium Doped Tellurite Glasses with Improved Thermal Properties as Promising Candidates for Laser Action and Amplification. *Opt. Mater. (Amsterdam, Neth.)* **2013**, *35* (12), 2234−2240.
(96) AbouDeif, Y. M.; Yousef, E. S.; Marzouk, S. Y. Investigation of Luminescence Parameters of Novel Glasses with Composition TeO_2-ZnO-NaF-MoO_2-Er_2O_3 as Laser Material. *J. Non-Cryst. Solids* **2018**, *498*, 72−81.
(97) Elkhoshkhany, N.; Marzouk, S. Y.; Moataz, N.; Kandil, S. H. Structural and Optical Properties of TeO_2-Li_2O-ZnO-Nb_2O_5-Er_2O_3 Glass System. *J. Non-Cryst. Solids* **2018**, *500*, 289−301.
(98) Effendy, N.; Abdul Wahab, Z.; Mohamed Kamari, H.; Matori, K. A.; Hj Ab Aziz, S.; Zaid, M. H. M. Structural and Optical Properties of Er^{3+}-Doped Willemite Glass-Ceramics from Waste Materials. *Optik (Munich, Ger.)* **2016**, *127* (24), 11698−11705.
(99) Choi, J. H.; Shi, F. G.; Margaryan, A.; Margaryan, A. Refractive Index and Low Dispersion Properties of New Fluorophosphate Glasses Highly Doped with Rare-Earth Ions. *J. Mater. Res.* **2005**, *20* (1), 264−270.
(100) Wang, Y.; Wang, L.; Zhao, Y.; Yuan, X. Color-Tunable up-Conversion Luminescence of Er^{3+}/Yb^{3+} Co-Doped (K,Na)NbO_3 Ceramics. *Mater. Lett.* **2016**, *179*, 210−213.
(101) Rivera-López, F.; Babu, P.; Basavapoornima, C.; Jayasankar, C. K.; Lavín, V. Efficient $Nd^{3+} \rightarrow Yb^{3+}$ Energy Transfer Processes in High Phonon Energy Phosphate Glasses for 1.0 μ m Yb 3+ Laser. *J. Appl. Phys.* **2011**, *109* (12), 123514.
(102) Yang, L.-q.; Zou, K.-s.; Yuan, X.; Xiong, B.-x.; Qin, Z.-x.; Zhang, X.; Zhang, G.-j. Spectroscopic Properties of Ytterbium-Doped TeO_2-Al_2O_3-Cs_2O Glass. *Guangzi Xuebao* **2013**, *42* (6), 679−683.
(103) Pang, L.; Pan, R.; Geng, P.; Ning, D.; Wang, B.; Yi, Y. The Research on Ytterbium-Doped Double-Clad Fiber for High Power Fiber Lasers. In *Advanced Laser Technology and Applications*; Jiang, S., Wang, L., Liu, Z., Zhou, P., Shi, W., Eds.; SPIE, 2018; p 30. DOI: 10.1117/12.2505459.
(104) Stępień, R.; Franczyk, M.; Pysz, D.; Kujawa, I.; Klimczak, M.; Buczyński, R. Ytterbium-Phosphate Glass for Microstructured Fiber Laser. *Materials* **2014**, *7* (6), 4723−4738.
(105) Venkata Krishnaiah, K.; Jayasankar, C. K.; Venkatramu, V.; León-Luis, S. F.; Lavín, V.; Chaurasia, S.; Dhareshwar, L. J. Optical Properties of Yb^{3+} Ions in Fluorophosphate Glasses for 1.0 Mm Solid-State Infrared Lasers. *Appl. Phys. B: Lasers Opt.* **2013**, *113* (4), 527−535.
(106) Li, Y.; Wang, J.; Jing, F.; Lin, A.; Liu, S.; Zhan, H.; Peng, K.; Sun, S.; Jiang, J.; Wang, X.; Ni, L.; Jiang, L. Fiber Design and Fabrication of Yb/Ce Codoped Aluminosilicate Laser Fiber With High Laser Stability. *IEEE Photonics J.* **2018**, *10* (4), 1−8.
(107) Liu, R.; Yan, D.; Chen, M.; Wang, J.; Shi, J.; Zhu, Q. Fabrication of Yb/Ce/P Co-Doped Fluoroaluminosilicate Fiber with Excellent Photodarkening Suppression and KW-Level Laser Performance. *Opt. Mater. Express* **2020**, *10* (3), 777.
(108) Kaewnuam, E.; Wantana, N.; Kim, H. J.; Kaewkhao, J. Development of Lithium Yttrium Borate Glass Doped with Dy^{3+} for Laser Medium, W-LEDs and Scintillation Materials Applications. *J. Non-Cryst. Solids* **2017**, *464*, 96−103.
(109) Li, B.; Li, D.; Pun, E. Y. B.; Lin, H. Dy^{3+} Doped Tellurium-Borate Glass Phosphors for Laser-Driven White Illumination. *J. Lumin.* **2019**, *206*, 70−78.
(110) Farooq, S.; Reddy, Y. M.; Padmasuvarna, R.; Kummara, V. K.; Viswanath, C. S. D.; Mahamuda, S. Photoluminescence of Dysprosium Doped Antimony-Magnesium-Strontium-Oxyfluoroborate Glasses. *Ceram. Int.* **2018**, *44* (17), 21303−21308.
(111) Sheng, K. C.; Korenowski, G. M. Laser-Induced Optical Emission Studies of Europium(3+) Sites in Polycrystalline Powders of Monoclinic and Bcc. Europium Sesquioxide. *J. Phys. Chem.* **1988**, *92* (1), 50−56.
(112) Ramteke, D. D.; Balakrishna, A.; Kumar, V.; Swart, H. C. Luminescence Dynamics and Investigation of Judd-Ofelt Intensity Parameters of Sm^{3+} Ion Containing Glasses. *Opt. Mater. (Amsterdam, Neth.)* **2017**, *64*, 171−178.
(113) Snetkov, I. L.; Yakovlev, A. I.; Permin, D. A.; Balabanov, S. S.; Palashov, O. V. Magneto-Optical Faraday Effect in Dysprosium Oxide (Dy_2O_3) Based Ceramics Obtained by Vacuum Sintering. *Opt. Lett.* **2018**, *43* (16), 4041.
(114) Ju, M.; Xiao, Y.; Sun, W.; Lu, C.; Yeung, Y. In-Depth Determination of the Microstructure and Energy Transition Mechanism for Nd^{3+}-Doped Yttrium Oxide Laser Crystals. *J. Phys. Chem. C* **2020**, *124* (3), 2113−2119.
(115) Sahoo, N. K.; Thakur, S.; Senthilkumar, M.; Bhattacharyya, D.; Das, N. C. Reactive Electron Beam Evaporation of Gadolinium Oxide Optical Thin Films for Ultraviolet and Deep Ultraviolet Laser Wavelengths. *Thin Solid Films* **2003**, *440* (1−2), 155−168.
(116) Shaaban, K. S.; Ali, A. M.; Saddeek, Y. B.; Aly, K. A.; Dahshan, A.; Amin, S. A. Synthesis, Mechanical and Optical Features of Dy_2O_3 Doped Lead Alkali Borosilicate Glasses. *Silicon* **2019**, *11* (4), 1853−1861.
(117) Yan, X.; Luo, S.; Lin, Z.; Yao, J.; He, R.; Yue, Y.; Chen, C. $ReBe_2B_5O_{11}$ (Re = Y, Gd): Rare-Earth Beryllium Borates as Deep-Ultraviolet Nonlinear-Optical Materials. *Inorg. Chem.* **2014**, *53* (4), 1952−1954.
(118) Singla, S.; Pandey, O. P.; Sharma, G. Z-Scan Study of Nonlinear Absorption in Gold Doped Borosilicate Glass: Effect of Dy^{3+}. *J. Non-Cryst. Solids* **2019**, *521*, 119481.
(119) Das, G. K.; Zhang, Y.; D'Silva, L.; Padmanabhan, P.; Heng, B. C.; Chye Loo, J. S.; Selvan, S. T.; Bhakoo, K. K.; Yang Tan, T. T. Single-Phase Dy_2O_3:Tb^{3+} Nanocrystals as Dual-Modal Contrast Agent for High Field Magnetic Resonance and Optical Imaging. *Chem. Mater.* **2011**, *23* (9), 2439−2446.
(120) Mandal, P.; Singh, U. P.; Roy, S. Co-Sputtering of Lu_2O_3, Eu_2O_3 and Ga_2O_3 for Optoelectronics Applications. *IOP Conf. Ser.: Mater. Sci. Eng.* **2020**, *872*, 012062.

(121) Bieza, M.; Guzik, M.; Tomaszewicz, E.; Guyot, Y.; Lebbou, K.; Boulon, G. Toward Optical Ceramics Based on Yb^{3+} Rare Earth Ion-Doped Mixed Molybdato-Tungstates: Part II - Spectroscopic Characterization. *J. Phys. Chem. C* **2017**, *121* (24), 13303−13313.
(122) Huang, Y.; Bai, G.; Zhao, Y.; Xie, H.; Yang, X.; Xu, S. Yb/Ho Codoped Layered Perovskite Bismuth Titanate Microcrystals with Upconversion Luminescence: Fabrication, Characterization, and Application in Optical Fiber Ratiometric Thermometry. *Inorg. Chem.* **2020**, *59* (19), 14229−14235.
(123) Zhao, Y.; Yuan, X.; Zhao, Y.; Zhou, H.; Li, J.; Jin, H. Improved Piezoelectricity and Luminescence Behavior in Er_2O_3 Doped (K,Na)NbO_3 Ceramics. *Mater. Lett.* **2016**, *162*, 226−229.
(124) Zhao, Y.; Wang, X.; Zhang, Y.; Li, Y.; Yao, X. Simultaneous Yb^{3+} -Induced Phase Transition and Sensitized Luminescence in Er^{3+}-Doped KNN-Based Lead-Free Ceramics for Optical Thermometry. *ACS Appl. Electron. Mater.* **2020**, *2* (9), 3028−3038.
(125) Ichoja, A.; Hashim, S.; Ghoshal, S. K.; Hashim, I. H.; Omar, R. S. Physical, Structural and Optical Studies on Magnesium Borate Glasses Doped with Dysprosium Ion. *J. Rare Earths* **2018**, *36* (12), 1264−1271.
(126) Feng, J.; Shan, G.; Maquieira, A.; Koivunen, M. E.; Guo, B.; Hammock, B. D.; Kennedy, I. M. Functionalized Europium Oxide Nanoparticles Used as a Fluorescent Label in an Immunoassay for Atrazine. *Anal. Chem.* **2003**, *75* (19), 5282−5286.
(127) Ramay, S. M.; Mahmood, A.; Ghaithan, H. M.; Al-Zayed, N. S.; Aslam, A.; Murtaza, A.; Ahmad, N.; Siddiqi, S. A.; Saleem, M. Magnetron Sputtered Dy_2O_3 with Chromium and Copper Contents for Antireflective Thin Films with Enhanced Absorption. *J. Rare Earths* **2019**, *37* (9), 989−994.
(128) Srinivasan, R.; Yogamalar, N. R.; Elanchezhiyan, J.; Joseyphus, R. J.; Bose, A. C. Structural and Optical Properties of Europium Doped Yttrium Oxide Nanoparticles for Phosphor Applications. *J. Alloys Compd.* **2010**, *496* (1−2), 472−477.
(129) Gasiorowski, A.; Szajerski, P. Particles Size Increase Assisted Enhancement of Thermoluminescence Emission in Gadolinium and Dysprosium Oxide Doped Phosphate Glasses. *J. Alloys Compd.* **2020**, *839*, 155479.
(130) Gopi, S.; Remya Mohan, P.; Sreeja, E.; Unnikrishnan, N. V.; Joseph, C.; Biju, P. R. Optical Characteristics of Dy^{3+} Ions in Alkali Fluoroborate Glasses for WLEDs. *J. Electron. Mater.* **2019**, *48* (7), 4300−4309.
(131) Zhang, L.; Luo, H.; Zhou, L.; Liu, Q.; Li, J.; Zhang, W. Preparation of γ-Aluminum Oxynitride Phosphor with Eu Doping by Direct Nitridation in Ammonia and Postannealing. *J. Am. Ceram. Soc.* **2018**, *101* (8), 3299−3308.
(132) Yang, Y.; Chen, J.; Li, G.; Mao, Z.; Xu, J.; Wang, D.-J.; Fahlman, B. D. Synthesis of Nitride Phosphor Using Entire Oxides Raw Materials and Their Photoluminescence Properties. *J. Am. Ceram. Soc.* **2017**, *100* (3), 1022−1029.
(133) Abdullah, M.; Azman, K.; Azhan, H.; Razali, W. A. W. Optical Characterization of Erbium Doped Sodium Borate Glass. *Adv. Mater. Res.* **2012**, *622*−*623*, 191−194.
(134) Nasser, K.; Aseev, V.; Ivanov, S.; Ignatiev, A.; Nikonorov, N. Spectroscopic and Laser Properties of Erbium and Ytterbium Co-Doped Photo-Thermo-Refractive Glass. *Ceram. Int.* **2020**, *46* (16), 26282−26288.
(135) Ouyang, Z.; Yang, Y.; Sun, J. Electroluminescent Yb_2O_3:Er and $Yb_2Si_2O_7$:Er Nanolaminate Films Fabricated by Atomic Layer Deposition on Silicon. *Opt. Mater. (Amsterdam, Neth.)* **2018**, *80*, 209−215.
(136) Erdem, M.; Örücü, H.; Cantürk, S. B.; Eryürek, G. Upconversion Yb^{3+}/Er^{3+}:Gadolinium Gallium Garnet Nanocrystals for White-Light Emission and Optical Thermometry. *ACS Appl. Nano Mater.* **2021**, *4* (7), 7162−7171.
(137) Tan, Y.; Zhang, S.; Liang, K. Photocurrent Response and Semiconductor Characteristics of Ce-Ce_2O_3-CeO_2-Modified TiO_2 Nanotube Arrays. *Nanoscale Res. Lett.* **2014**, *9* (1), 67.
(138) El Desouky, F. G.; Saadeldin, M. M.; Mahdy, M. A.; Wahab, S. M. A.; El Zawawi, I. K. Impact of Calcination Temperature on the Structure, Optical and Photoluminescence Properties of Nano-crystallineCerium Oxide Thin Films. *Mater. Sci. Semicond. Process.* **2020**, *111*, 104991.
(139) Josephine, G. A. S.; Sivasamy, A. Nanocrystalline ZnO Doped Dy_2O_3 a Highly Active Visible Photocatalyst: The Role of Characteristic f Orbital's of Lanthanides for Visible Photoactivity. *Appl. Catal., B* **2014**, *150*−*151*, 288−297.
(140) Tanko, Y. A.; Sahar, M. R.; Ghoshal, S. K. Samarium activated absorption and emission of zinc tellurite glass. *J. Teknol.* **2016**, *78* (3−2). DOI: 10.11113/jt.v78.7834.
(141) Zhang, H.; Dai, H.; Liu, Y.; Deng, J.; Zhang, L.; Ji, K. Surfactant-Mediated PMMA-Templating Fabrication and Characterization of Three-Dimensionally Ordered Macroporous Eu_2O_3 and Sm_2O_3 with Mesoporous Walls. *Mater. Chem. Phys.* **2011**, *129* (1−2), 586−593.
(142) Prakash, M. R.; Neelima, G.; Kummara, V. K.; Ravi, N.; Kiran, N.; Viswanath, C. S. D.; Rao, T. S.; Venkatramu, V. Optical and Radiative Properties of Sm^{3+} ions Activated Alkali-Bismuth-Germanate Glasses. *J. Lumin.* **2019**, *214*, 116566.
(143) Al-Hadeethi, Y.; Ahmed, M.; Al-Heniti, S. H.; Sayyed, M. I.; Rammah, Y. S. Rare Earth Co-Doped Tellurite Glass Ceramics: Potential Use in Optical and Radiation Shielding Applications. *Ceram. Int.* **2020**, *46* (11), 19198−19208.
(144) Linganna, K.; Basavapoornima, C.; Jayasankar, C. K. Luminescence Properties of Sm^{3+}-Doped Fluorosilicate Glasses. *Opt. Commun.* **2015**, *344*, 100−105.
(145) Lewandowski, T.; Seweryński, C.; Walas, M.; Łapiński, M.; Synak, A.; Sadowski, W.; Kościelska, B. Structural and Luminescent Study of TeO_2-BaO-Bi_2O_3-Ag Glass System Doped with Eu^{3+} and Dy^{3+} for Possible Color-Tunable Phosphor Application. *Opt. Mater. (Amsterdam, Neth.)* **2018**, *79*, 390−396.
(146) Xing, Y.; Zhu, Y.; Chang, C.; Wang, Y.; Wang, Y. New Synthetic Method and the Luminescent Properties of Green-Emitting β-Sialon:Eu^{2+} Phosphors. *J. Mater. Sci.: Mater. Electron.* **2017**, *28* (13), 9464−9470.
(147) Jiménez, J. A. Photoluminescence of Eu^{3+}-Doped Glasses with Cu^{2+} Impurities. *Spectrochim. Acta, Part A* **2015**, *145*, 482−486.
(148) Azlan, M. N.; Halimah, M. K.; El-Mallawany, R.; Faznny, M. F.; Eevon, C. Optical Properties of Zinc Borotellurite Glass System Doped with Erbium and Erbium Nanoparticles for Photonic Applications. *J. Mater. Sci.: Mater. Electron.* **2017**, *28* (5), 4318−4327.
(149) Gaafar, M. S.; Marzouk, S. Y. Judd−Ofelt Analysis of Spectroscopic Properties of Er^{3+} Doped TeO_2-BaO-ZnO Glasses. *J. Alloys Compd.* **2017**, *723*, 1070−1078.
(150) Charitidis, C.; Patsalas, P.; Logothetidis, S. Optical and Mechanical Performance of Nanostructured Cerium Oxides for Applications in Optical Devices. *J. Phys.: Conf. Ser.* **2005**, *10*, 226−229.
(151) Ma, R.; Jahurul Islam, M.; Amaranatha Reddy, D.; Kim, T. K. Transformation of CeO_2 into a Mixed Phase CeO_2/Ce_2O_3 Nano-hybrid by Liquid Phase Pulsed Laser Ablation for Enhanced Photocatalytic Activity through Z-Scheme Pattern. *Ceram. Int.* **2016**, *42* (16), 18495−18502.
(152) Niu, J.; Chen, H.; Song, Z. Preparation and Spectral Properties of the Yb^{3+} Doped Silicate Glass. In *9th International Conference on Optical Communications and Networks (ICOCN 2010)*; IET, 2010; pp 391−394. DOI: 10.1049/cp.2010.1233.
(153) Venkatramu, V.; Vijaya, R.; León-Luis, S. F.; Babu, P.; Jayasankar, C. K.; Lavín, V.; Dhareshwar, L. J. Optical Properties of Yb^{3+}-Doped Phosphate Laser Glasses. *J. Alloys Compd.* **2011**, *509* (16), 5084−5089.

https://doi.org/10.1021/acsaelm.1c00682
ACS Appl. Electron. Mater. 2021, 3, 3715−3746